Origin and Fate of Dissolved Organic Matter in Boreal Lakes Under the Environmental Changes of the 21st Century

Dissertation for the degree of Philosophiae Doctor

Camille Crapart

Department of Chemistry

Faculty of Mathematics and Natural Sciences

University of Oslo

2023

Series of dissertations submitted to the
Faculty of Mathematics and Natural Sciences, University of Oslo
No. 2684

ISSN 1501-7710

Cover: UiO.
Print production: Graphic center, University of Oslo.

Acknowledgments

I must thank first my two successive supervisors, Rolf and Tom. Rolf, you gave me the opportunity to begin and pursue a PhD fellowship in Oslo, helped me launch the first projects, and followed up on my work up even after leaving UiO. Tom, you trusted me in the end of the PhD when I wasn't sure of where I was going. Thank you for your valuable scientific intuition and knowledge! I would also like to thank Dag who has been there throughout, for work and ski talks.

Thanks to the crew who welcomed me at the Kjemisk Institutt: Jenny, Eline, Suzanne, Maya and Alexander. My first fully Norwegian colleague crew! Special thanks for Alexander and all the time spent on long discussions by the coffee machine. Many others at KI and IBV accompanied my journey there, bringing life and fun: Isabelle, Nico, Felix, Baptiste, JP, Deniz, and Eirik.

To all my friends, who never doubted me and never asked me when I would finish, going climbing or skiing with me instead: thank you. Special thanks to some of you: Marion, for the home you provided me in the mountains, and your support through the years. Louise, for your guaranteed fun and kindness. Flora, for your loyalty and your care. Your friendships are precious.

To Morgan, who discovered what it meant to pursue an academic career when he met me. Thank you for your loving and patient support. You have been there daily, and I hope this will continue for a long time.

And of course, thanks to my family: my parents who always support me unconditionally; Clémence who is a great listener; Cécile who will soon become a doctor too; and Théo who is now on the other side of the world. I hope you are as proud of me as I am proud of you!

Table of contents

Acknowledgments

Table of contents 1

List of papers 3

Abbreviations 5

Abstract 7

Abstrakt 9

1. Introduction: Organic matter in lakes and the carbon cycle in Fennoscandia 11

1.1. The pool of organic carbon in lakes: from the soils to the atmosphere 13

1.1.1. Lakes are the mirror of their catchment 13

1.1.2. Carbon pathways in the water column 16

1.1.3. Carbon evasion to the atmosphere 17

1.2. Past, present, and future anthropogenic impacts on the carbon cycle 20

1.2.1. Land use changes 20

1.2.2. Impact of atmospheric deposition of Sulphur and Nitrogen 21

1.2.3. Impact of climate change 22

2. Scope of this thesis 23

3. Material and Methods 26

3.1. Datasets and surveys 26

3.2. Experimental analysis 30

3.3. Statistical analysis 32

4. Main findings & Discussion 33

4.1 Drivers of TOC load in freshwater – Paper 1 & Appendix 33

4.1.1. Forecast of TOC in the future 33

4.1.2. Hindcast of TOC concentration 38

4.2. Heterotrophic respiration in boreal lakes – Paper 2 40

4.3. TOC driving CO_2 evasion in boreal lakes – Paper 3 42

5. Conclusion and future perspectives 46

References 48

Appendix - TOC concentration and coastal darkening in the 20th century

Paper 1 - Spatial Predictors and Temporal Forecast of Total Organic Carbon Levels in Boreal Lakes

Paper 2 - Factors Governing Biodegradability of Dissolved Natural Organic Matter in Lake Water

Paper 3 - Effect of Organic Carbon Concentration on CO_2 Evasion from Boreal Lakes

List of papers

Paper 1

Crapart Camille, Anders G. Finstad, Dag Olav Hessen, Rolf David Vogt, and Tom Andersen. 2023. "Spatial Predictors and Temporal Forecast of Total Organic Carbon Levels in Boreal Lakes." *Science of the Total Environment* 870 (April): 161676. https://doi.org/10.1016/j.scitotenv.2023.161676.

Paper 2

Crapart Camille, Tom Andersen, Dag Olav Hessen, Nicolas Valiente, and Rolf David Vogt. 2021. "Factors Governing Biodegradability of Dissolved Natural Organic Matter in Lake Water." *Water (Switzerland)* 13 (16). https://doi.org/10.3390/w13162210.

Paper 3

Crapart, Camille, Dag Olav Hessen, Tom Andersen. "Effect of Organic Carbon Concentration on CO_2 Evasion from Boreal Lakes". *Submitted to Global Biogeochemical Cycles*

Appendix

Crapart Camille, Tom Andersen, Anders Martin Frugård Opdal, "TOC concentration and coastal darkening in the 20th century". *Material, Methods, and Results*

Abbreviations

Parameters

CO_2: Carbon Dioxide

CH_4: Methane

HCO_3^-: Bicarbonate

CO_3: Carbonate

N_2O: Nitrous Oxide

O_2: Dioxygen

C:N: Carbon to Nitrogen ratio

DP: Dissolved Phosphate

DN: Dissolved Nitrogen

DIC: Dissolved Inorganic Carbon

DOM: Dissolved Organic Matter

LMW: Low Molecular Weight (DOM)

HMW: High Molecular Weight (DOM)

TA: Total Alkalinity

TIC: Total Inorganic Carbon

TOC: Total Organic Carbon

pCO_2: partial pressure of CO_2

NDVI: Net Differential Vegetation Index

sUVa: Specific Ultraviolet Absorbance at 254 nm

SARuv: UV Specific Absorbance Ratio

TNdep: Total Nitrogen Deposition

TSdep: Total Sulphur Deposition

RR: Respiration Rate

RRn: Normalized Respiration Rate

BdgT: Biodegradability period

Acronyms

CBA: Center for Biogeochemistry in the Anthropocene

CMIP: Coupled Model Intercomparison Project

IPCC: Intergovernmental Panel on Climate Change

LULUCF: Land Use, Land Use Change and Forestry

NCC: Norwegian Coastal Current

NorESM: Norwegian Earth System Model

NELS: Northern European Lakes Survey

RCP: Representative Concentration Pathway

SSP: Shared Socio-economic Pathway

LM: Linear Model

GLM: Generalized Linear Model

SELM: Spatial Error Linear Model

Units

Pg: petagram

Tg: teragram

$MtCO_{2eq}$: Megaton CO_2 equivalent

Abstract

Lakes are a typical feature of boreal landscapes, covering up to 10% of the land surface in Sweden and Finland. The water in most lakes has a brown colour due to a substantial influx of dissolved organic matter (DOM) from surrounding forests and peatlands. The organic matter, originating from the biomass, is transported to rivers and lakes by surface runoff. Once in lakes, this DOM undergoes various processes, including microbial uptake for secondary production. The in-situ decomposition of organic matter and import of inorganic carbon from the catchment leads to notable emissions of greenhouse gases from these inland waters.

Presently, the boreal region faces climate changes, including rising temperatures, changes in precipitation patterns, changes in cloud cover, and reduced snow cover. These changes are affecting the growth of vegetation. Evergreen species suffer from droughts, while the tree line rises in the mountains and the boreal forest moves upwards to the north in previously frozen areas. Additionally, anthropogenic activities are influencing the carbon cycle in lakes. Historical land use changes such as afforestation following abandonment of pastures, peatland draining, and timber industry expansion have increased the forested area. Acid deposition resulting from industrial activities further south in Europe was a major environmental factor in the 1970s-1980s, from which freshwater is still recovering. All these shifts are influencing the production, transport, and decomposition of dissolved organic matter in boreal freshwaters.

The main aim of this thesis was to assess how these climate and anthropogenic changes are impacting the fate of organic matter in boreal lakes. The goal was to understand how the biogeochemical carbon cycle has been and will be affected by these changes. The thesis consists of three separate papers, each focusing on a specific aspect of this cycle: the transfer of DOM from land to water, the heterotrophic respiration of DOM in the watercourse, and the evasion of carbon dioxide from surface waters to the atmosphere.

The first paper explores the relationship between the catchment characteristics and the concentration of total organic carbon (TOC), as a proxy for organic matter in lakes. This study builds upon existing knowledge about the drivers of DOM load and extends the use of a single set of parameters to predict TOC across the entire Fennoscandia region, despite wide variations in land use and climate. The analysis utilizes data from Northern European Lakes Survey conducted in 1995 across Norway, Sweden, and Finland. Additionally, the study attempts to predict potential changes in TOC load for the years 2050 and 2100, under two different Shared Socioeconomic Pathways. Using a similar

model, we also conducted a "historical" experiment reconstituting the concentration of TOC from 1900 to 2020. The historical trends were compared to actual TOC concentration in the past century, obtained from measurements of the chemical oxygen demand in several Swedish location. The research highlights the significant impact of land use on TOC load, modulated by trends in runoff and the deposition of sulphur and nitrogen from the atmosphere.

The second paper shifts focus to the heterotrophic decomposition of DOM in lakes. The study involves sampling seventy-three lakes in southern Norway in 2019. The rate of DOM respiration by microorganism was assessed with an incubation experiment during which the concentration of dioxygen was regularly measured. The study aimed at discerning how specific characteristics of DOM, such as mass, aromaticity, and elemental composition, influence its "recalcitrant" or "labile" nature. Results show that microorganisms preferably consume "labile" DOM, comprised of lighter, nutrient-rich molecules. Interestingly, even "recalcitrant" DOM can quickly be degraded when nutrient limitations are removed, indicating that it is used for respiration rather than microbial production.

The third paper involves estimating the efflux of CO_2 from boreal lakes. This estimation is based on using TOC as a predictor for the partial pressure of CO_2 (pCO_2) in the water. The study proceeds in two stages. Firstly, the best method of estimating pCO_2 was explored, considering the range of pH, alkalinity, and TOC concentrations in the two training datasets. It is found that TOC is the most reliable predictor in both cases. Secondly, this linear relationship was used to estimate pCO_2 in lakes from the Northern European Lakes Survey. Subsequently the evasion rate of CO_2 and the total efflux from inland waters in Norway, Sweden, and Finland is calculated. The results confirmed that inland water substantially contribute to greenhouse gas emissions that should be accounted for into national carbon budgets.

The research conducted in this thesis underscores the interconnectedness of catchment areas, lakes, rivers, and the global climate. It traces the journey of organic carbon from the soil to water and back to the atmosphere, highlighting its intricate cycle. However, quantifying future changes in this cycle poses challenges. Further investigations are required to refine the estimates presented here, as well as to account for methane production, sedimentation of organic matter and specific processes occurring in rivers. Nevertheless, these results advocate for the necessity of acknowledging the contribution of inland waters to the global carbon cycle.

Abstrakt

Innsjøer er et karakteristisk element i boreale landskapet og dekker opptil 10% av landoverflaten i Sverige og Finland. Vannet i de fleste innsjøene har en brun farge på grunn av oppløst organisk materiale (DOM) fra omkringliggende skoger og myrer. Det organiske materialet som stammer fra vegetasjonen i landskapet, transporteres til elver og innsjøer gjennom overflateavrenning. Når dette organiske materialet når innsjøene gjennomgår det ulike prosesser, slik som sekundærproduksjon gjennom mikrobielt opptak. Nedbrytning av organisk materiale fra nedbørfeltet fører til betydelige utslipp av klimagasser fra elver og innsjøer.

Den boreale sonen står overfor klimaendringer, inkludert økende temperaturer, endringer i nedbørsmønstre og redusert snødekke. Disse endringene påvirker vegetasjonens vekstbetingelser. Eviggrønne arter lider under tørke, samtidig som tregrensen stiger i fjellene og den boreale skogen forflytter seg oppover mot nord i tidligere isdekte områder. I tillegg påvirker menneskelig aktivitet karbonsyklusen i innsjøer. Historiske endringer i arealbruk, som skogplanting etter at beitemarker ble forlatt, myrgrøfting og utvidelse av tømmerindustrien, har økt skogsarealet. Sur nedbør som følge av industriaktiviteter lenger sør i Europa var en betydelig miljøfaktor på 1970-80-tallet, som ferskvannet fremdeles gjenoppretter seg fra. Alle disse endringene påvirker produksjonen, transporten og nedbrytningen av oppløst organisk materiale i boreale ferskvann.

Hovedmålet med denne avhandlingen var å vurdere hvordan klima- og arealbruksendringer påvirker skjebnen til organisk materiale i boreale innsjøer. Målet var å forstå hvordan den biogeokjemiske karbonsyklusen har blitt påvirket og vil bli påvirket av disse endringene. Avhandlingen består av tre separate artikler, hver fokusert på en bestemt del av denne syklusen: overføringen av oppløst organisk materiale fra land til vann, den heterotrofe respirasjonen av oppløst organisk materiale i vannet, og avgivelsen av karbondioksid fra overflatevann til atmosfæren.

Den første artikkelen utforsker sammenhengen mellom nedbørfeltsegenskaper og konsentrasjonen av totalt organisk karbon (TOC), som et mål på organisk materiale i innsjøer. Denne studien bygger på eksisterende kunnskap om faktorene som påvirker belastningen av oppløst organisk materiale og utvider bruken av et enkelt parameteroppsett for å forutsi TOC over hele Fennoskandia-regionen, til tross for betydelige variasjoner i arealbruk og klima. Analysen bruker data fra den Nordeuropeiske Innsjøundersøkelsen gjennomført i 1995 over Norge, Sverige og Finland. I tillegg forsøker studien å forutsi potensielle endringer i TOC-belastning for årene 2050 og 2100,

under to forskjellige sosioøkonomiske utviklingsbaner. Ved hjelp av en lignende modell gjennomførte vi også et "historisk" eksperiment der vi rekonstruerte konsentrasjonen av TOC fra 1900 til 2020. Forskningen fremhever den betydelige påvirkningen av arealbruk på TOC-belastningen, som moduleres av trender i overflateavrenning og avsetningen av svovel og nitrogen fra atmosfæren.

Den andre artikkelen skifter fokus til den heterotrofe nedbrytningen av oppløst organisk materiale (DOM) i innsjøer. Studien involverer prøvetaking av syttitre sørnorske innsjøer i 2019. Vi målte hastigheten til mikroorganismenes DOM-nedbrytning gjennom inkubasjonseksperimenter med tilsetning av næringsstoffer og regelmessige målinger av oksygenkonsentrasjon. Studien hadde som mål å avgjøre hvordan spesifikke egenskaper som molekylmasse, aromatisitet og elementsammensetning, påvirker DOMs "resistente" eller "labile" natur. Resultatene viser at mikroorganismer foretrekker å konsumere "labilt" DOM, som består av lettere, næringsrike molekyler. Interessant nok kan selv "resistent" DOM raskt nedbrytes når næringsstoffbegrensninger fjernes, noe som indikerer at DOM brukes til respirasjon i stedet for mikrobiell produksjon.

Den tredje artikkelen søker å estimere utslippet av CO_2 fra boreale innsjøer. Estimatet er basert på bruk av TOC som prediktor for partialtrykket av CO_2 (pCO_2) i vannet. Studien gjennomføres i to trinn. Først utforskes den beste metoden for å estimere pCO_2 i forhold til variasjonen i pH, alkalitet og TOC-konsentrasjoner i to treningsdatasett. Vi fant at TOC er den mest pålitelige prediktoren i begge tilfellene. Vi brukte denne lineære sammenhengen til å estimere pCO_2 i innsjøer fra den Nordeuropeiske Innsjøundersøkelsen. Deretter blir CO_2-avgivelsesraten og det totale utslippet fra innsjøer i Norge, Sverige og Finland beregnet. Resultatene bekreftet at innlandsfarvann i betydelig grad bidrar til utslipp av klimagasser og at dette bør tas med i nasjonale karbonbudsjetter.

Forskningen utført i denne avhandlingen understreker sammenhengen mellom nedbørsfeltområder, innsjøer, elver og det globale klimaet. Den følger reisen til organisk karbon fra jord til vann og tilbake til atmosfæren, og fremhever et intrikate kretsløp. Imidlertid innebærer kvantifisering av fremtidige endringer i denne syklusen utfordringer. Videre undersøkelser er nødvendige for å forbedre estimatene som er presentert her, samt å ta hensyn til metanproduksjon, sedimentering av organisk materiale og spesifikke prosesser som skjer i elver. Likevel argumenterer disse resultatene for nødvendigheten av å ta hensyn til innlandsfarvannenes bidrag til det globale karbonkretsløpet.

1. Introduction: Organic matter in lakes and the carbon cycle in Fennoscandia

The northernmost European regions encompass the boreal and arctic regions of Norway, Sweden, and Finland. These three countries are part of the Fennoscandia region, which also includes the Russian Kola peninsula and Karelia. The region is characterized by a bedrock consisting of igneous granite and gneiss and was entirely covered by ice during the last ice age. Today, the landscape is dominated by forests, mires, and lakes, with rocky archipelagos lining the coast. The climate, morphology, and land use differ from west to east and from north to south. The landscape along the west coast of Norway is marked by steep slopes and frequent rainfalls, whereas Finland is predominantly flat and covered by forested areas. The arctic regions are characterized by shrubs and permafrost, while agricultural activities are concentrated in the southern areas. Lakes are a distinctive marker of the region. Freshwater covers 5% of the Norwegian land surface, and almost 10 % in Sweden and Finland. Generally, lakes are larger in Sweden and Finland. In Sweden, the four largest lakes - Vänern (5 648 km^2), Vättern (1 912 km^2), Mälaren (1 140 km^2) and Hjälmaren (484 km^2) - cover 25% of the total inland water area in Sweden (Larson 2012). In Finland, the largest lakes are Saimaa (1 393 km^2), Päijänne (1 082 km^2), Inarijäarvi (1 082 km^2), Oulujärvi (912 km^2) and Pielinen (895 km^2), accounting for 15% of the country's surface water (Statistics Finland 2023). In contrast, Norway's largest lake, Mjøsa, covers 365 km^2, and only five other lakes surpass 100 km^2 (Figure 1).

Typically, boreal lakes exhibit a brownish hue due to the high concentration of DOM and associated iron in the water. In contrast, mountain and arctic lakes, surrounded by relatively barren catchment areas, tend to be more transparent. The pool of DOM comprises a diverse range of organic compounds originating from residues of dead organic matter or exudates of living biomass. The molecules of DOM are conventionally defined as being smaller than to 0.2-0.45 µm in size. This DOM constitutes a significant carbon reservoir within the boreal carbon cycle.

Over the past few decades, a widespread browning of water has been observed in the northern hemisphere, often attributed to the decrease of sulphur deposition. However, there are broader changes at play. As highlighted by Williamson et al. (2008), "lakes and streams are sentinels of environmental changes". This thesis aims to deconvolute the environmental factors driving this browning phenomenon and how the changes in these factors also affect the subsequent stages of the carbon cycle.

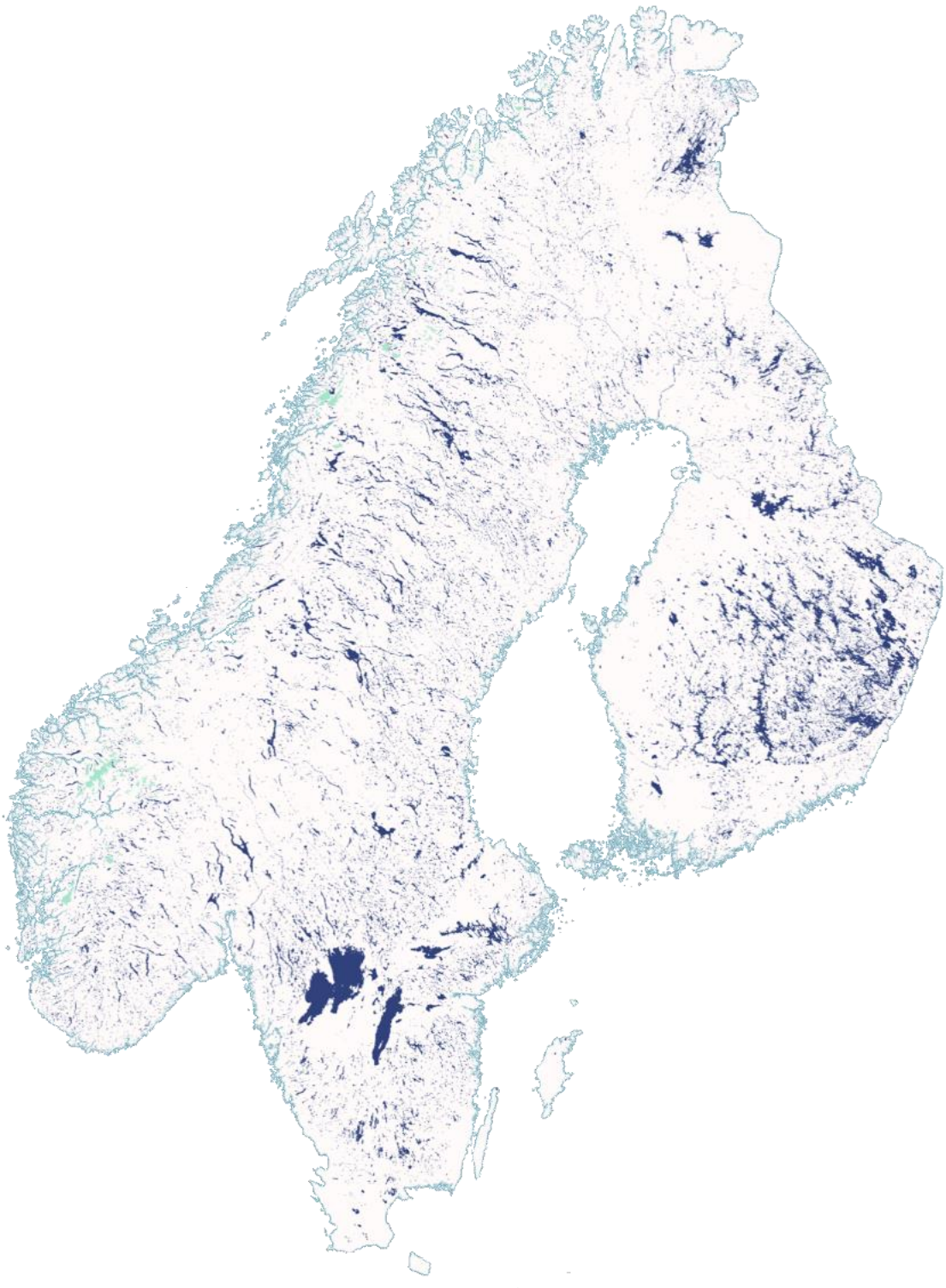

Figure 1 - Lakes and watercourses in Norway, Sweden, and Finland (CORINE Land Cover 2006). Dark blue represents inland waters; cyan blue represents glaciers and perpetual snow.

1.1. The pool of organic carbon in lakes: from the soils to the atmosphere

1.1.1. Lakes are the mirror of their catchment

In the boreal regions most of the organic matter in freshwater originates from the associated catchment (Wilkinson, Pace, and Cole 2013). Hence, the cycle of carbon in boreal freshwaters starts in the catchment soil. Forests, whether mixed or coniferous, dominate Norway, Sweden, and Finland's landscapes, although a considerable portion of Norway's land is mountainous and largely devoid of forest. Peatlands and mires are also widespread in all three countries, especially in Finland. Agricultural regions, on the other hand, are relatively modest in extension, with large fields concentrated mainly in the southern parts. Globally, boreal soils store a significant amount of carbon, with dry soils potentially storing up to 69,1 PgC and wet soils up to 356,7 PgC (Scharlemann et al. 2014).

The boreal forest

Boreal forests form a large biome with low diversity of fir, larch, pine, spruce, birch, alder, and poplar. Freezing temperature often persist for 6 to 8 months (Gauthier et al. 2015). Forested land account for 38% of Norway, 68% of Sweden, and 87% of Finland (SSB 2021; Statistics Sweden 2022; Statistics Finland 2023). Human activity significantly influences the expansion of the boreal forest, despite natural factors like fires, insect outbreaks and windstorms. In the Fennoscandian region, 90% of the forest areas are managed for the forest industry, which enhance biomass production but diminishes biodiversity and resilience.

Forests contribute to the organic soil pool through several mechanisms (Bolan et al. 2011). Rainwater falling on the leaves, branches, and trunks (throughfall and stemflow) carries organic molecules to the soil. Root exudation of sugars is another pathway. These sugars are intended for the associated mycorrhiza fungi that in exchange provide nutrients to the tree. Decomposition of tree litter, consisting in dead leaves and wood, is facilitated by microorganisms and fungi producing enzymes to break down complex organic molecules. Physical and chemical processes like fragmentation, erosion, and fire also contribute to the decomposition of soil organic matter (Cornwell et al. 2009) into DOM. Over time soil organic matter stabilizes through these processes, making it less available to microorganisms.

As a result, a significant amount of carbon in stored in the soil rather than in the biomass. For instance, in a forest in Ontario, Liu et al. (2002) estimated that 1.70 Pg C is stored in living biomass while 10.95 PgC is stored in the soil. The total carbon store in the boreal

forest, with a mean value of 1 041,5 Pg, surpasses that of tropical forests (Bradshaw and Warkentin 2015). This exceptional storage capacity is explained by several factors enhancing the stabilization of DOM such as the low nitrogen availability, organic matter chelation with Al and Fe, and the interaction with fungi that produce recalcitrant necromass residues (Adamczyk 2021).

Lands of mires

Peatlands cover 5.3% of Norway, 7.2% of Sweden (SSB 2021; Statistics Sweden 2022). In Finland, mires cover 29% of the territory, with some areas being forested (Sallinen et al. 2019). These peatlands rank among the world's largest carbon stores, second only to oceans (Barthelmes et al. 2015), due to permanently water-logged soils that impede the decomposition of organic matter (Bridgham et al. 2013). Forested peatlands in the Canadian Clay Belt region can accumulate 22.6 to 66.9 kgC/m^2, while standing tree biomass only accounts for 2.8 to 5.7 kgC/m^2 (Beaulne et al. 2021). The export of dissolved organic carbon (DOC), a proxy for DOM, from peatland to water bodies is estimated to average 13.7 gC/m^2/year by Rosset et al. (2022)

Agriculture and carbon storage

Agricultural soils also have some capacity to store carbon. The proportion of cultivated land is modest in the Nordic countries: 3.5% in Norway (SSB 2021), 6.26% in Sweden (Statistics Sweden 2022), and 7.5% in Finland (Natural Resources Institute Finland 2022). DOM in agricultural soils originates from plant residues, root exudates, and organic amendments (Bolan et al. 2011). These amendments, such as manure and sludges, acts as a fresh source of DOM and nutrients, having a "priming effect" that mobilizes recalcitrant organic compounds within the soil carbon pool. As a result, the organic matter in agricultural soils is less stabilized compared to forest and peatland soils.

Sources of inorganic carbon

In addition to organic carbon, soils are also involved in producing and storing inorganic carbon (TIC, total inorganic carbon). The TIC pool in boreal soil primarily originates from the complete mineralization of soils organic matter by soil microorganisms and fungi. Following mineralization, CO_2 is temporarily dissolved in water and trapped in soil pores and is subsequently transported by runoff to surface waters. In regions with carbonate-rich soils, some inorganic carbon can be imported by groundwater (Marcé et al. 2015; Guo et al. 2015). However, in boreal areas with limited alkalinity production and lower temperatures, CO_2 supersaturation is mostly driven by the mineralization of organic matter both in soils and in lakes (Allesson et al. 2022).

From the soils to the lakes

Both TOC and TIC are transported from the topsoil to the water bodies by runoff (Hagedorn et al. 2000). The mobilization of DOM has been shown to increase during heavy rainfalls (Håland 2017), with increased precipitation linked to increased transport of DOM from soils to lakes (Heleen A. De Wit et al. 2016).

Once within the aquatic system, DOM becomes a major carbon and nutrients source for aquatic microorganisms.

Figure 2- Land Cover from CORINE 2000 for Norway, Sweden, and Finland, used in Paper 1

1.1.2. Carbon pathways in the water column

During its residency in rivers and lakes, approximately 40% of the imported DOC is released from the water system as CO_2, while 50% continues its journey through the watercourse to the coastal areas. The remaining 10% becomes trapped in lakes sediments (J. J. Cole et al. 2007).

Imbalance between secondary and primary production

The substantial influx of organic matter from the catchment area provides resources for heterotrophic organisms, a process known as secondary production. Conversely, primary production increases the DOM pool in lakes by producing biomass via photosynthesis. High DOM concentration are suggested to hinder primary production by shading the light required for photosynthesis (Seekell et al. 2015). However, Bogard et al. (2020) demonstrated that both primary and secondary production depend less on light availability and more on nitrogen concentration. Additionally, primary production can prime secondary production by releasing labile DOM (Guenet et al. 2010). Generally, secondary production dominates over primary production in lakes with high DOM concentration, resulting in negative net ecosystem production.

Heterotrophic microorganisms feeding on DOM in the water include bacteria (Deshpande et al. 2016) and some groups of protists (Jones 2000). Some of these are mixotrophic organisms that can utilize both autotrophic and heterotrophic pathways. These microorganisms assimilate organic carbon and use it either for respiration, releasing energy and CO_2, or for their own biomass production. DOM imported from the catchment, having previously been exposed to bacteria and fungi, tends to be more recalcitrant than the DOM produced in situ (Shasha Liu et al. 2020). The most labile compounds is used first, causing the proportion of recalcitrant DOM to increases with water residence time (Soares et al. 2019).

The stratification of lakes influences autotrophic and heterotrophic metabolisms. During summer, a warmer epilimnion forms at the surface, while a colder layer remains at the bottom. In winter, the colder top layer with a temperature below 4 °C is less dense than the bottom layer. Most lakes are dimictic, which means that the layers mix twice a year. Some arctic lakes are monomictic, mixing only once due to temperature never exceeding 4 °C (Huttula 2012). Some shallow lakes never stratify. Stratified lakes experience limited exchange of gases and nutrients between the layers (Kankaala et al. 2013). In summer, the epilimnion is in equilibrium with the atmosphere, with favourable light conditions supporting both photosynthesis and heterotrophic metabolism. On the contrary, in lakes where the hypolimnion is anoxic, the production of methane is notable through anaerobic

respiration in the water column (Bastviken et al. 2004) and in the sediments (Clayer et al. 2020). As the allochthonous, aromatic DOM is hydrophobic, it is expelled from ice during the freezing of the lakes, increasing seasonally the relative concentration of recalcitrant DOM compared to labile COM (Zhou et al. 2023). This enhances the methane production and the carbon burial in sediments via flocculation of DOM.

Photo-mineralization, sedimentation, and export

Photo-mineralization involves ultraviolet light breaking down large organic matter molecules into smaller ones, rendering them more available to bacteria. According to Allesson et al. (2021), it accounts for only 3% of total direct CO_2 production, and is in that regard negligible compared to heterotrophic respiration.

Sedimentation constitutes a sink of organic carbon in lakes. Particulate carbon flocculates and settles at the lake's bottom, where it can be respired and reintroduced as CO_2 into the water column, significantly contributing to the inorganic carbon pool in the lakes (Weyhenmeyer et al. 2015). Von Wachenfeldt and Tranvik (2008) estimated an annual sedimentation rate of 55 +/- 44 gC/m^2/year, peaking in spring. The TOC concentration is generally a good predictor of sedimentation rates. Sedimentation rates have been increasing during the Holocene along with TOC concentration (Chmiel et al. 2015).

Organic carbon that is neither assimilated by microorganisms nor sedimented continues its journey through the watercourse to the sea. Cole et al. (2007) estimated that nearly half of the carbon entering the watercourse flows to the sea, while around 12% remains in the sediments, and the remaining 40% escapes to the atmosphere.

1.1.3. Carbon evasion to the atmosphere

Most boreal lakes are supersaturated with CO_2, having a partial pressure of CO_2 exceeding atmospheric levels. Therefore, these lakes emit CO_2 into the atmosphere. While carbon is accumulated at the catchment scale, lakes display remarkably high CO_2 evasion rates (Jonsson et al. 2007). Despite mounting evidence that their substantial contribution to global greenhouse gas emissions, they have not yet been accounted for in the overall global carbon budgets.

Contribution of lakes to global CO_2 emissions

Global emissions from lakes were initially estimated at 0.3 PgC/year by Raymond et al. (2013), with streams and rivers contributing 1.8 PgC/year. These numbers are likely underestimated, mainly because the database used by the authors underestimate the actual lake and reservoir surfaces. Based on estimates from Raymond et al. (2013), Hastie et al. (2018) calculated that the boreal forest would be responsible for emitting 79 TgC/year, a

figure that rose to 189 TgC/year when using their own database. Also using data from Raymond et al. (2013), Lindroth and Tranvik (2021) calculated that the Swedish rivers release 9.9 $MtCO_2$/year, while lakes and reservoirs emit 8.2 $MtCO_2$/year. Combined, these emissions offset nearly half of the forest sink in Sweden and may even cancel a higher proportion of it in some regions.

Technical challenges in accurately estimating pCO_2

Accurately gauging the partial pressure of CO_2 in freshwater presents technical difficulties. pCO_2 depends on carbonate equilibrium, hence on pH and on the concentration of dissolved inorganic carbon (DIC). DIC is the sum of all carbonate species: H_2CO_3 (or mainly dissolved CO_2), HCO_3^- and CO_3^{2-}. It is common to consider that the concentration of HCO_3 and CO_3^{2-} constitute a major part of the total alkalinity (TA) in a sample, and to use TA as a proxy for DIC. However, especially in the acid and soft boreal waters the total alkalinity is strongly constituted by the presence of organic acid anions and hydroxide bases (Shaoda Liu, Butman, and Raymond 2020). Several attempts have been made to quantify the organic alkalinity based on TOC and pH (Oliver 1983, Hruška et al. 2003; Liu et al. 2020). Other authors directly use the concentration of TOC to predict pCO_2 (Larsen, Andersen, and Hessen 2011; Raymond et al. 2013). This approach is justified by the high contribution of heterotrophic respiration to the supersaturation of CO_2, even though part of the inorganic carbon in lakes is stemming from groundwater influx (Allesson et al. 2022; Yang et al. 2015).

Methane evasion

DOM in lakes also serve as a substrate for methane production through anaerobic respiration and fermentation. Methane is produced in the anoxic, deep layers of the lakes, resulting in higher concentration of methane in these layers, whereas CO_2 is more evenly distributed throughout the water column (Huttunen et al. 2003). Methane production is also enhanced by the fermentation in the sediments (Bastviken et al. 2004). During wintertime, when the lake is covered with ice, the O_2 is depleted by heterotrophic respiration, leading to a higher production of methane. Upon ice melt, CO_2 emissions may constitute 20 to 30% of the annual emissions, with CH_4 emissions at ice melt accounting for 20 to 50%. Both CH_4 and CO_2 concentrations are closely linked to substantial DOM import from the catchment to the lakes (Valiente et al. 2022). Larger lakes tend to foster CH_4 production, while higher temperature increase CO_2 production.

Historically, atmospheric sulphur deposition and changing land use has considerably effected catchment-based biomass production, lake metabolism, and CO_2 evasion

processes over the past century. Presently, climate change accelerates the carbon cycle, while new challenges arise from changing land use patterns and nitrogen deposition.

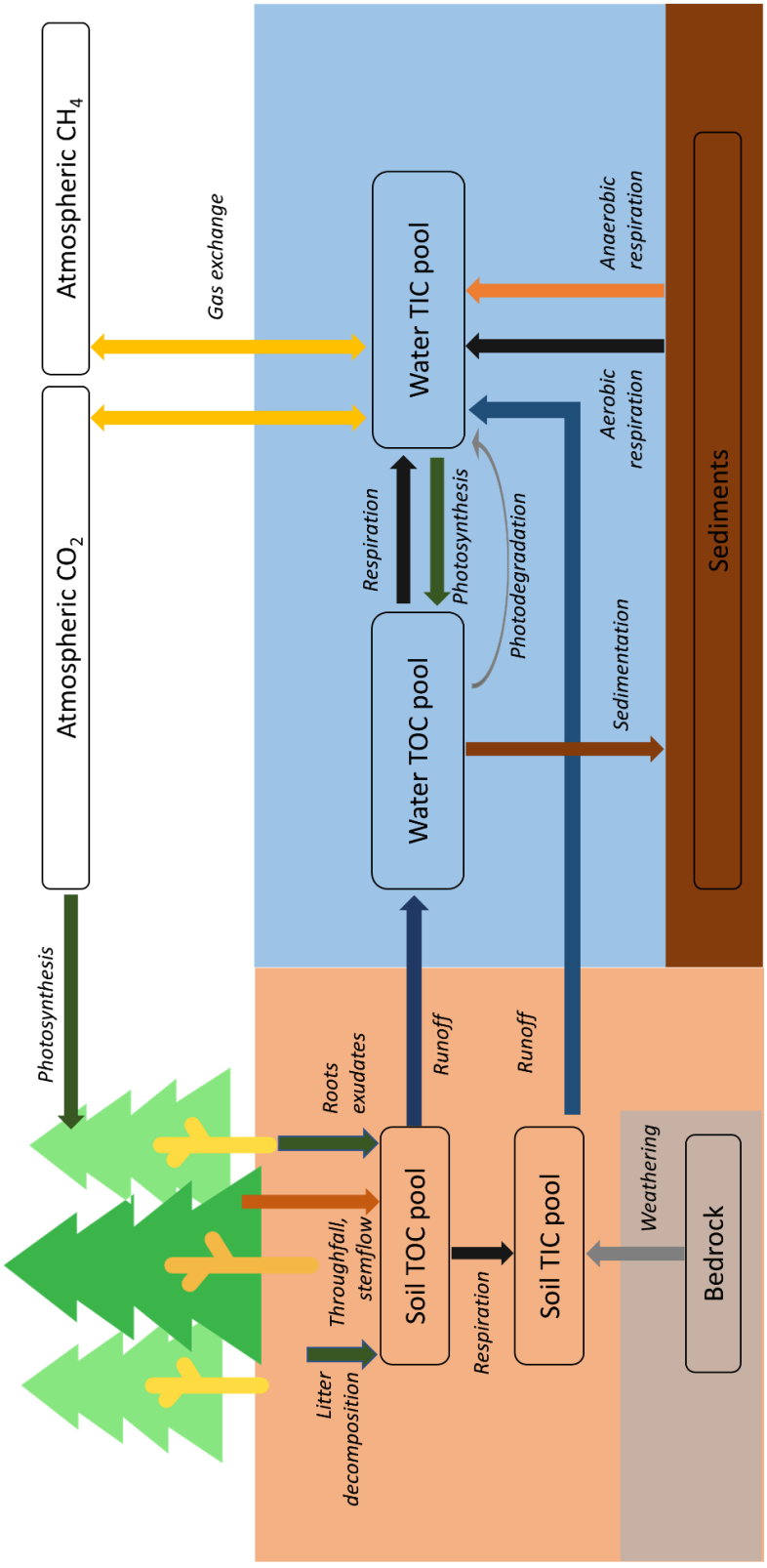

Figure 3 –Summary: Carbon pools and processes in a boreal lake and its catchment

1.2. Past, present, and future anthropogenic impacts on the carbon cycle

1.2.1. Land use changes

Two main trends in land use have been observed in the Nordics. On the one hand, substantial ditching and draining of the peatland have led to a reduction in the carbon store. On the over hand, the forest cover expanded over previously pastured land. Whether this afforestation resulted in changes in the soil carbon pool is unsure, but it contributed to an increased export of DOM to water bodies.

Expansion and intensification of forestry

Since 1850, land use changes, with a decreasing share of agriculture and the growth of timber industry, have resulted in an expansion of productive forest area in the Nordic region. In the Nordic countries, forestry holds significant economic importance, with governmental policies supporting afforestation and reforestation (Rolf D Vogt, De Wit, and Koponen 2022). Additionally, forest growth is considered as a substantial leverage for offsetting carbon emissions and reaching carbon neutrality. In Norway, incentives are therefore offered for the densification of planted areas and the afforestation of new forests (Futter et al. 2019). Similarly, Sweden's thriving timber industry constitutes a major economical resource, with wood products accounting for 23% of total exports (Royal Swedish Academy of Agriculture and Forestry 2015). This industry has seen a substantial growth, with standing biomass doubling over the past century (Näringsdepartementet 2018). The Federation of Swedish Forest Industries even published a report highlighting their crucial role in climate mitigation (Swedish Forest Industries 2019). Finland also greatly benefits from the wood industry, as 20% of its exported goods stem from this sector (Ministry of Agriculture and Forestry 2014). The forest legislation was updated in the 2010s to enhance competitiveness while maintaining its sustainability goals, with national subsidy schemes aiming to intensify the forestry sector.

Increased forest cover has contributed to the increase of DOM concentration in water bodies, raising concerns about surface water quality (Vogt et al. 2023; Finstad et al. 2016; Futter et al. 2019). Forestry practices exert direct impact on the organic matter pools in both soils and water. Activities like site preparation and clear-cutting temporarily increase the DOM export to watercourses, thereby reducing the carbon pool in soils stored during forest growth (Schelker et al. 2012).

Drainage of peatlands

Over the past century mires and peatlands have been subject to extensive drainage. This drainage leads to increased carbon and nutrient export from soils to watercourses,

depleting soil resources (Finér et al. 2021). The drained land has been repurposed for agriculture or forestry, and peat extraction for fuel has further contributed to this trend, especially during the World Wars. In Norway, drainage for agriculture started around 1750, followed by forestry drainage around 1860. The area of peatland drained for agriculture increased from 111 000 ha in 1921 to 150 000 ha in 1963. While around 13 000 ha of peatland was drained annually in the early 1960s, this decreased to 2 000 ha/year from 2000-2010. New drainage for forest production is now prohibited by law. In total, around 200 000 ha of peats have been drained for agriculture and 400 000 for forestry in Norway, representing 30% of the original mire area under the coniferous limit (Joosten et al. 2017, in Barthelmes et al. 2015). The area affected by ditches is even larger. In Sweden, a quarter of peatlands have been drained for conversion to arable land, mainly between 1850 and 1900, peaking between 1920 and 1950 (Barthelmes et al. 2015). In Finland, mires originally covered 5 million hectares, mainly located in the north. Including wooded mires, this number rises to 10.4 million hectares, with half of them drained to enhance forest production. Peatland agriculture boomed after World War II with a maximum use of 1.2 million hectares. Recent efforts focus on protecting peatlands, including monitoring and restoration initiatives (Barthelmes et al. 2015).

1.2.2. Impact of atmospheric deposition of Sulphur and Nitrogen

Acid rain deposition plays a pivotal role in the mobilisation and transport of DOM. Sulphur and nitrogen deposition, originating from long-range transport of pollutants, was first reported in Norway in 1880 and peaked during the 1980s. As a results, a decrease of pH was observed in numerous lakes across the Nordic region, as evidenced by surveys conducted in 1986 and 1995 (Henriksen et al. 1998). The acidification of soils and waters led to a decrease in pH, release of the trivalent cations (i.e., Al and Fe), and increased ionic strength of freshwater. Consequently, the humic charge and solubility of DOM decreased, resulting in lower concentrations of DOM in water (Heleen A. De Wit et al. 2007). After the enforcement of three sulphur protocols (UNECE 1985; 1992; and 1999), sulphur emission and deposition has decreased significantly. This reduction has led to a subsequent rise in the DOM concentration in rivers and lakes (Monteith et al. 2007, Finstad et al. 2016). Nitrogen emissions mainly come from the use of intrants for agriculture. Its deposition in the Nordic countries mirrors the same atmospheric patters as sulphur deposition but has contrasting effects on TOC. While it can have fertilizing effects on biomass production and respiration in the N-poor Scandinavian soils (Kortelainen et al. 2013), prolonged N enrichment may decrease microbial biomass and microbial respiration over time (Treseder 2008).

1.2.3. Impact of climate change

Increased temperature and changes in precipitation pattern will impact both primary production within catchments and the subsequent export to the watercourse, as well as secondary production in lakes. Positioned at high latitudes, the Nordic countries have already started to experience the effects of climate change.

Expected changes in temperature and precipitation patters

The average temperature in Norway has increased by 1 ºC between 1900 and 1941 (Hanssen-Bauer et al. 2017), particularly in spring and winter. The RCP8.5 scenario in the CMIP5 model ensemble, which represents a worst-case scenario, forecasts an temperature increase of 4.5 ºC in the annual average, coupled with an 18% increase in precipitation. Increased temperature lead to higher evapotranspiration, resulting in minor changes in the overall runoff. However, seasonal patterns will be modified, with runoff increasing in the winter and decreasing in summer. Moreover, Norway will encounter more frequent heavy rainfalls and flooding episodes. Lowlands area will have shorter snow cover, resulting in longer growing seasons. In the northern regions, permafrost will thaw, and sea-level increase is expected to range between 15 and 55 cm, depending on location along the coast. In Sweden, the average temperature is projected to increase by 3 to 6 ºC (Eklund et al. 2015). Precipitations will also increase, especially in the north. Conversely, water availability in the south will dwindle because of increased evapotranspiration. Like Norway, Sweden will experience intensified torrential rains. While the sea-level rise could reach 1 m, it is counterbalanced by the ongoing land rise. In Finland, the mean annual temperature has already increased by 2.3 ºC since 1850 and could rise up an additional 5.6 ºC by 2080 (Venäläinen et al. 2020). Precipitations will also increase, spanning from 6 to 18%, mainly during winter. The frequency of drought and forest fire will increase.

Impacts on biomass production & transport

Climate zones are moving northwards and upwards. Warmer temperature and longer growing season will enhance biomass and litter production (Gauthier et al. 2015), even though this will be countered by increased tree mortality stemming from droughts. The mortality among pine and spruce trees will increase, whereas birch trees might prosper (Venäläinen et al. 2020). Deciduous tree litter, being less recalcitrant than conifers litter (Kritzberg et al. 2020), will enhance the decomposition of the soil organic pool. This will diminish the pool of recalcitrant DOM, resulting in a larger share of labile DOM and TIC in carbon exports to lakes. Altered precipitation patterns with higher frequency of heavy

rainfall events will also transiently impact the export of TOC and TIC from top soils to watercourse (Hagedorn et al. 2000; Håland 2017).

Impacts on biomass mineralization

Increased temperature within boreal and arctic regions, along with the concurrent release of phosphate linked to temperature increase, are expected to accelerate soil biomass decomposition rates. The transformation of soil microbial composition might take several years, with a stronger response to nutrient availability than to temperature rise (Rinnan et al. 2007). However, warmer temperature increase the efficiency of C utilization by bacterial biomass (Curtin et al. 2012). Conversely, reduced snow cover might impede litter decomposition during winter by failing to act as an insulator preventing the soil to freeze (Wang et al. 2022).

In the water, the impacts of climate change are slightly different. Comparable to soil conditions, increased temperature might favour aerobic respiration within the surface layer, hence more CO_2 efflux. In addition, the increased browning and eutrophication could lead to longer and stronger lake stratification, resulting in prolonged anoxia conditions at the bottom of the lake, and hence to more production of CH_4 (Bartosiewicz et al. 2019).

2. Scope of this thesis

Knowledge gaps remain in each of the steps of the carbon journey through boreal lakes. By understanding better these intricate processes, the overarching aim of this dissertation is to predict the repercussions of climate change and other anthropogenic disturbances on the carbon cycle in boreal lakes.

Firstly, the relative contributions of the various drivers of TOC concentration in freshwater have not been assessed at a regional level. The impact of acid deposition has been estimated for Fennoscandia by Monteith et al.(2007). However, other studies integrating land-use or climate variables rather focus on local scales, i.e. Erlandsson et al. (2008) in Sweden, Kortelainen et al. (2006) and Palviainen et al.(2016) in Finland; and Larsen et al. (2011) and De Wit et al. (2007) in Norway.

Therefore, **Paper 1** focuses on impact of land use and climate characteristics of the catchment on the TOC loading in lakes at the Fennoscandian scale (defined as Norway, Sweden Finland). This study draws on data gathered from the Northern European Lakes Survey conducted in 1995, the last harmonized dataset available at that scale. This model aims at encompassing the entire gradient of Fennoscandian lakes under a unified

framework. The aim is to disentangle the respective impacts of land use, acidification, and precipitation patterns. Moreover, we used this model to forecast TOC concentration over the coming century, using two socio-economic pathways from the CMIP6 model ensemble: one outlining a scenario where climate change is restricted to 2 °C and in which the world becomes more (SSP1), and another portraying a world with potential global warming up to 5 °C, characterized by regional rivalry and limited focus on environmental challenges (SSP3). Supplementary work presented in **Appendix** relates to this paper, employing a similar model fitted to land cover, runoff, and atmospheric deposition to hindcast the concentration of organic carbon and its coastal exports over the last century.

In a second step, this dissertation focuses on heterotrophic respiration within boreal lakes. The controls over biodegradability of organic matter are still discussed (Coble et al. 2016; Rajakumar 2018; Shasha Liu et al. 2020). Most incubation experiments involved week-long measurements of biodegradable organic carbon (BDOC) over long periods of time (Vonk et al. 2015). While these experiments reflect naturally happening processes, they say little about the respiration process itself. **Paper 2** builds upon the results of the CBA lakes survey conducted in 2019 of 73 Norwegian lakes. The investigation involves measurements of respiration rates during short incubation experiments, based on optical measurements of oxygen consumption. These data are coupled with a plethora of chemical and physical characteristics of the sampled DOM, such as absorbance data and DOM composition. The experimental setup involves incubating samples at 25 °C with nutrient excess to investigate which DOM characteristics promote its respiration.

Finally, national estimations of CO_2 emissions from surface water are nowhere available, despite their significant contribution to the carbon balance. An attempt was made by Lindroth and Tranvik (2021) to compute CO_2 emissions from Swedish surface water, but the results are based on data from Raymond et al. (2013), that likely underestimates the CO_2 efflux by underestimating the share of surface waters. (Hastie et al. 2018) use a large database of pCO_2 values to estimate CO_2 emissions from boreal regions, but no Norwegian lakes are included in the original database. Hence, **Paper 3** assesses the carbon dioxide evasion from boreal lakes specifically for Norway, Sweden, and Finland. It also includes methodological considerations of the most suitable approach for estimating partial pressure of CO_2 in lakes, given that the alkalinity, often used as a proxy for DIC concentration, is influenced by the high concentration of organic matter. Drawing

on data from two sources - the CBA lakes survey and the N112 survey (Larsen, Andersen, and Hessen 2011) - the study confirms that TOC is the best predictor for CO_2, which can be used directly to estimate CO_2 evasion from lakes. We then compare the evasion rates in the different surveys and compute the CO_2 efflux from inland waters in 1995 based on the Northern European Lakes Survey data.

3. Material and Methods

3.1. Datasets and surveys

Paper 1 and the results presented in the Appendix are based on the TOC data from the Northern European Lakes Survey (NELS) conducted in 1995 (Henriksen et al. 1998). These data, sources from the NOFA database (Finstad 2017), encompasses the TOC concentration in mg/L for a total of 4 160 lakes. In this survey, lakes were sampled either manually or by helicopter after the autumn turnover (Henriksen et al. 1996), in order to obtain samples representative of the entire lake. In addition, the NOFA database contained the catchment polygons determined by a digital elevation model for all lakes in Norway, Sweden, and Finland. The sampling points of the NELS were matched to the corresponding catchment in SQL. In addition, the database contained polygons outlining coastal drainage basins in the three countries, encompassing the catchment areas of watercourses that drains into the sea within specific coastal sections (NVE 2022). These coastal drainage basins served as the foundation for predicting past and future TOC concentrations. Their utility rested on their ability to cover the entire territory while being less in number than individual lakes, thereby reducing computational demands. Moreover, they facilitated direct computation of TOC export from inland waters to the coast. After removing artificially small basins, as well as basins with missing data, a total of 1 392 polygons were retained for Paper 1, and 1 440 for the Appendix.

Climate and land-use data were acquired from various sources, summarised in Table 1 The Northern Lakes Survey data was complemented by satellite data and earth model products. The Net Differential Vegetation Index (NDVI) from GIMMS (The National Center for Atmospheric Research 2018) served as proxies for biomass. Present land use data was acquired from CORINE Land Cover for year 2000 (Figure 2), the first year that includes Norway, issued by Copernicus Land Monitoring Service (Copernicus Land Monitoring Service n.d.). Past land use data was acquired from the HILDA database (Winkler et al. 2021). Precipitation and temperature data was acquired from downscaled CMIP6 model products (World Climate Resarch Program n.d.), while future surface runoff was downloaded from CORDEX (CORDEX 2021) and past surface runoff from historical models of NorESM for CMIP6(Seland et al. 2020). Historical model product were used to fit the models on the data from 1995, and projections were based on the SSP 1-2.6 scenario (maintaining warming around 2 °C) and the SSP 3-7.0 (where warming will average 5°C). Sulphur and nitrogen deposition for the last decades were extracted from EMEP model products (EMEP 2022), while historical deposition data was obtained

from a NorESM model product (Bentsen et al. 2013), used in the Appendix. Additionally, the dataset of the Norwegian Lakes Survey of 2019 was graciously provided by NIVA and served as a test dataset for the spatial error model of TOC concentration in lakes in Paper 1.

Paper 3 uses the concentration of TOC, DOC, and alkalinity, along with pH measured during the CBA lakes survey (see following section) to model the partial pressure of CO_2 in lakes. An additional dataset of 104 lakes sampled in 2004 and published in Larsen et al. (2011) was incorporated into the training dataset. It contained TOC, pH, alkalinity, temperature, DIC and lake area. The resulting model performance was evaluated using data from the Northern European Lakes Survey, from which we used TOC, pH, alkalinity, water temperature, and lake area. In the three studies, pH was measured separately from alkalinity, with combination electrodes.

To estimate CO_2 evasion from lakes, the pCO_2 along with wind speed data were required to calculate the gas transfer coefficient. Wind speed was downloaded from Copernicus Land Services (Boogaard et al. 2020).

Table 1 - Sources of data for paper 1, 3 and Appendix

Parameter	*Dataset*	*Paper 1*	*Appendix*	*Paper 3*
TOC	Training	Northern European Lakes Survey (Henriksen et al. 1998)	Northern European Lakes Survey (Henriksen et al. 1998)	N112 dataset (Larsen, Andersen, and Hessen 2011) CBA Sampling Campaign (Crapart and Parra 2019)
	Test	NIVA 1000 lakes survey (Helene A. De Wit et al. 2023)	SLU historical measurements (as chemical oxygen demand) (Eriksson 1929; SLU 2020)	Northern European Lakes Survey (Henriksen et al. 1998)
Catchment & Lakes polygons		NOFA database (Finstad 2017)	NOFA database (Finstad 2017)	NOFA database (Finstad 2017)
Alkalinity, pH, water temperature	Training			N112 dataset (Larsen, Andersen, and Hessen 2011) CBA sampling campaign (Crapart and Parra 2019)
	Test			Northern European Lakes Survey (Henriksen et al. 1998)

Parameter	*Dataset*	*Paper 1*	*Appendix*	*Paper 3*
Land cover		CORINE Land Cover (Copernicus Land Monitoring Service n.d.)	HILDA database ("The HILDA+ Project – Land Change Stories" n.d.)	
Precipitation, surface temperature		1970-2000: Worldclim (WorldClim n.d.) Future data: Worldclim downscaling of CMIP6		
Surface runoff		CORDEX (CNRM) (Voldoire et al. 2019)	Historical surface runoff from NorESM (Seland et al. 2020)	
NDVI		GIMMS (The National Center for Atmospheric Research 2018)		
Nitrogen and Sulphur deposition		EMEP (EMEP 2022)	NorESM1 for CMIP5 (1850-2015) (Bentsen et al. 2013) EMEP (1990-2002) (EMEP 2022)	
Wind speed				Copernicus (Hassell et al. 2017)

3.2. Experimental analysis

Paper 2 is based on data acquired during a lake survey conducted by the Centre of Biogeochemistry in the Anthropocene in autumn 2019, encompassing 73 lakes in southern Norway (Crapart and Parra 2019). The lakes were selected to match a national survey conducted by NIVA, aiming at repeating the sampling undertaken in 1995 (Helene A. De Wit et al. 2023). They were chosen to represent a wide range of characteristics, from agricultural regions in South-east Norway, to mountain lakes at the North-west of Oslo. The 73 lakes were sampled and analysed for a range of chemical and biological parameters. We used the concentration of DOC, dissolved nitrogen, phosphate and iron, and absorbance data such as specific ultraviolet absorbance (sUVa), and the quantification of bacterial population in each sample.

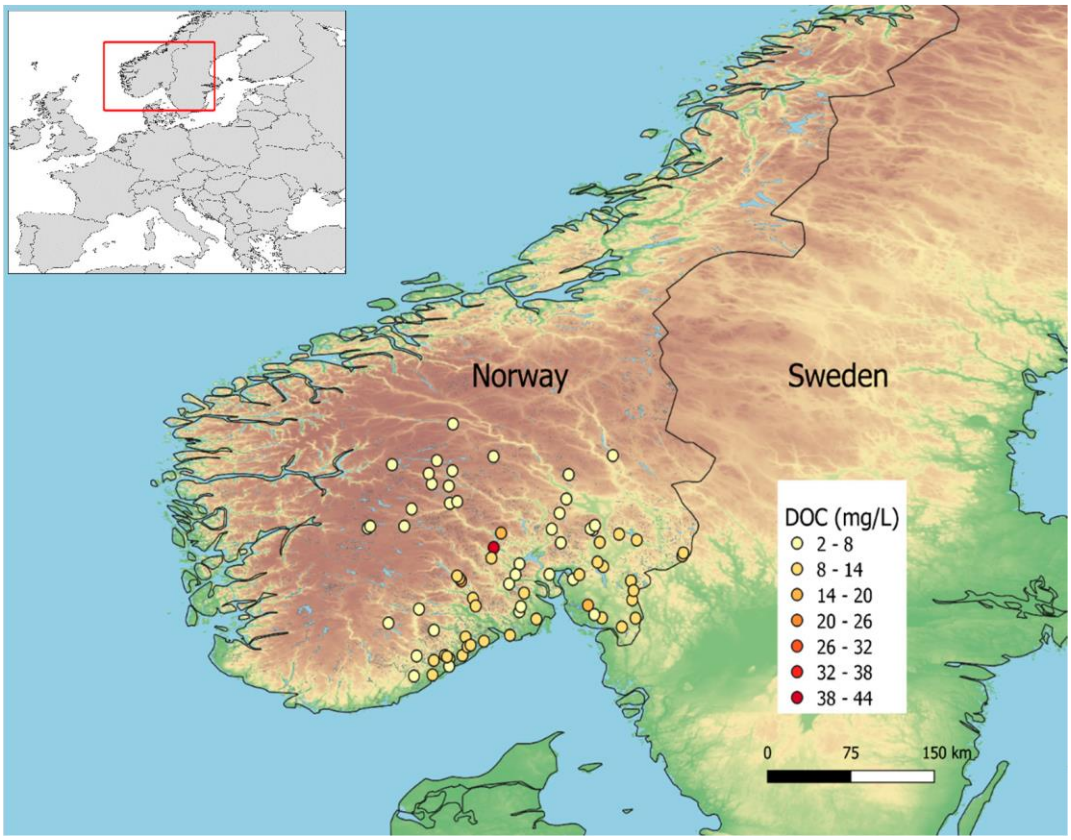

Figure 4 - Map of the 73 lakes sampled during the CBA lake survey and their Dissolved Organic Carbon Concentration in mg/L

An incubation experiment was used to measure the respiration rate of DOM, measured as the oxygen consumption rate per minute. This incubation was conducted using vials equipped with Presens© optical sensors, which employ fluorescence decay to measure the oxygen concentration. Water samples collected from the lakes were filtered through 0.22 µm filters and were stored at 4°C. Before incubation, the samples were inoculated

with bacteria sourced from Lake Langtjern, and nutrients (i.e., nitrate, phosphate) were added. Four replicates were prepared for each lake. The vials containing the inoculated samples were sealed to avoid any exchange with ambient air and were subsequently placed in an incubator set to maintain a temperature of 25°C. The incubation process spanned a duration of 30h.

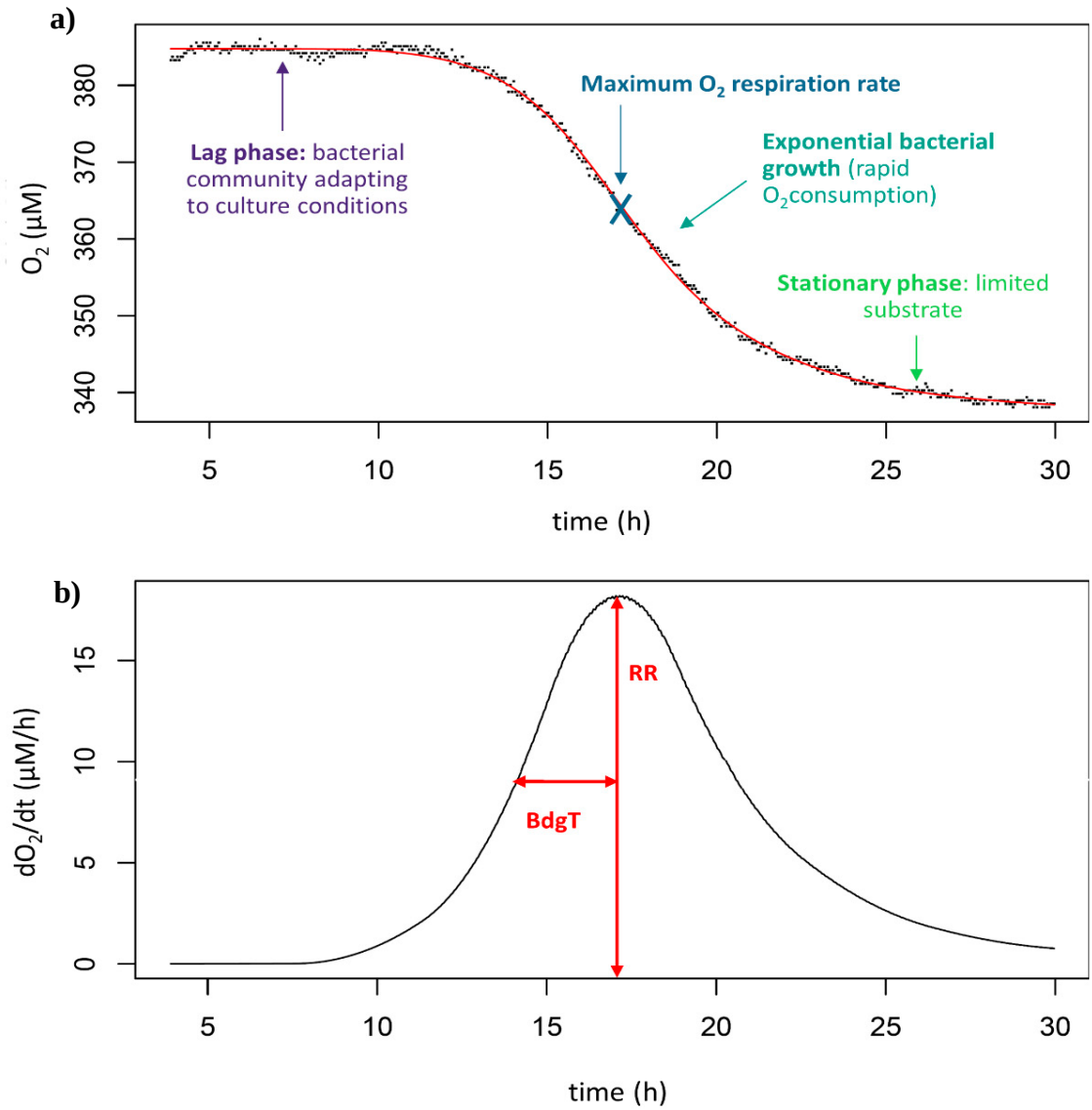

Figure 5 - Typical oxygen consumption curve observed during the incubation experiment, and method for estimating the respiration rate (RR) and the biodegradation period (BdgT). The normalized respiration rate, RRn, corresponds to RR divided by the concentration in dissolved organic carbon.

A typical oxygen curve measured during the incubation experiment is illustrated in Figure 5. This curve demonstrates distinct phases: an initial prolonged plateau where oxygen concentration remains relatively stable, corresponding to the microbial community's acclimation to its new environment. Subsequently, a decrease of oxygen concentration is

observed, corresponding to a rapid growth of the microbial community. Finally, the curve reaches a second plateau at a lower oxygen concentration, signifying the gradual demise of the microbial community. We obtained a curve of oxygen concentration depending on time, from which we calculated the derivative to obtain the speed of oxygen consumption in µM/min. The respiration rate, RR, was defined as the maximum oxygen consumption speed. We used the median respiration rate of each set of replicates to obtain the final value. In a similar fashion, we computed the duration of the growth phase for each sample, termed the "biodegradation period" (BdgT). The full protocol for this experiment is described online ("Biodegradability of DNOM" n.d.).

3.3. Statistical analysis

All the statistical analysis were conducted using the R software (R Core Team 2023).

Geographical data was analysed within the R environment. Runoff, temperature, wind speed and atmospheric deposition raster files were acquired from the sources cited above. The average value for each of the catchment polygon was computed with the "extract" function combined with the "mean" function from the raster package (Hijmans et al. 2018).

Multiple linear models were used to fit the TOC concentration in lakes based on catchment parameters. The "lm" function from the "stats" package, included in the core version of R, was used for this purpose. A Spatial Error Linear Model (SELM), which considers spatial autocorrelation in the error term, was also tested using the "spatialreg" package (Bivand 2019). These two methods were used in Paper 1 and in Appendix.

Generalized linear models (GLMs) were used to model pCO_2 and DIC based on pH, alkalinity, and TOC in Paper 3. They allow the use of Gamma distribution, which is adapted to the distribution of pCO_2 and DIC. The "glm" function from the core "stats" package in R was employed for this purpose.

A lasso regression was used in Paper 2 to help select the relevant variables that best explain the variation in the respiration rate. Lasso regression penalizes some of the predicting variables so that their coefficient is equal to zero when they lack sufficient significance (James et al. 2013). Subsequently, the selected variables were then used to fit a multiple linear model.

4. Main findings & Discussion

4.1 Drivers of TOC load in freshwater – Paper 1 & Appendix

4.1.1. Forecast of TOC in the future

In Paper 1, we modelled the effect size of a change in the main predictors of TOC. This was based on a dataset gathered from more than 4 000 lakes in 1995. We used these data to predict the average TOC concentration in Norway, Sweden, and Finland in 2050 and 2100. These forecasts were based on two socio-economic pathways as described in the last IPCC report (Masson-Delmotte et al. 2021).

It has been shown that most of the TOC in boreal lakes originates from the catchment (Tranvik et al. 2009). The model was therefore fitted using catchment characteristics rather than lake characteristics. The proportion of bogs and arable land were included as predictors. NDVI was used as a proxy for forest. It proved to be more correlated to TOC than the proportion of forest land use, probably because it reflects the overall "greenness" in the catchment, and not only the part of it that is categorized as forest (more than 10% canopy cover). The model included surface runoff, the main pathway for TOC transportation, along with acid deposition, as it is proven to have a negative impact on TOC. In this context, nitrogen deposition was chosen instead of sulphur deposition. Both are nevertheless highly correlated because they are predicted by the same atmospheric model. The level of atmospheric sulphur deposition has substantially decreased since the 90s though remains now stable. In contrast, nitrogen deposition, that mainly depends on the use of agricultural fertilizers, will continue to change in the coming century.

We formulated and fitted both a multiple linear model and a spatial error linear model using these five predictors. A spatial error model is similar to a multiple linear model but accommodates the spatial autocorrelation of the predictors within the error component. For both models, we used the formula:

$$\begin{aligned}\log(TOC) \sim \alpha + \beta_1 \times NDVI + \beta_2 \times \log(Surface\ Runoff) \\ + \beta_3 \times Proportion\ of\ bogs + \beta_4 \times Proportion\ of\ arable\ land \\ + \beta_5 \times Total\ Nitrogen\ Deposition\end{aligned}$$

To describe better the impact wielded by each predictor, we converted each estimate (β) into an effect size. This effect size delineates the percentage change of TOC concentration given a 1% change in the predicting parameter. This corresponds to a0.01 change in bog cover, arable cover, and NDVI (ranging from 0 and 1), as well as a 1% increment in TNdep and Runoff. In Figure 6, we compare the results of the impact of each predictor,

showcasing the findings of both the linear model (LM) and in the Spatial Linear Error Model (SELM). For example, a 1% change in NDVI would result in a 3.3% increase in TOC compared to the original concentration. The results were similar, yet with higher values for the linear model. We attribute this effect to the strong spatial autocorrelation within the predictor variables.

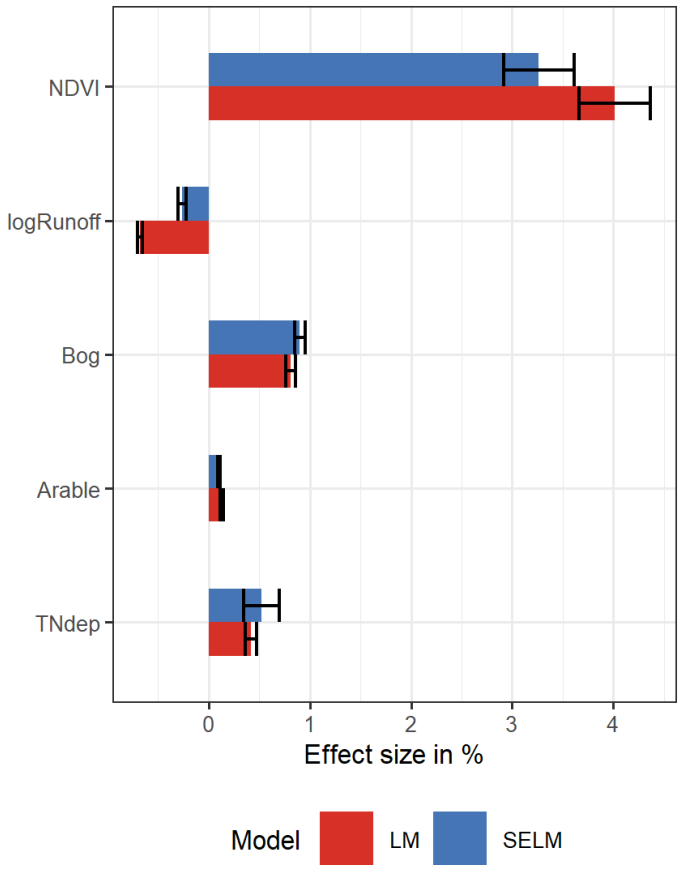

Figure 6 – Effect size of the 5 predictors of TOC concentration in the Linear Model and the Spatial Error Linear Model

Our model shows that changes in the catchment vegetation, as shown by NDVI, had the strongest impact on TOC concentration in lakes. This highlights the intrinsic link between DOM production within the catchment and the ensuing export of TOC. As anticipated, the proportion of bogs also plays an important role, while the proportion of arable land on TOC export was comparatively modest. Remarkably, TNdep had a positive effect in both models. In contrast to sulphur deposition's negative impact on TOC concentration, the fertilizer effect of TNdep had a more significant influence than its role as an acidifier. Despite being the predominant predictor of DOM mobilization, Runoff has a counterintuitive negative effect on TOC concentration. This counteraction was attributed to a dilution effect: increased runoff, related to more precipitation, results in increased

volume of water and hence inducing a diluted concentration, even when the total amount of transported DOM increases.

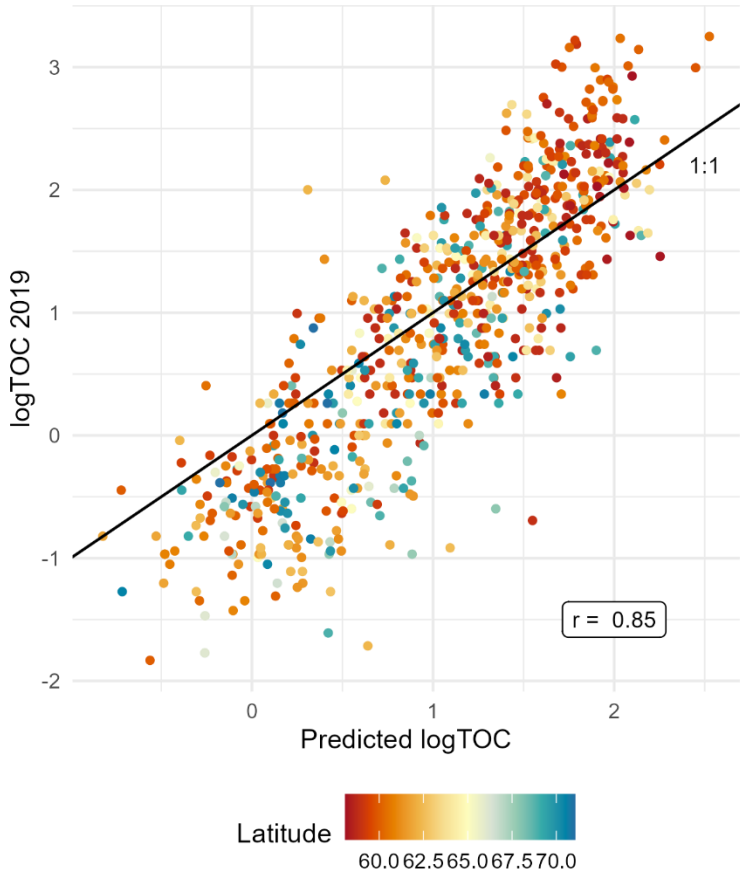

Figure 7 - Observed vs predicted log(TOC) concentration in the ThousandLakes

This model was validated against the ThousandLakes data, provided by NIVA (Helene A. De Wit et al. 2023). Figure 7 shows the correlation between observed and predicted values.

To anticipate the trajectory of TOC concentration in the future, the future evolution of each of the predictors was estimated by various approaches. As no model for NDVI exists, we resorted to predicting its future values based on temperature and precipitation forecast derived from CMIP6 model products. However, this approach has its limitations as it does not consider possible land use changes, such as afforestation or development of agricultural areas. Without any concrete data about these possible changes, the proportion of bogs and arable land were retained at their 2000 levels. The predicted surface runoff was also extracted from a CMIP6 model product. The forecasted evolution of TNdep was assumed to decline under SSP 1-2.6, and rise under SSP 3-7.0, based on the emissions prediction described in the last IPCC report (Masson-Delmotte et al. 2021). These

assumptions entail a degree of uncertainty that is difficult to quantify. The forecasts must therefore be interpreted with caution.

This forecast (Figure 8) shows that the browning trends observed in the last decade is likely to persist, particularly in the regions that have already experienced pronounced browning in the past decade. These regions encompass the southern part of Fennoscandia, where temperature increase is expected to have a positive impact on biomass production, nitrogen deposition exerts a significant impact, and runoff is projected to decrease. In contrast, in mountains and western coastal regions, the dilution by increase in runoff offsets the potential effect of biomass increase. In the northern territories, the proliferation of vegetation growth within the catchment due to a warmer climate is anticipated to increase browning trends. While the trends are consistent across both scenarios, they are a lot more extreme in the SSP 3-7.0.

The forecasted outlook is accompanied by several sources of uncertainty. These include the evolution of forest composition, as well as of forestry choices, which can impact both the biomass production and the organic matter decomposition in the soils. In addition, the long-term effects of nitrogen deposition remain relatively enigmatic. Finally, further work would be necessary to gauge the uncertainty inherent in our forecast and to suggest more precise estimates of changes in TOC concentration.

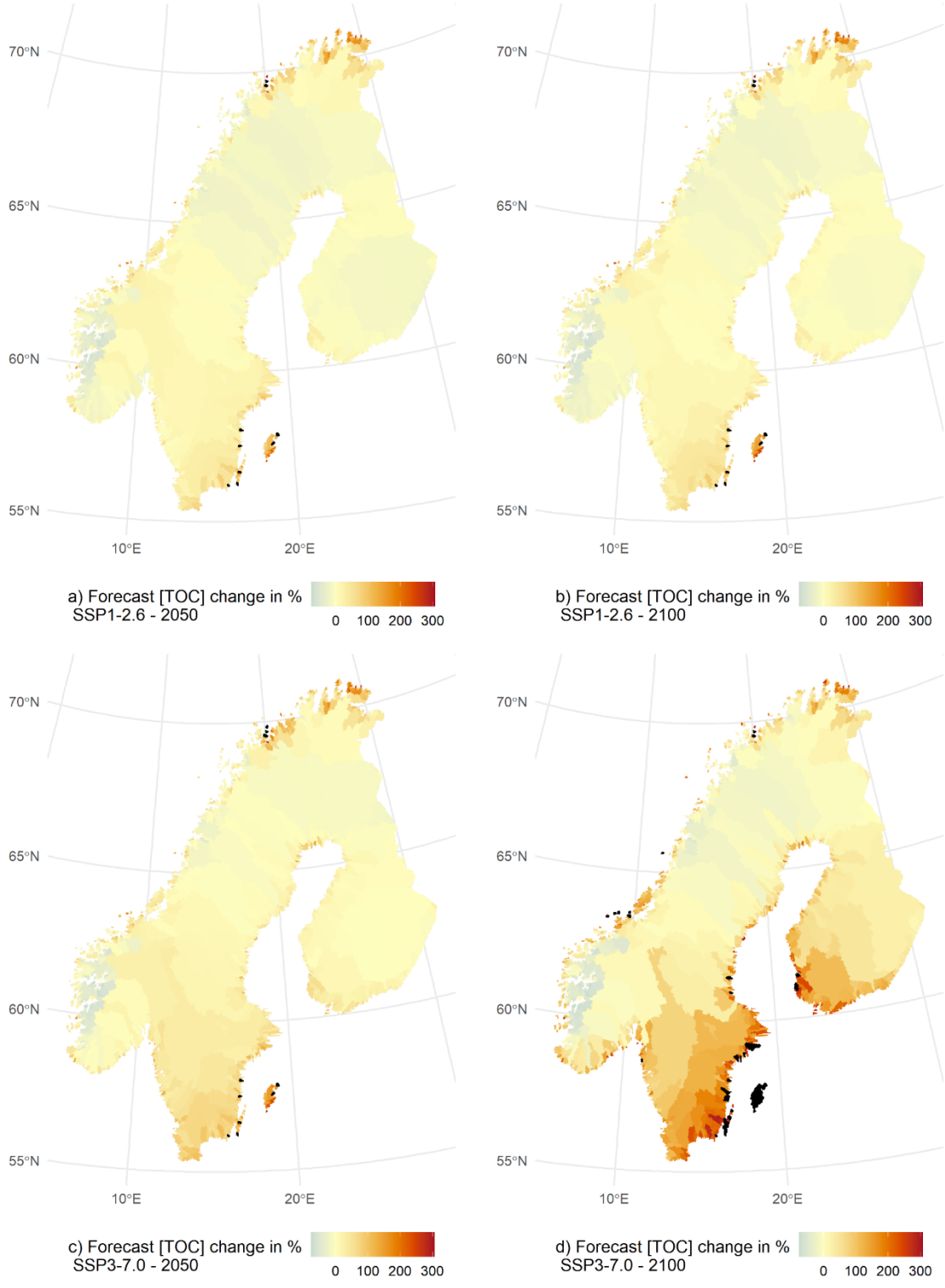

Figure 8 - Forecast of TOC concentration in coastal drainage basins in 2050 and 2100, under SSP 1-2.6 and SSP 3-7.0

4.1.2. Hindcast of TOC concentration

This prognostic endeavour was not confined to future projections alone; it was extended to the past through the implementation of a slightly different model. The global land cover in the last century was reconstructed by Winkler et al. (2021) and grouped in the HILDA database, while historical models of runoff and atmospheric deposition are available in the CMIP5 and CMIP6 model ensembles. Given that sulphur deposition predominantly drove acid rain in the past century, the hindcast used total sulphur deposition instead of TNdep. Additionally, to avoid having to reconstruct NDVI in the past the proportion of forest land use was retained as a predictor.

The land cover categories encapsulated in HILDA are less precise compared to those in the Corine Land Cover dataset. While it accounts for forest cover and arable land, peatlands lack their own category. Shrubland and grassland are however included and were grouped into the same category. Using forest, shrubland and arable land from HILDA yielded similar results as using forest, bogs, and arable land from CORINE. Therefore, the new model is fitted as:

$$\begin{aligned}\log(TOC) \sim \alpha + \beta_1 \times Proportion\ of\ forest + \beta_2 \times Proportion\ of\ shurbland \\ + \beta_3 \times Proportion\ of\ arable\ land + \beta_4 \times \log(Surface\ Runoff) \\ + \beta_5 \times \log(Total\ sulfur\ Deposition)\end{aligned}$$

Similarly, the model was fitted on the 1995 dataset with 4 160 lakes. Subsequently, it was hindcasted on 1 440 coastal drainage basins. We grouped the results by the sea into which the coastal drainage basins is draining: Baltic Sea, North Sea, or Norwegian Coastal Current. The outcomes are shown in Figure 9.

To bolster the credibility of our results, we compared them with actual measurements conducted in Swedish rivers. Data from the beginning of the 19th century, published by Eriksson (1929), was compiled with data from SLU dating back to 1950 (SLU 2020). By averaging the available measurements for each coastal drainage basin, we were able to compare actual values with the predicted average TOC concentrations. While our hindcast aligned with the trend observed in measured TOC concentration, it commonly had slightly lower values. This divergence can be partly ascribed to the distinction between river measurements and lake predictions. Since both the water residence time and the direct contribution of precipitation to the water volume are higher in lakes, TOC concentration in lakes tend to be lower than in rivers. This is particular the case for the largest lakes.

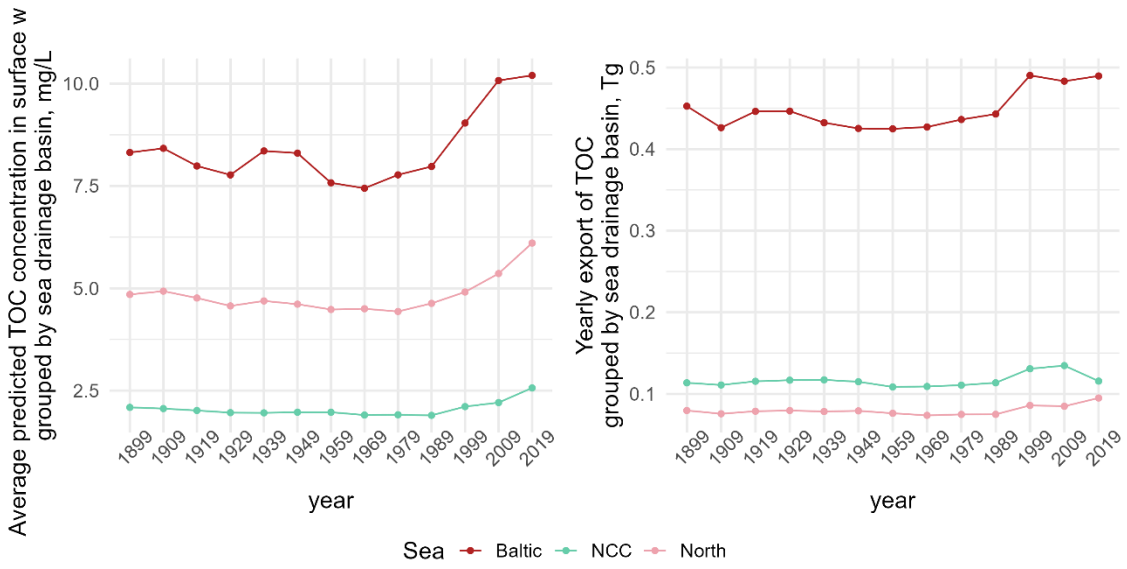

Figure 9 - Predicted TOC concentration by decade since 1899 in mg/L, and predicted export to coastal waters in Tg; gathered by sea: Baltic Sea, North Sea, and Norwegian Coastal Current

The good match between the empirical measurements and the hindcast show the capacity of the combined explanatory factors – namely sulphur deposition, changes in land cover, and changes in runoff – to effectively explain the main fluctuations and trends in TOC concentration since 1900. Notably, TOC concentrations are today higher than they were in the beginning of the last century, after a drop due to the negative impact of sulphur deposition. This resurgence in recent decades is plausibly mainly attributed to the "greening" effect of increased afforestation.

The computed export of TOC to coastal water (Figure 9) was accomplished through a simple multiplication of the TOC concentration, the specific surface runoff, and the costal drainage basin area. However, this approach disregards the many processes that contribute to the removal of TOC from the water column during its journey through the watercourse. The most significant of these processes is studied in Paper 2: the mineralization of DOM via heterotrophic respiration.

4.2. Heterotrophic respiration in boreal lakes – Paper 2

The substantial influx of organic matter into lakes favours secondary production in comparison to primary production in boreal lakes. Heterotrophic microorganisms use organic carbon as a source of energy through respiration, a process that releases carbon dioxide. The bioavailability of DOM for the bacterial community in lakes is determined by its lability, with microorganisms preferring low-molecular weight aliphatic compounds. Most of the organic matter in lakes is allochthonous, originating from forests and mires in the catchments, and has already undergone degradation in the soil. Therefore, most of the DOM in lakes is constituted of complex high-molecular-weight molecules that are less accessible to microorganisms, rendering them "recalcitrant".

The aim of this study was to investigate which of the characteristics of the organic matter, such as its mass, absorbance, elemental composition, alongside lakes characteristics such as pH, conductivity, base cations concentration etc., exert influence on heterotrophic respiration. To assess the respiration rate of heterotrophic microorganisms, an incubation method based on monitoring oxygen concentration with optical sensors was applied. Typical oxygen curves are shown in Figure 5 (Material and Methods). The respiration rate (RR) was defined as the maximum speed at which the microbial community consumed oxygen. The duration of the exponential growth of the bacterial community was computed and is referred to as Biodegradation period (BdgT). Since the respiration rate is likely to be affected by the amount of available organic matter, the normalized respiration rate (RRn), i.e., the respiration rate divided by the concentration of dissolved organic carbon in the sample, was studied independently. RR, RRn and BdgT were then correlated with DOM and lake characteristics, and multiple linear models were then fitted on selected predictors (Figure 10).

We found that parameters linked to aromaticity and molecular weight (sUVa, SARuv, Fe) exerted a negative impact on RR, RRn and BdgT. This implies that DOM characterized by lower molecular weight and less aromaticity was respired faster compared to high molecular weight and aromatic DOM. This corresponds to the common definition of "labile" and "recalcitrant" DOM. Conversely, in samples originally deficient in nutrients, RR was higher than in samples with originally rich content of nutrients. This can be attributed to a priming effect due to the addition of nutrients in the incubation experiment. The barrier between "labile" and "recalcitrant" is therefore not strict as it varies depending on available nutrients. The underlying processes might, however, differ. While low molecular weight (LMW) DOM serves both bacterial respiration (metabolism) and bacterial production (anabolism), high molecular weight (HMW) DOM seems to favour

respiration over production. This is illustrated by the positive relationship between RR and the C:N ratio. This has been suggested as a microbial pathway to utilize excess carbon, consequently making DOM more amendable for other uses. Therefore, alleviating nutrient limitation in lakes characterized by HMW DOM would result in the use of a greater proportion of the DOM by the microbial community, although primarily for mineralization through respiration, rather than biomass production.

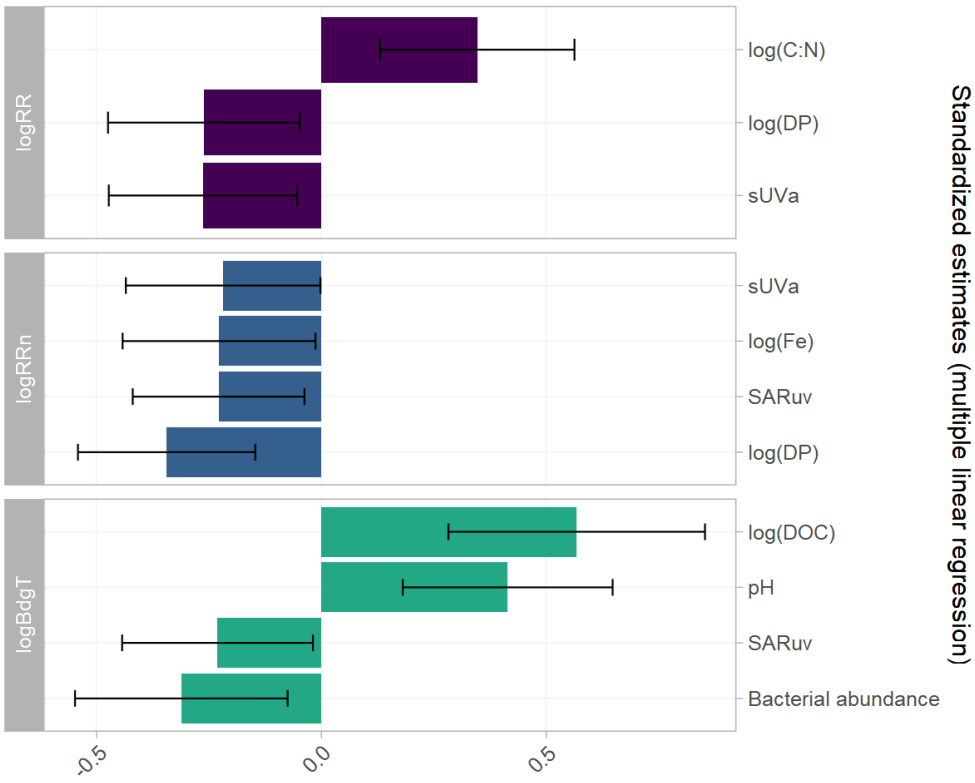

Figure 10 - Multiple linear regression with selected predictors for RR (respiration rate), RRn (normalized respiration rate), and BdgT (biodegradation period).

RR and RRn also display a negative relationship with nutrients (DP, C:N ratio), while the biodegradation was sustained longer (high BdgT) for samples with high pH and low bacterial abundance, which are associated to more eutrophic lakes with a higher share of photosynthesis.

Most DOM in boreal lakes is allochthonous originating from conifer forests and peatland. These sources are recognized for generating HMW, aromatic DOM. This makes heterotrophic respiration a major process for transforming DOM with high mineralization rate. This contributes to explaining the strong relationship between the concentration of TOC and the partial pressure of CO_2, which is investigated in Paper 3.

4.3. TOC driving CO_2 evasion in boreal lakes – Paper 3

Greenhouse gas emissions from inland waters are rarely accounted for in national carbon budgets, and do not have their own category in the guidelines for Land Use – Land Use Change and Forestry (LULUCF). In this paper, we aimed at estimating the partial pressure of CO_2 in boreal lakes using sampling surveys conducted in Norway in 2004 and 2019: the survey conducted in 2004 by Larsen et al (2011), referred to as N112 survey), and the survey conducted by the CBA in 2019 (Crapart and Parra 2019). The data from the NELS, which encompasses Norway, Sweden, and Finland, is used to extend the results to Fennoscandia. In addition, the study seeks to estimate the CO_2 evasion from inland waters in these three countries.

The partial pressure of CO_2 is commonly calculated using the total alkalinity (TA) as a proxy for DIC: i.e., TA = HCO_3^- + 2 x CO_3^{2-}. However, this approach disregards the fact that alkalinity in boreal waters is strongly impacted by the presence of weak organic acid anions and hydroxy bases, which contribute to the alkalinity. In addition, at pH < 5.4, most of the dissolved inorganic carbon is converted in CO_2 (Guo et al. 2015). The remaining alkalinity must stem from other sources, rendering the use of alkalinity as a proxy for DIC invalid under this pH threshold.

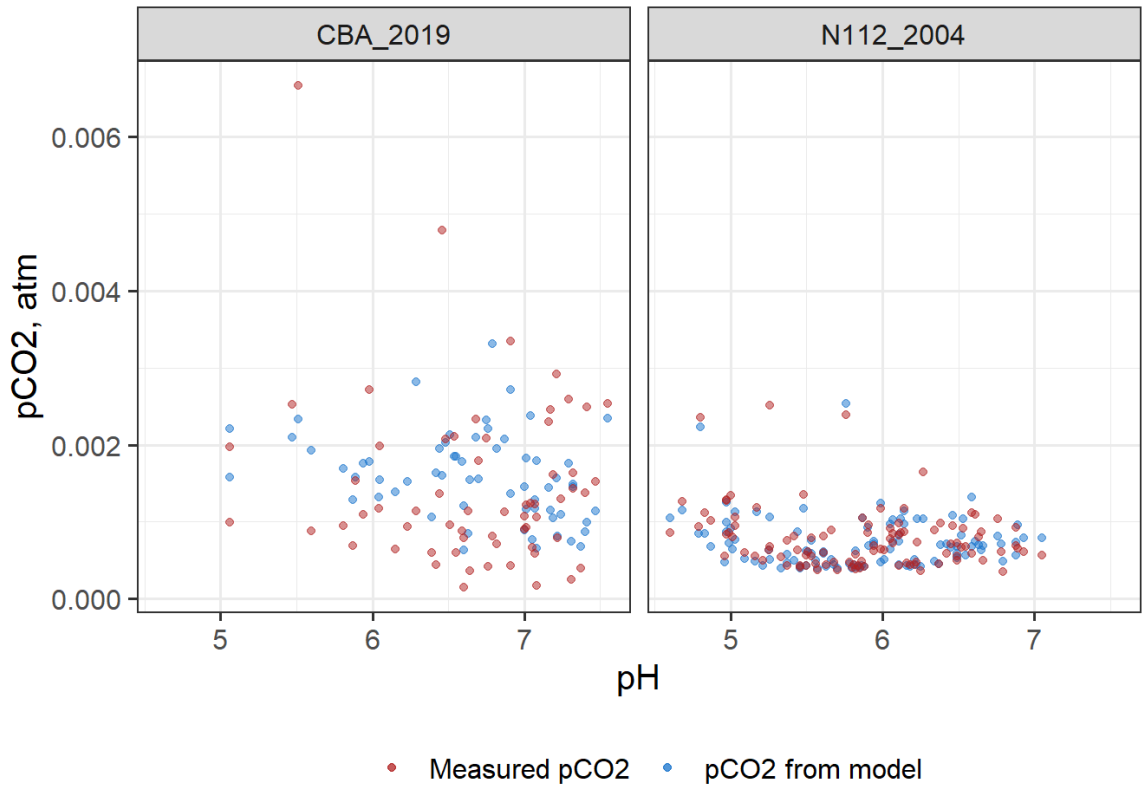

Figure 11 - Measured pCO_2 and pCO_2 modelled from TOC in the training datasets: CBA lakes survey 2019 (left) and N112 lakes survey 2004 (right)

We experimented with several methodologies suggested in the literature to remove the organic alkalinity from the total alkalinity, all yielding unsatisfactory outcomes. We then investigated whether it was possible to predict the concentration of DIC in the samples as means to back-calculate pCO_2. Another avenue explored was the direct fitting of pCO_2 based on the commonly measured parameters: TA, pH, and TOC. We found that fitting a linear model with TOC as predictor for pCO_2 offered the most straightforward and reliable approach to predict pCO_2 when the concentration of DIC was unknown. This model, fitted using data from the two surveys conducted in 2004 and 2019 (Figure 11), was then validated using the dataset of 4 106 lakes from the Northern European Lakes Survey. Utilizing the derived pCO_2 values, we computed CO_2 evasion rates, both on a Fennoscandian scale and specifically for Norway, Sweden, and Finland.

We used two estimates for the gas transfer coefficient of CO_2 from water to the atmosphere. The first estimate only accounted for the wind speed over the lake (Cole and Caraco 1998), while the second included both wind speed and lake area (Vachon and Prairie 2013). The latter estimate tended to result in higher values, resulting in a low and high estimate for CO_2 evasion. Within the Northern European Lakes Survey, we found a median evasion rate of 107.5 to 176.3 gC/m^2/year for the Northern European Lakes

Survey. For Norway, the mean evasion rate of 38.3 to 62.6 gC/m^2/year, while it spanned from 169 to 243 gC/m^2/year for Sweden and 161 to 253 gC/m^2/year for Finland. The similar conditions of Sweden and Finland contrast with Norway's situation, which features numerous mountain lakes exhibiting lower CO_2 concentrations and less forested catchments. In addition, lakes in Sweden and Finland tend to be larger than the Norwegian lakes.

To estimate the contribution of inland waters to national greenhouse gases emissions, we categorized the total inland water area into five segments based on surface area within the three countries. Subsequently, we calculated the CO_2 efflux for each category. The results, expressed in $MtCO_2$/year, were compared to the overall greenhouse gases emissions of each country (Bjønness 2020; Swedish Environmental Protection Agency 2022; Forsell et al. 2022).

Table 2 – National greenhouse gases emissions in $MtCO_2eq$/year for 1995, and estimated CO_2 efflux from inland waters in $MtCO_2$

	Norway	Sweden	Finland
Total GHG emissions	38.7	36.9	58.4
GHG emissions from the LULUCF category	-12	-36.5	-13.2
GHG emissions from the "wetland" category (including lakes)	0.26	0.1	1.6
CO_2 efflux from inland waters, computed from TOC, low estimate	2.84	23.01	24.49
CO_2 efflux from inland waters, computed from TOC, high estimate	4.64	46.08	53.06

Our estimations show that the carbon sink represented by the LULUCF category, driven primarily by forest growth, is largely counterbalanced by the CO_2 emissions originating from inland waters. This is particularly evident in Sweden and in Finland. In fact, in certain cases the highest estimates of CO_2 emissions even exceed the estimated sink. This observation underscores the dynamic interplay between carbon sequestration during forest growth eventually returns to the atmosphere, through microbial respiration in the soil and in the lakes.

These estimates would be improved by distinguishing between lakes, reservoirs, and rivers, and by integrating CH_4 emissions from inland waters. Despite their smaller surface area, rivers and streams tend to have a higher gas transfer coefficient compared to lakes,

potentially leading to a more substantial contribution to CO_2 efflux than that of lakes (Lindroth and Tranvik 2021). Finally, although emissions of CH_4 are lower in magnitude than CO_2 emissions, methane has a higher global warming potential. The inclusion of CH_4 efflux is anticipated to significantly increase the total GHG emissions from inland waters.

5. Conclusion and future perspectives

The organic matter in lakes, measured by its proxies such as total and dissolved organic carbon, holds strong significance for understanding the carbon cycle within the boreal biome. This thesis delves into the intricate relationship between catchments and lakes exploring how the organic matter traverses from the former to the latter, influencing the metabolic processes within boreal lakes, and ultimately governing the emissions of CO_2 emissions from their surface waters.

The hindcast and forecast of TOC concentration, presented in **Paper 1** and in the **Appendix**, show that the current drivers of TOC in lakes serve also as good predictors of past and future changes. Surface runoff intensity, despite being the main vector for mobilization and transport of DOM, has an overall negative impact on TOC concentration due to the diluting of organic matter in an increased water volume. The historical role of sulphur-based acid rain deposition in reducing the solubility of the organic matter is now less prevalent. However, nitrogen deposition will continue to play a key role in the Nordics, where nutrient availability limits the primary and secondary productions. The land uses characteristics within the catchment emerge as strong predictors, with the biomass quantity holding prominence, but better predictions arise from incorporating peatlands, shrubland, and agricultural land. The resulting forecast of TOC concentration must however be considered with caution, as the evolution of these predictors in the future are highly uncertain.

In boreal lakes, where most of the organic matter originates from the catchment and predominantly consist of recalcitrant compounds, heterotrophic respiration is the main process through which the bacteria community in the lakes decomposes and uses the organic matter. In **Paper 2**, we show that removing the nutrient limitation allows the microbial community to use more of the recalcitrant DOM, even though this favours microbial respiration over production, and therefore increase the mineralization rate of DOM. The concentration of inorganic carbon in lakes, though partially imported through groundwaters, can be associated to the aerobic respiration of organic matter, as shown by the linear relationship between TOC and pCO_2, investigated in **Paper 3**.

The high export of organic carbon from catchment to lakes, accompanied by the prevalence of heterotrophic metabolism within the water column, magnified by the large surface area covered by lakes, transforms the boreal inland waters into substantial conduits for C exchange with the atmosphere. This process counters the carbon accumulation in boreal forests, as the mineralization of DOM in the watercourses offsets

this storage. The forecast for TOC concentration, developed in **Paper 1,** tends to indicate that mountainous lakes along the Norwegian west coast, already characterized by low TOC concentration and, hence minimal CO_2 emissions, will become even less concentrated. In contrast, lakes in the southern regions of Sweden and Finland will experience even more browning, leading to increased CO_2 emissions. These results bolster the necessity of integrating inland waters and the DOM into the global C cycle framework.

However, more prospective work is needed to accurately quantify the impact of climate and land use changes on TOC concentration, quality, mineralization, and evasion. Beyond the uncertainty associated with climate models, predicting the adaptations of soil and aquatic ecosystems to changing climate patterns poses considerable challenges. A more accurate forecast of the predictors intertwined with public policies and human activities further underscore the need for prospective work.

References

Adamczyk, Bartosz. 2021. “How Do Boreal Forest Soils Store Carbon?” *BioEssays* 43 (7): 2100010. https://doi.org/10.1002/bies.202100010.

Allesson, Lina, Birgit Koehler, Jan Erik Thrane, Tom Andersen, and Dag O Hessen. 2021. “The Role of Photomineralization for CO2 Emissions in Boreal Lakes along a Gradient of Dissolved Organic Matter.” *Limnology and Oceanography* 66 (1): 158–70. https://doi.org/10.1002/lno.11594.

Allesson, Lina, Nicolas Valiente, Peter Dörsch, Tom Andersen, Alexander Eiler, and Dag O Hessen. 2022. “Drivers and Variability of CO2:O2 Saturation along a Gradient from Boreal to Arctic Lakes.” *Scientific Reports* 12 (1): 18989. https://doi.org/10.1038/s41598-022-23705-9.

Barthelmes, Alexandra, John Couwenberg, Mette Risager, Cosima Tegetmeyer, and Hans Joosten. 2015. “Peatlands and Climate in a Ramsar Context, a Nordic-Baltic Perspective.” *Peatlands and Climate in a Ramsar Context*. https://doi.org/10.6027/tn2015-544.

Bartosiewicz, Maciej, Anna Przytulska, Jean François Lapierre, Isabelle Laurion, Moritz F. Lehmann, and Roxane Maranger. 2019. “Hot Tops, Cold Bottoms: Synergistic Climate Warming and Shielding Effects Increase Carbon Burial in Lakes.” *Limnology And Oceanography Letters* 4 (5): 132–44. https://doi.org/10.1002/lol2.10117.

Bastviken, David, Jonathan Cole, Michael Pace, and Lars Tranvik. 2004. “Methane Emissions from Lakes: Dependence of Lake Characteristics, Two Regional Assessments, and a Global Estimate.” *Global Biogeochemical Cycles* 18 (4): 1–12. https://doi.org/10.1029/2004GB002238.

Beaulne, Joannie, Michelle Garneau, Gabriel Magnan, and Étienne Boucher. 2021. “Peat Deposits Store More Carbon than Trees in Forested Peatlands of the Boreal Biome.” *Scientific Reports* 11 (1): 2657. https://doi.org/10.1038/s41598-021-82004-x.

Bentsen, M., I. Bethke, J. B. Debernard, T. Iversen, A. Kirkevåg, Ø. Seland, H. Drange, et al. 2013. “The Norwegian Earth System Model, NorESM1-M – Part 1: Description and Basic Evaluation of the Physical Climate.” *Geoscientific Model Development* 6 (3): 687–720. https://doi.org/10.5194/gmd-6-687-2013.

“Biodegradability of DNOM.” n.d. Accessed August 2, 2020. https://www.protocols.io/view/biodegradability-of-dnom-biyykfxw.

Bivand, Roger. 2019. “Estimation Methods for Models of Spatial Interaction.” *CRAN - R Package*. https://doi.org/10.1080/01621459.1975.10480272.

Bjønness, Kathrine Loe. 2020. “Greenhouse Gas Emissions 1990-2018, National Inventory Report.”

Bogard, Matthew J, Nicolas F St-Gelais, Dominic Vachon, and Paul A. del Giorgio. 2020. “Patterns of Spring/Summer Open-Water Metabolism Across Boreal Lakes.” *Ecosystems* 23 (8): 1581–97. https://doi.org/10.1007/s10021-020-00487-7.

Bolan, Nanthi S., Domy C. Adriano, Anitha Kunhikrishnan, Trevor James, Richard McDowell, and Nicola Senesi. 2011. *Dissolved Organic Matter. Biogeochemistry, Dynamics, and Environmental Significance in Soils. Advances in Agronomy*. 1st ed.

Vol. 110. Elsevier Inc. https://doi.org/10.1016/B978-0-12-385531-2.00001-3.

Boogaard, H., J. Schubert, A. De Wit, J. Lazebnik, R. Hutjes, and G. Van der Grijn. 2020. "Copernicus Climate Change Service (C3S) Climate Data Store (CDS)." Agrometeorological Indicators from 1979 to Present Derived from Reanalysis. 2020. https://doi.org/10.24381/cds.6c68c9bb.

Bradshaw, Corey J.A., and Ian G. Warkentin. 2015. "Global Estimates of Boreal Forest Carbon Stocks and Flux." *Global and Planetary Change* 128 (May): 24–30. https://doi.org/10.1016/j.gloplacha.2015.02.004.

Bridgham, Scott D., Hinsby Cadillo-Quiroz, Jason K. Keller, and Qianlai Zhuang. 2013. "Methane Emissions from Wetlands: Biogeochemical, Microbial, and Modeling Perspectives from Local to Global Scales." *Global Change Biology* 19 (5): 1325–46. https://doi.org/10.1111/gcb.12131.

Chmiel, Hannah E., Jutta Niggemann, Jovana Kokic, Marie Ève Ferland, Thorsten Dittmar, and Sebastian Sobek. 2015. "Uncoupled Organic Matter Burial and Quality in Boreal Lake Sediments over the Holocene." *Journal of Geophysical Research: Biogeosciences* 120 (9): 1751–63. https://doi.org/10.1002/2015JG002987.

Clayer, François, Yves Gélinas, André Tessier, and Charles Gobeil. 2020. "Mineralization of Organic Matter in Boreal Lake Sediments: Rates, Pathways, and Nature of the Fermenting Substrates." *Biogeosciences* 17 (18): 4571–89. https://doi.org/10.5194/bg-17-4571-2020.

Coble, Ashley A., Amy M. Marcarelli, Evan S. Kane, David Toczydlowski, and Robert Stottlemyer. 2016. "Temporal Patterns of Dissolved Organic Matter Biodegradability Are Similar across Three Rivers of Varying Size." *Journal of Geophysical Research: Biogeosciences* 121 (6): 1617–31. https://doi.org/10.1002/2015JG003218.

Cole, J. J., Y. T. Prairie, N. F. Caraco, W. H. McDowell, L. J. Tranvik, R. G. Striegl, C. M. Duarte, et al. 2007. "Plumbing the Global Carbon Cycle: Integrating Inland Waters into the Terrestrial Carbon Budget." *Ecosystems* 10 (1): 171–84. https://doi.org/10.1007/S10021-006-9013-8/TABLES/1.

Cole, Jonathan J., and Nina F. Caraco. 1998. "Atmospheric Exchange of Carbon Dioxide in a Low-Wind Oligotrophic Lake Measured by the Addition of SF6." *Limnology and Oceanography* 43 (4): 647–56. https://doi.org/10.4319/lo.1998.43.4.0647.

Copernicus Land Monitoring Service. n.d. "CHA 2000-2006." Accessed January 26, 2022. https://land.copernicus.eu/pan-european/corine-land-cover/lcc-2000-2006.

CORDEX. 2021. "CORDEX Experiment Design for Dynamical Downscaling of CMIP6," no. May: 1–8. https://cordex.org/wp-content/uploads/2021/05/CORDEX-CMIP6_exp_design_RCM.pdf.

Cornwell, William K., Johannes H.C. Cornelissen, Steven D. Allison, Jürgen Bauhus, Paul Eggleton, Caroline M. Preston, Fiona Scarff, James T. Weedon, Christian Wirth, and Amy E. Zanne. 2009. "Plant Traits and Wood Fates across the Globe: Rotted, Burned, or Consumed?" *Global Change Biology* 15 (10): 2431–49. https://doi.org/10.1111/j.1365-2486.2009.01916.x.

Crapart, Camille, Anders G. Finstad, Dag O. Hessen, Rolf D. Vogt, and Tom Andersen. 2023. "Spatial Predictors and Temporal Forecast of Total Organic Carbon Levels in Boreal Lakes." *Science of the Total Environment* 870 (April): 161676.

https://doi.org/10.1016/j.scitotenv.2023.161676.

Crapart, Camille, and Nicolas Parra. 2019. “CBA 100 Lakes.” 2019. https://osf.io/r39ng/?view_only=d1b8c4c2c68c4ca59bb4c78a817fc64b.

Curtin, Denis, Michael H. Beare, and Guillermo Hernandez-Ramirez. 2012. “Temperature and Moisture Effects on Microbial Biomass and Soil Organic Matter Mineralization.” *Soil Science Society of America Journal* 76 (6): 2055–67. https://doi.org/10.2136/sssaj2012.0011.

Deshpande, Bethany N., Sophie Crevecoeur, Alex Matveev, and Warwick F. Vincent. 2016. “Bacterial Production in Subarctic Peatland Lakes Enriched by Thawing Permafrost.” *Biogeosciences* 13 (15): 4411–27. https://doi.org/10.5194/bg-13-4411-2016.

Eklund, Anna, Jenny Axén Mårtensson, Sten Bergström, Emil Björck, Joel Dahné, Lena Lindström, Daniel Nordborg, Jonas Olsson, Lennart Simonsson, and Elin Sjökvist. 2015. “Sveriges Framtida Klimat Underlag till Dricksvattenutredningen.” *KLIMATOLOGI Nr*. Vol. 14.

EMEP. 2022. “EMEP MSC-W HOME.” 2022. https://emep.int/mscw/mscw_moddata.html#Comp.

Eriksson, J.V. 1929. “Den Kemiska Denudationen i Sverige (The Chemical Denudation of Sweden).” Stockholm. http://info1.ma.slu.se/max/www_max.acgi$Project?ID=Intro&pID=23.

Erlandsson, Martin, Ishi Buffam, Jens Fölster, Hjalmar Laudon, Johan Temnerud, Gesa A. Weyhenmeyer, and Kevin Bishop. 2008. “Thirty-Five Years of Synchrony in the Organic Matter Concentrations of Swedish Rivers Explained by Variation in Flow and Sulphate.” *Global Change Biology* 14 (5): 1191–98. https://doi.org/10.1111/j.1365-2486.2008.01551.x.

Finér, Leena, Ahti Lepistö, Kristian Karlsson, Antti Räike, Laura Härkönen, Markus Huttunen, Samuli Joensuu, et al. 2021. “Drainage for Forestry Increases N, P and TOC Export to Boreal Surface Waters.” *Science of the Total Environment* 762: 144098. https://doi.org/10.1016/j.scitotenv.2020.144098.

Finstad, Anders G. 2017. “Environmental Data · NINAnor/NOFA Wiki.” 2017. https://github.com/NINAnor/NOFA/wiki/Environmental-data.

Finstad, Anders G., Tom Andersen, Søren Larsen, Koji Tominaga, Stefan Blumentrath, Heleen A. De Wit, Hans Tømmervik, and Dag Olav Hessen. 2016. “From Greening to Browning: Catchment Vegetation Development and Reduced S-Deposition Promote Organic Carbon Load on Decadal Time Scales in Nordic Lakes.” *Scientific Reports* 6:31944 (7485): 1–8. https://doi.org/10.1038/srep31944.

Forsell, Pia, Kari Grönfors, Jutta Kallanto, Timo Kareinen, Päivi Lindh, Sini Niinistö, Riitta Pipatti, et al. 2022. “National Inventory Report, Greenhouse Gas Emissions in Finland 1990 to 2020.”

Frances, Martinez Elena. 2017. “Biodegradability and Spectroscopic Properties of Dissolved Natural Organic Matter Fractions Linked to Hg and MeHg Transport and Uptake.” *Department of Chemistry Faculty of Mathematics and Natural Sciences* Master (URN:NBN:no-62116). https://www.duo.uio.no/bitstream/handle/10852/59440/5/Elena-Mart-nez-Franc-s-Master-thesis-final.pdf.

Futter, Martyn, Nicholas Clarke, Øyvind Kaste, and Salar Valinia. 2019. "The Potential Effects on Water Quality of Intensified Forest Management for Climate Mitigation in Norway," no. 7363–2019. www.niva.no.

Gauthier, S., P. Bernier, T. Kuuluvainen, A. Z. Shvidenko, and D. G. Schepaschenko. 2015. "Boreal Forest Health and Global Change." *Science* 349 (6250): 819–22. https://doi.org/10.1126/science.aaa9092.

Guenet, Bertrand, Michael Danger, Luc Abbadie, and Gérard Lacroix. 2010. "Priming Effect: Bridging the Gap between Terrestrial and Aquatic Ecology." *Ecology* 91 (10): 2850–61. https://doi.org/10.1890/09-1968.1.

Guo, Jingheng, Fushun Wang, Rolf David Vogt, Yuhang Zhang, and Cong Qiang Liu. 2015. "Anthropogenically Enhanced Chemical Weathering and Carbon Evasion in the Yangtze Basin." *Scientific Reports* 5: 1–8. https://doi.org/10.1038/srep11941.

Hagedorn, Frank, Patrick Schleppi, Peter Walnder, and Hannes Flühler. 2000. "Export of Dissolved Organic Carbon and Nitrogen from Gleysol Dominated Catchments--the Significance of Water Flow Paths." *Biogeochemistry* 50: 137–61. https://link.springer.com/article/10.1023/A:1006398105953.

Håland, Alexander. 2017. "Characteristics and Bioavailability of Dissolved Natural Organic Matter in a Boreal Stream during Storm Flow." DUO, University of Oslo, Norway. http://urn.nb.no/URN:NBN:no-61154.

Hanssen-Bauer, I, E J Førland, I Haddeland, H Hisdal, D Lawrence, S Mayer, A Nesje, S Sandven, A B Sandø, and A Sorteberg. 2017. "Climate in Norway 2100 – a Knowledge Base for Climate Adaptation." *Norwegian Environmental Agency, Report No. 1/2017*. www.miljodirektoratet.no/M741.

Hassell, David, Jonathan Gregory, Jon Blower, Bryan N. Lawrence, and Karl E. Taylor. 2017. "A Data Model of the Climate and Forecast Metadata Conventions (CF-1.6) with a Software Implementation (Cf-Python v2.1)." *Geoscientific Model Development* 10 (12): 4619–46. https://doi.org/10.5194/GMD-10-4619-2017.

Hastie, Adam, Ronny Lauerwald, Gesa Weyhenmeyer, Sebastian Sobek, Charles Verpoorter, and Pierre Regnier. 2018. "CO2 Evasion from Boreal Lakes: Revised Estimate, Drivers of Spatial Variability, and Future Projections." *Global Change Biology* 24 (2): 711–28. https://doi.org/10.1111/gcb.13902.

Henriksen, Arne, Brit Lisa Skjelvåle, Leif Lien, Tor S Traaen, Jaakko Mannio, Martin Forsius, J Kämari, et al. 1996. "Regional Lake Surveys in Finland - Norway - Sweden - Northern Kola - Russian Karelia - Scotland - Wales 1995, Coordination and Design." https://niva.brage.unit.no/niva-xmlui/bitstream/handle/11250/208733/3420_72dpi.pdf?sequence=1&isAllowed=y.

Henriksen, Arne, Brit Lisa Skjelvåle, Jaakko Mannio, Anders Wilander, Ron Harriman, Chris Curtis, Jens Peder Jensen, Erik Fjeld, and Tatyana Moiseenko. 1998. "Northern European Lake Survey 1995: Finland, Norway, Sweden, Denmark, Russian Kola, Russian Karelia, Scotland and Wales." *Ambio* 2 (27): 80–91. https://www.jstor.org/stable/4314692.

Hijmans, Robert J, Jacob Van Etten, Joe Cheng, Michael Sumner, Matteo Mattiuzzi, Jonathan A Greenberg, Oscar Perpinan, et al. 2018. "Package 'raster' Type Package Title Geographic Data Analysis and Modeling." https://github.com/rspatial/raster/issues/.

Hruška, Jakub, Stephan Köhler, Hjalmar Laudon, and Kevin Bishop. 2003. "Is a Universal Model of Organic Acidity Possible: Comparison of the Acid/Base Properties of Dissolved Organic Carbon in the Boreal and Temperate Zones." *Environmental Science and Technology* 37 (9): 1726–30. https://doi.org/10.1021/es0201552.

Huttula, Timo. 2012. "Stratification in Lakes." In *Encyclopedia of Earth Sciences Series*, 743–47. Springer Netherlands. https://doi.org/10.1007/978-1-4020-4410-6_12.

Huttunen, Jari T., Jukka Alm, Anu Liikanen, Sari Juutinen, Tuula Larmola, Taina Hammar, Jouko Silvola, and Pertti J. Martikainen. 2003. "Fluxes of Methane, Carbon Dioxide and Nitrous Oxide in Boreal Lakes and Potential Anthropogenic Effects on the Aquatic Greenhouse Gas Emissions." *Chemosphere* 52 (3): 609–21. https://doi.org/10.1016/S0045-6535(03)00243-1.

Jones, Roger I. 2000. "Mixotrophy in Planktonic Protists: An Overview." *Freshwater Biology* 45 (2): 219–26. https://doi.org/10.1046/j.1365-2427.2000.00672.x.

Jonsson, A., G. Algesten, A. K. Bergström, K. Bishop, S. Sobek, L. J. Tranvik, and M. Jansson. 2007. "Integrating Aquatic Carbon Fluxes in a Boreal Catchment Carbon Budget." *Journal of Hydrology* 334 (1–2): 141–50. https://doi.org/10.1016/j.jhydrol.2006.10.003.

Joosten, Hans, Franziska Tanneberger, and Asbjørn Moen. 2017. *Mires and Peatlands in Europe Status, Distribution and Conservation*. Schweizerbart Sience Publisher. https://www.schweizerbart.de/publications/detail/isbn/9783510653836/Joosten_Tanneberger_Moen_Mires_and_peat.

Kankaala, Paula, Jessica Lopez Bellido, Anne Ojala, Tiina Tulonen, and Roger I. Jones. 2013. "Variable Production by Different Pelagic Energy Mobilizers in Boreal Lakes." *Ecosystems* 16 (6): 1152–64. https://doi.org/10.1007/S10021-013-9674-Z/FIGURES/5.

Kortelainen, Pirkko, Tuija Mattsson, Leena Finér, Marketta Ahtiainen, Sari Saukkonen, and Tapani Sallantaus. 2006. "Controls on the Export of C, N, P and Fe from Undisturbed Boreal Catchments, Finland." *Aquatic Sciences* 68 (4): 453–68. https://doi.org/10.1007/s00027-006-0833-6.

Kortelainen, Pirkko, Miitta Rantakari, Hannu Pajunen, Tuija Mattsson, Sari Juutinen, Tuula Larmola, Jukka Alm, Jouko Silvola, and Pertti J. Martikainen. 2013. "Carbon Evasion/Accumulation Ratio in Boreal Lakes Is Linked to Nitrogen." *Global Biogeochemical Cycles* 27 (2): 363–74. https://doi.org/10.1002/gbc.20036.

Kritzberg, Emma S., Eliza Maher Hasselquist, Martin Škerlep, Stefan Löfgren, Olle Olsson, Johanna Stadmark, Salar Valinia, Lars Anders Hansson, and Hjalmar Laudon. 2020. "Browning of Freshwaters: Consequences to Ecosystem Services, Underlying Drivers, and Potential Mitigation Measures." *Ambio* 49 (2): 375–90. https://doi.org/10.1007/s13280-019-01227-5.

Langtjern - Norway DEIMS-SDR. (n.d.). Retrieved November 1, 2023, from https://deims.org/2610fbc1-8eee-4223-8c27-367aa67feddc

Larsen, Søren, Tom Andersen, and Dag O. Hessen. 2011. "The PCO2 in Boreal Lakes: Organic Carbon as a Universal Predictor?" *Global Biogeochemical Cycles* 25 (2): 1–8. https://doi.org/10.1029/2010GB003864.

Larson, Magnus. 2012. "Sweden's Great Lakes." In *Encyclopedia of Lakes and Reservoirs*, 761–64. Springer, DOrdrecht. https://doi.org/10.1007/978-1-4020-4410-6_269.

Lindroth, Anders, and Lars Tranvik. 2021. "Accounting for All Territorial Emissions and Sinks Is Important for Development of Climate Mitigation Policies." *Carbon Balance and Management* 16 (1): 8–10. https://doi.org/10.1186/s13021-021-00173-8.

Liu, Jinxun, Changhui Peng, Mike Apps, Qinglai Dang, Edwin Banfield, and Werner Kurz. 2002. "Historic Carbon Budgets of Ontario's Forest Ecosystems." *Forest Ecology and Management* 169 (1–2): 103–14. https://doi.org/10.1016/S0378-1127(02)00301-8.

Liu, Shaoda, David E. Butman, and Peter A. Raymond. 2020. "Evaluating CO2 Calculation Error from Organic Alkalinity and PH Measurement Error in Low Ionic Strength Freshwaters." *Limnology and Oceanography: Methods* 18 (10): 606–22. https://doi.org/10.1002/lom3.10388.

Liu, Shasha, Zhongqi He, Zhi Tang, Leizhen Liu, Junwen Hou, Tingting Li, Yahe Zhang, Quan Shi, John P. Giesy, and Fengchang Wu. 2020. "Linking the Molecular Composition of Autochthonous Dissolved Organic Matter to Source Identification for Freshwater Lake Ecosystems by Combination of Optical Spectroscopy and FT-ICR-MS Analysis." *Science of the Total Environment* 703 (February): 134764. https://doi.org/10.1016/j.scitotenv.2019.134764.

Marcé, Rafael, Biel Obrador, Josep Anton Morguí, Joan Lluís Riera, Pilar López, and Joan Armengol. 2015. "Carbonate Weathering as a Driver of CO2 Supersaturation in Lakes." *Nature Geoscience* 8 (2): 107–11. https://doi.org/10.1038/ngeo2341.

Masson-Delmotte, V., P. Zhai, A. Pirani, S.L. Connors, C. Péan, S. Berger, N. Caud, et al. 2021. "IPCC. 2021: Summary for Policymakers." In *Climate Change 2021: The Physical Science Basis. Contribution of Working Group I to the Sixth Assessment Report of the Intergovernmental Panel on Climate Change*, Cambridge, 3–32. Cambridge, United Kingdom and New Yoak, USA. https://www.ipcc.ch/report/ar6/wg1/.

Ministry of Agriculture and Forestry. 2014. "Government Report on Forest Policy 2050."

Monteith, D. T., J. L. Stoddard, C. D. Evans, H. A. De Wit, M. Forsius, T. Høgåsen, A. Wilander, et al. 2007. "Dissolved Organic Carbon Trends Resulting from Changes in Atmospheric Deposition Chemistry." *Nature* 450 (7169): 537–40. https://doi.org/10.1038/nature06316.

Näringsdepartementet. 2018. "Strategi För Sveriges Nationella Skogsprogram."

Natural Resources Institute Finland. 2022. "Land Classes on Forestry Land (1000 Ha) by Inventory, Region and Land Class." Statistical Database. 2022. https://statdb.luke.fi/PXWeb/pxweb/en/LUKE/LUKE__04 Metsa__06 Metsavarat/1.01_Metsatalousmaa.px/table/tableViewLayout2/.

NVE. 2022. "Watersheds (REGINE)." 2022. https://www.nve.no/kart/kartdata/vassdragsdata/nedborfelt-regine/.

Oliver, Barry G., Earl M. Thurman, and Ronald L. Malcolm. 1983. "The Contribution of Humic Substances to the Acidity of Colored Natural Waters." *Geochimica et Cosmochimica Acta* 47 (11): 2031–35. https://doi.org/10.1016/0016-

7037(83)90218-1.

Palviainen, Marjo, Ari Laurén, Samuli Launiainen, and Sirpa Piirainen. 2016. "Predicting the Export and Concentrations of Organic Carbon, Nitrogen and Phosphorus in Boreal Lakes by Catchment Characteristics and Land Use: A Practical Approach." *Ambio* 45 (8): 933. https://doi.org/10.1007/S13280-016-0789-2.

R Core Team. 2023. "R: A Language and Environment for Statistical Computing." Vienna, Austria: R Foundation for Statistical Computing. https://www.r-project.org/.

Räike, Antti, Pirkko Kortelainen, Tuija Mattsson, and David N. Thomas. 2012. "36 Year Trends in Dissolved Organic Carbon Export from Finnish Rivers to the Baltic Sea." *Science of the Total Environment* 435–436: 188–201. https://doi.org/10.1016/j.scitotenv.2012.06.111.

Rajakumar, Janaki. 2018. "Effect of Photo-Oxidation on Size, Structure and Biodegradability of Dissolved Natural Organic Matter." Oslo: University of Oslo. https://www.duo.uio.no/handle/10852/65724.

Raymond, Peter A., Jens Hartmann, Ronny Lauerwald, Sebastian Sobek, Cory McDonald, Mark Hoover, David Butman, et al. 2013. "Global Carbon Dioxide Emissions from Inland Waters." *Nature* 503 (7476): 355–59. https://doi.org/10.1038/nature12760.

Rinnan, Riikka, Anders Michelsen, Erland Bååth, and Sven Jonasson. 2007. "Fifteen Years of Climate Change Manipulations Alter Soil Microbial Communities in a Subarctic Heath Ecosystem." *Global Change Biology* 13 (1): 28–39. https://doi.org/10.1111/j.1365-2486.2006.01263.x.

Rosset, Thomas, Stéphane Binet, François Rigal, and Laure Gandois. 2022. "Peatland Dissolved Organic Carbon Export to Surface Waters: Global Significance and Effects of Anthropogenic Disturbance." *Geophysical Research Letters* 49 (5). https://doi.org/10.1029/2021GL096616.

Royal Swedish Academy of Agriculture and Forestry. 2015. "Forests and Forestry in Sweden."

Sallinen, A., S. Tuominen, T. Kumpula, and T. Tahvanainen. 2019. "Undrained Peatland Areas Disturbed by Surrounding Drainage: A Large Scale GIS Analysis in Finland with a Special Focus on AAPA Mires." *Mires and Peat* 24: 1–22. https://doi.org/10.19189/MaP.2018.AJB.391.

Scharlemann, Jörn Pw, Edmund Vj Tanner, Roland Hiederer, and Valerie Kapos. 2014. "Global Soil Carbon: Understanding and Managing the Largest Terrestrial Carbon Pool." *Carbon Management*. https://doi.org/10.4155/cmt.13.77.

Schelker, J., K. Eklöf, K. Bishop, and H. Laudon. 2012. "Effects of Forestry Operations on Dissolved Organic Carbon Concentrations and Export in Boreal First-Order Streams." *Journal of Geophysical Research: Biogeosciences* 117 (1): 1011. https://doi.org/10.1029/2011JG001827.

Seekell, David A., Jean Francois Lapierre, Jenny Ask, Ann Kristin Bergstreom, Anne Deininger, Patricia Rodriguez, and Jan Karlsson. 2015. "The Influence of Dissolved Organic Carbon on Primary Production in Northern Lakes." *Limnology and Oceanography* 60 (4): 1276–85. https://doi.org/10.1002/lno.10096.

Seland, Øyvind, Mats Bentsen, Dirk Olivié, Thomas Toniazzo, Ada Gjermundsen, Lise Seland Graff, Jens Boldingh Debernard, et al. 2020. *Overview of the Norwegian Earth System Model (NorESM2) and Key Climate Response of CMIP6 DECK, Historical, and Scenario Simulations*. *Geoscientific Model Development*. Vol. 13. https://doi.org/10.5194/gmd-13-6165-2020.

SLU. 2020. "Miljödata MVM." Swedish University of Agricultural Sciences. 2020. https://miljodata.slu.se/MVM/Search.

Soares, Ana R.A., Jean François Lapierre, Balathandayuthabani P. Selvam, Göran Lindström, and Martin Berggren. 2019. "Controls on Dissolved Organic Carbon Bioreactivity in River Systems." *Scientific Reports* 9 (1): 1–9. https://doi.org/10.1038/s41598-019-50552-y.

SSB. 2021. "Land Use and Land Cover." 2021. https://www.ssb.no/en/natur-og-miljo/areal/statistikk/arealbruk-og-arealressurser.

Statistics Finland. 2023. "Environment and Nature." 2023. https://www.stat.fi/tup/suoluk/suoluk_alue_en.html.

Statistics Sweden. 2022. "Statistical Database - Select Table." Statistical Database. 2022. https://www.statistikdatabasen.scb.se/pxweb/en/ssd/START__MI__MI0803__MI0803A/.

Swedish Environmental Protection Agency. 2022. "National Inventory Report Sweden 2022." Stockholm. https://www.naturvardsverket.se/upload/sa-mar-miljon/statistik-a-till-o/vaxthusgaser/2014/national-inventory-report-2014.pdf.

Swedish Forest Industries. 2019. "Contribution of the Swedish Forestry Sector to Global Climate Efforts." https://www.forestindustries.se/siteassets/dokument/rapporter/swedish-forestry-sectors-climate-contribution.pdf.

"The HILDA+ Project – Land Change Stories." n.d. Accessed June 22, 2023. https://landchangestories.org/hildaplus/.

The National Center for Atmospheric Research. 2018. "Global GIMMS NDVI3g v1 Dataset (1981-2015)." *A Big Earth Data Platform for Three Poles*. http://poles.tpdc.ac.cn/en/data/9775f2b4-7370-4e5e-a537-3482c9a83d88/.

Tranvik, Lars J., John A. Downing, James B. Cotner, Steven A. Loiselle, Robert G. Striegl, Thomas J. Ballatore, Peter Dillon, et al. 2009. "Lakes and Reservoirs as Regulators of Carbon Cycling and Climate." *Limnology and Oceanography* 54 (6 PART 2): 2298–2314. https://doi.org/10.4319/lo.2009.54.6_part_2.2298.

Treseder, Kathleen K. 2008. "Nitrogen Additions and Microbial Biomass: A Meta-Analysis of Ecosystem Studies." *Ecology Letters*. https://doi.org/10.1111/j.1461-0248.2008.01230.x.

UNECE. 1985. "The 1985 Helsinki Protocol on the Reduction of Sulphur Emissions or Their Transboundary Fluxes by at Least 30 per Cent." Helsinki. https://doi.org/10.18356/25457837-en-fr.

———. 1992. "The 1994 Oslo Protocol on Further Reduction of Sulphur Emissions." Oslo. https://unece.org/environment-policy/air/protocol-further-reduction-sulphur-emissions.

———. 1999. "The 1999 Gothenburg Protocol to Abate Acidification, Eutrophication

and Ground-Level Ozone." Gothenburg. https://unece.org/environment-policy/air/protocol-abate-acidification-eutrophication-and-ground-level-ozone.

Vachon, Dominic, and Yves T. Prairie. 2013. "The Ecosystem Size and Shape Dependence of Gas Transfer Velocity versus Wind Speed Relationships in Lakes." *Canadian Journal of Fisheries and Aquatic Sciences* 70 (12): 1757–64. https://doi.org/10.1139/cjfas-2013-0241.

Valiente, Nicolas, Alexander Eiler, Lina Allesson, Tom Andersen, François Clayer, Camille Crapart, Peter Dörsch, et al. 2022. "Catchment Properties as Predictors of Greenhouse Gas Concentrations across a Gradient of Boreal Lakes." *Frontiers in Environmental Science* 10 (September): 1–16. https://doi.org/10.3389/fenvs.2022.880619.

Venäläinen, Ari, Ilari Lehtonen, Mikko Laapas, Kimmo Ruosteenoja, Olli Pekka Tikkanen, Heli Viiri, Veli Pekka Ikonen, and Heli Peltola. 2020. "Climate Change Induces Multiple Risks to Boreal Forests and Forestry in Finland: A Literature Review." *Global Change Biology* 26 (8): 4178–96. https://doi.org/10.1111/GCB.15183.

Vogt, Rolf D, Heleen A De Wit, and Kati Koponen. 2022. "Case Study on Impacts of Large-Scale Re-/Afforestation on Ecosystem Services in Nordic Regions. In: Quantifying and Deploying Responsible Negative Emissions in Climate Resilient Pathway." *Negemproject.Eu* 3.1.4. https://www.negemproject.eu/wp-content/uploads/2022/06/NEGEM_D3.6_Case-study-on-impacts-of-large-scale-re-afforestation-on-ecosystem-services-in-Nordic-regions.pdf.

Vogt, Rolf David, Petr Porcal, Josef Hejzlar, Ma. Cristina Paule-Mercado, Ståle Haaland, Cathrine Brecke Gundersen, Geir Orderud, and Bjørnar Eikebrokk. 2023. "Distinguishing between Sources of Natural Dissolved Organic Matter (DOM) by Means of Its Characteristics." *Preprint*. https://doi.org/10.20944/preprints202307.

Voldoire, A., D. Saint-Martin, S. Sénési, B. Decharme, A. Alias, M. Chevallier, J. Colin, et al. 2019. "Evaluation of CMIP6 DECK Experiments With CNRM-CM6-1." *Journal of Advances in Modeling Earth Systems* 11 (7): 2177–2213. https://doi.org/10.1029/2019MS001683.

Vonk, J E, S E Tank, P J Mann, R. G.M. Spencer, C C Treat, R G Striegl, B W Abbott, and K P Wickland. 2015. "Biodegradability of Dissolved Organic Carbon in Permafrost Soils and Aquatic Systems: A Meta-Analysis." *Biogeosciences* 12 (23): 6915–30. https://doi.org/10.5194/bg-12-6915-2015.

Wachenfeldt, Eddie Von, and Lars J Tranvik. 2008. "Sedimentation in Boreal Lakes - The Role of Flocculation of Allochthonous Dissolved Organic Matter in the Water Column." *Ecosystems* 11 (5): 803–14. https://doi.org/10.1007/s10021-008-9162-z.

Wang, Dingyi, Xiangyin Ni, Hongrong Guo, and Wenyuan Dai. 2022. "Alpine Litter Humification and Its Response to Reduced Snow Cover: Can More Carbon Be Sequestered in Soils?" *Forests* 13 (6): 897. https://doi.org/10.3390/f13060897.

Weyhenmeyer, Gesa A, Sarian Kosten, Marcus B Wallin, Lars J Tranvik, Erik Jeppesen, and Fabio Roland. 2015. "Significant Fraction of CO2 Emissions from Boreal Lakes Derived from Hydrologic Inorganic Carbon Inputs." *Nature Geoscience* 8 (12): 933–36. https://doi.org/10.1038/ngeo2582.

Wilander, Anders. 1988. "ORGANISKT MATERIAL I VATTEN. – EN JÄMFÖRELSE

AV RESULTAT FRÅN OLIKA ANALYSMETODER, Organic Substances in Natural Water. A Comparison of Results from Different Analytical Methods." *Vatten* 3: 217–24. https://www.tidskriftenvatten.se/tsv-artikel/organiskt-material-i-vatten-en-jamforelse-av-resultat-fran-olika-analysmetoder-organic-substances-in-natural-water-a-comparison-of-results-from-different-analytical-methods/.

Wilkinson, Grace M, Michael L Pace, and Jonathan J Cole. 2013. "Terrestrial Dominance of Organic Matter in North Temperate Lakes." *Global Biogeochemical Cycles* 27 (1): 43–51. https://doi.org/10.1029/2012GB004453.

Williamson, Craig E, Walter Dodds, Timothy K Kratz, and Margaret A Palmer. 2008. "Lakes and Streams as Sentinels of Environmental Change in Terrestrial and Atmospheric Processes." *Frontiers in Ecology and the Environment*. https://doi.org/10.1890/070140.

Winkler, Karina, Richard Fuchs, Mark Rounsevell, and Martin Herold. 2021. "Global Land Use Changes Are Four Times Greater than Previously Estimated." *Nature Communications* 12 (1): 1–10. https://doi.org/10.1038/s41467-021-22702-2.

Wit, Heleen A. De, Jan Mulder, Atle Hindar, and Lars Hole. 2007. "Long-Term Increase in Dissolved Organic Carbon in Streamwaters in Norway Is Response to Reduced Acid Deposition." *Environmental Science and Technology* 41 (22): 7706–13. https://doi.org/10.1021/es070557f.

Wit, Heleen A. De, Salar Valinia, Gesa A. Weyhenmeyer, Martyn N. Futter, Pirkko Kortelainen, Kari Austnes, Dag O. Hessen, Antti Räike, Hjalmar Laudon, and Jussi Vuorenmaa. 2016. "Current Browning of Surface Waters Will Be Further Promoted by Wetter Climate." *Environmental Science and Technology Letters* 3 (12): 430–35. https://doi.org/10.1021/acs.estlett.6b00396.

Wit, Helene A. De, Øyvind A. Garmo, Leah Jackson-Blake, François Clayer, Rolf D. Vogt, Øyvind Kaste, Cathrine Brecke Gundersen, Jose Luis Guerrero, and Atle Hindar. 2023. "Changing Water Chemistry in One Thousand Norwegian Lakes During Three Decades of Cleaner Air and Climate Change." *Global Biogeochemical Cycles* 37 (2). https://doi.org/https://doi.org/10.1029/2022GB007509.

World Climate Resarch Program. n.d. "CMIP6." Accessed March 3, 2022. https://www.wcrp-climate.org/wgcm-cmip/wgcm-cmip6.

WorldClim. n.d. "Data Format — WorldClim 1 Documentation." Accessed November 1, 2021. https://worldclim.org/data/v1.4/formats.html.

Yang, Hong, Tom Andersen, Peter Dörsch, Koji Tominaga, Jan Erik Thrane, and Dag O. Hessen. 2015. "Greenhouse Gas Metabolism in Nordic Boreal Lakes." *Biogeochemistry* 126 (1–2): 211–25. https://doi.org/10.1007/s10533-015-0154-8.

Zhou, Yongqiang, Carolin Hiller, Sara Andersson, Elizabeth Jakobsson, Lei Zhou, Jeffery A Hawkes, Dolly N Kothawala, and Lars J Tranvik. 2023. "Selective Exclusion of Aromatic Organic Carbon During Lake Ice Formation." *Geophysical Research Letters* 50 (4). https://doi.org/10.1029/2022GL101414.

Appendix - TOC concentration and coastal darkening in the 20th century

This work is related to the Green-Blue project, financed by the Research Council of Norway, and conducted jointly by the Department of Biological Sciences at the University of Bergen, the Department of Biosciences and Department of Geosciences of the University of Oslo. The project leader is Anders Frugård Opdal. The Material & Methods are presented here, as well as the main results. A manuscript based on these results will be written jointly by Anders Frugård Opdal, Camille Crapart and Tom Andersen.

Material & Methods

A model predicting TOC concentration in lakes water, based on catchment characteristics, was fitted in the Northern European Lakes Survey dataset (Henriksen et al. 1998). The concentration of total organic carbon (TOC) of 4160 lakes, in mg/L, as well as the lakes catchments polygons, were stored and downloaded from the NOFA database (Finstad 2017).

Then, we used this model to predict the average TOC concentration back in time in larger areas: coastal drainage basins. These basins encompass all the lakes and rivers that discharge into the sea at a specific point. Using these larger areas for the predictions not only saved computing resources, but also allowed us to estimate the export of TOC from land to coastal waters. The coastal drainage basins polygons were generated with a seamless digital elevation model for Fennoscandia (Finstad 2017). The elevation model resulted in more than 200 000 coastal drainage basins, most of which were extremely small polygons covering the coastal regions. To simplify the model and reduce the data size, we keep only the 0,001% of the coastal drainage basins that are the biggest, i.e., 1440 polygons. They accounted for more than 93% of the total surface covered by the initial set of polygons. Finally, we matched all the coastal drainage basins to the sea in which they discharge: Baltic Sea (“Baltic”), North Sea (“North”) or Norwegian Coastal Current (“NCC”).

Information on land cover, i.e. the proportion of forest, shrubland and cropland, were obtained from the HILDA+ database (Winkler et al. 2021). HILDA+ is a reconstruction of land use and land cover in the past, using a limited number of categories: forest, grassland/shrubland, pasture, cropland, urban area, and water. This database was first constructed from 1960 to 2019, and then expanded to include data back to 1890. The

proportion of each land cover category for both catchment polygons and coastal drainage basin polygons were extracted and averaged over a 10-year period centred around 1899, 1909 etc., until 2019.

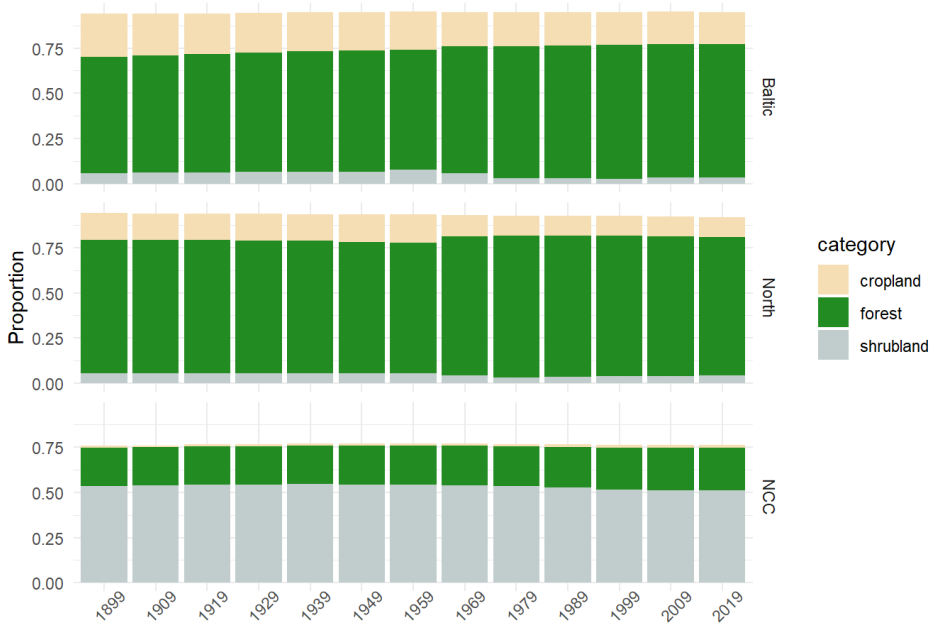

Figure 1 - Evolution of the proportion of forest, cropland and shrubland during the 20th century, grouped by sea drainage area.

Figure 2 - Evolution of surface runoff during the 20th century, grouped by sea drainage area.

We used historical surface runoff from the NorESM2 model (Seland et al. 2020), conducted as part of the Coupled Model Intercomparison Project phase 6 ensemble (World Climate Resarch Program n.d.). The historical model runs until 2015. Since the historical model runs were not available for the ten-year period around 2019, we used a model run with the parameters for the Shared Socioeconomic Pathway SP 2-4.5 (SSP 2-4.5). This run considers the impact of COVID-19 events and was also conducted using the NorESM2 model. As for the land-cover data, we averaged the layers corresponding to each decade and extracted the average value for all the polygons in the study.

Historical sulphur deposition was extracted from a historical model calculated for the Coupled Model Intercomparison Project Phase 5 (CMIP5) model ensemble. This model was run using the previous version of NorESM (Bentsen et al. 2013), and covers the period 1850-2005. The average sulphur deposition for the decades around 1999, 2009 and 2019 was extracted from EMEP model results (EMEP 2022). For all models, we added dry and wet deposition of SO_2 and SO_4 to obtain total sulphur deposition in mg/m2/s, that we converted in mg/m2/year. We compared the value for the 1999 decade obtained from the historical model and obtained from the EMEP model to ensure the continuity of the data. The result is presented in Figure 3.

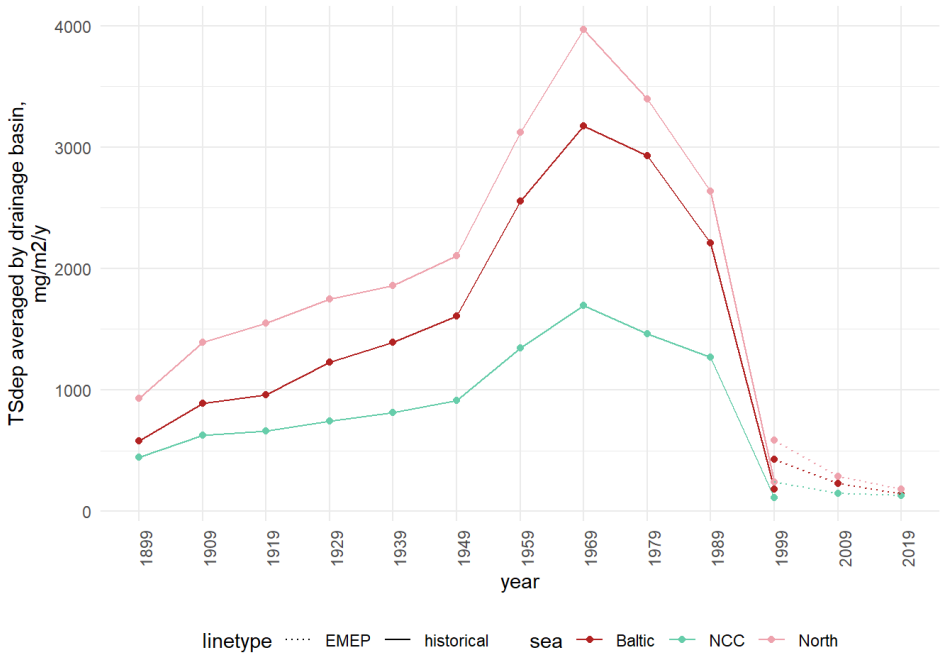

Figure 3 –Total sulphur deposition, averaged by decade and grouped by sea drainage area. The full line represents the historical model (CMIP5), and the dotted line represents the EMEP model. We used the EMEP value for 1999 to ensure good continuity between CMIP5 and EMEP models.

We fitted a linear model using the proportion of forest, cropland and shrubland, total sulphur deposition and surface runoff as predictors for TOC concentration. This model was fitted using the base package in R. The distribution of TOC, runoff and sulphur deposition were normalized by taking the log10 of each variable. Following Crapart et al. (2023), we also fitted a spatial error model with the same predictors, using the package "spatialreg" in R (Bivand 2019).

Then, using the resulting model, we predicted the average TOC concentration for each coastal drainage basins and each decade. The predictions were grouped depending on the sea in which each basin drained: Baltic Sea, North Sea/Skagerrak, and Norwegian Coastal Current. The average TOC concentration was multiplied by the average surface runoff and the area of the corresponding coastal drainage basin to obtain the average TOC export to the sea.

We compared the results of the hindcast to actual measurements of coloured dissolved organic matter in Swedish rivers. Observations from the early 20th century originate from a study conducted by Erikkson in 1929, which data was digitalized by the Swedish University of Agricultural Sciences (Eriksson 1929). Observations dating from after 1950 were extracted from the Swedish University of Agricultural Sciences database (SLU 2020). Erikkson data is provided as chemical oxygen demand, first measured with KMnO4 (1909-1915), then as CODMn (1916-1925). SLU data also uses both methods, with KMnO4 data from 1959 to 2022 and CODMn data from 2003 to 2021). To compare, we used the CODMn data from SLU. CODMn in mgO/L is obtained from KMnO4 by multicating the amount of potassium permanganate added by 3.95 (Wilander 1988). In boreal freshwaters, the COD/TOC is close to 1 (Erlandsson et al. 2008; Räike et al. 2012). Therefore, we chose to directly compare the measured COD (in mgO/L) to the predicted TOC (in mgC/L).

We reconstituted stime series for the rivers sampled by Eriksson et al. by matching their sampling coordinates to the sampling coordinates of the rivers sampled after 1950, using a 5 km radius around the original sampling point. We also averaged all the available datapoints sampled during the same decade in each of the coastal drainage basin, to compared it with the value predicted by the model. For this second comparison, we only kept rivers and lakes for which more than 20 datapoints were available, over at least four decades in a row, before averaging all the values in the same coastal drainage basin.

All the data cleaning, analysis and visualization was done in R (R Core Team 2023).

Results

The analysis of the models revealed that both the linear model (LM) and the spatial error linear model (SELM) accurately fitted the training dataset, as indicated by low Akaike Information Criterion (AIC) values and normally distributed residuals. Consistent with the findings of Crapart et al. (2023), the proportion of forest, cropland, and shrubland showed a positive impact on the concentration of total organic carbon (TOC) in both models. Conversely, surface runoff had a negative coefficient, indicating a dilution effect on TOC concentration, which was found to be more significant than its contribution to TOC transportation.

However, a discrepancy arose when analysing the coefficient for total sulphur deposition in the SELM. Contrary to the expected negative relationship observed in previous studies (Finstad et al. 2016; Heleen A. De Wit et al. 2007; Monteith et al. 2007)., the SELM yielded a positive coefficient, suggesting that increased sulphur deposition would lead to higher TOC concentration. In contrast, the LM aligned with the theoretical expectation by attributing a negative coefficient to total sulphur deposition. Therefore, we discarded the SELM and used the LM to predict the average TOC concentration and export for each decade. The hindcast, grouped by sea drainage area, are presented on Figure 4

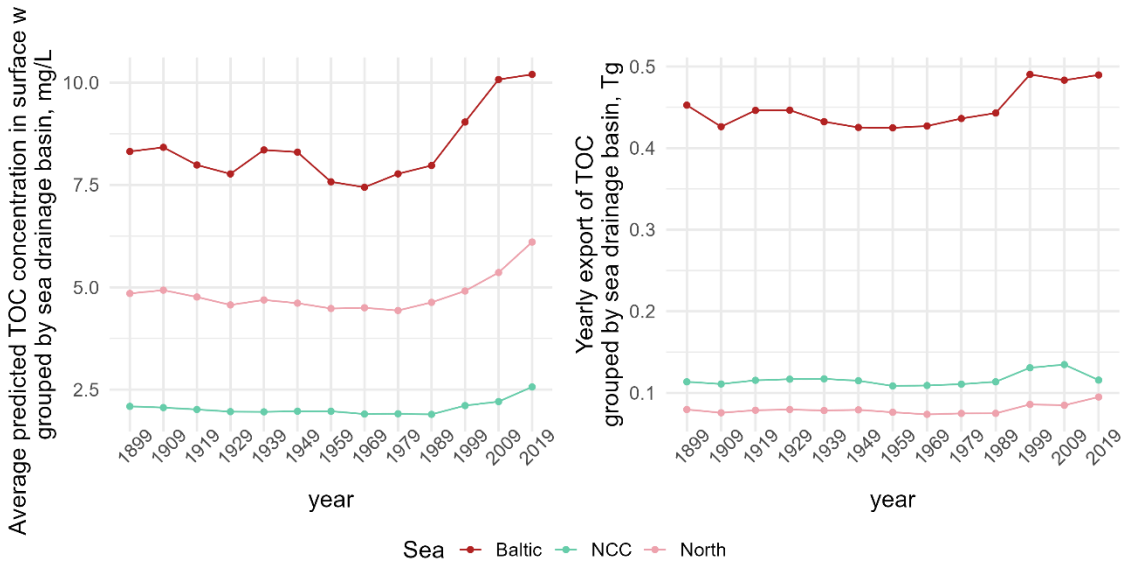

Figure 4 - Predicted TOC concentration (mg/L) and export by surface runoff (Tg/year), grouped by drainage basin

The fluctuations in TOC concentration can largely be explained by the changes in total sulphur deposition. A notable pattern is the sharp increase in TOC concentration after 1990, coinciding with a decline in sulphur deposition level. This is especially evident in the Baltic Sea basin. In addition, the proportion of forest in the catchment area gradually

increased after 1959, reaching a plateau approximately 20 years later. However, the positive impact of this forest expansion on TOC concentration becomes noticeable only after 1990, suggesting that the acid deposition from previous years may have delayed the response. The fluctuations in TOC concentration and export before 1950 are likely influenced by variations in average runoff for each decade. Changes in runoff levels during these periods likely contribute to the observed fluctuations in TOC concentration and subsequent export to the sea.

16 rivers were sampled both in the Eriksson survey between 1916 and 1925 and by the Swedish University of Agricultural sciences after 1950 (SLU 2020). The time series were assembled, and the average annual TOC concentration for the selected rivers was compared with the average TOC concentration in the corresponding coastal drainage basin. The results are presented on Figure 5. The observations for each river were fitted by a "loess" smooth to visualize the changes. The line representing the period between 1930 and 1980 is only indicative, due to the lack of data. Nevertheless, the observed TOC concentrations mostly fitted our hindcast. For some rivers, like Tidan or Närkes Svartå, the measured TOC increased a lot faster than the predicted average TOC. For others, like Tornehalven, the trend was similar but the observations lower than the predicted average TOC.

When averaging the available observations within each coastal drainage basin, the focus was primarily on comparing the absolute total organic carbon (TOC) concentrations observed after 1950. The analysis revealed that the model fit was generally better in the northern regions compared to the southern regions. In the northernmost coastal drainage basin, the predicted average TOC concentrations closely aligned with the observed values. The model performed well in capturing the TOC dynamics in this region. However, in the southern coastal drainage basins, the average predicted TOC concentrations consistently appeared to be underestimated. In some cases, the predicted values were approximately half of the observed concentrations. It is important to note that the observed average values are derived from a subset of lakes and rivers within the catchment that were regularly sampled, and that the model was primarily fitted using TOC from lakes while the comparison with real observation includes mainly rivers. Therefore, the observed averages may not represent the entire range of TOC concentrations in the catchment. A comparison of the river catchments compared to the corresponding coastal drainage basin is shown on Table 3. The rivers catchments were obtained from SMHI.

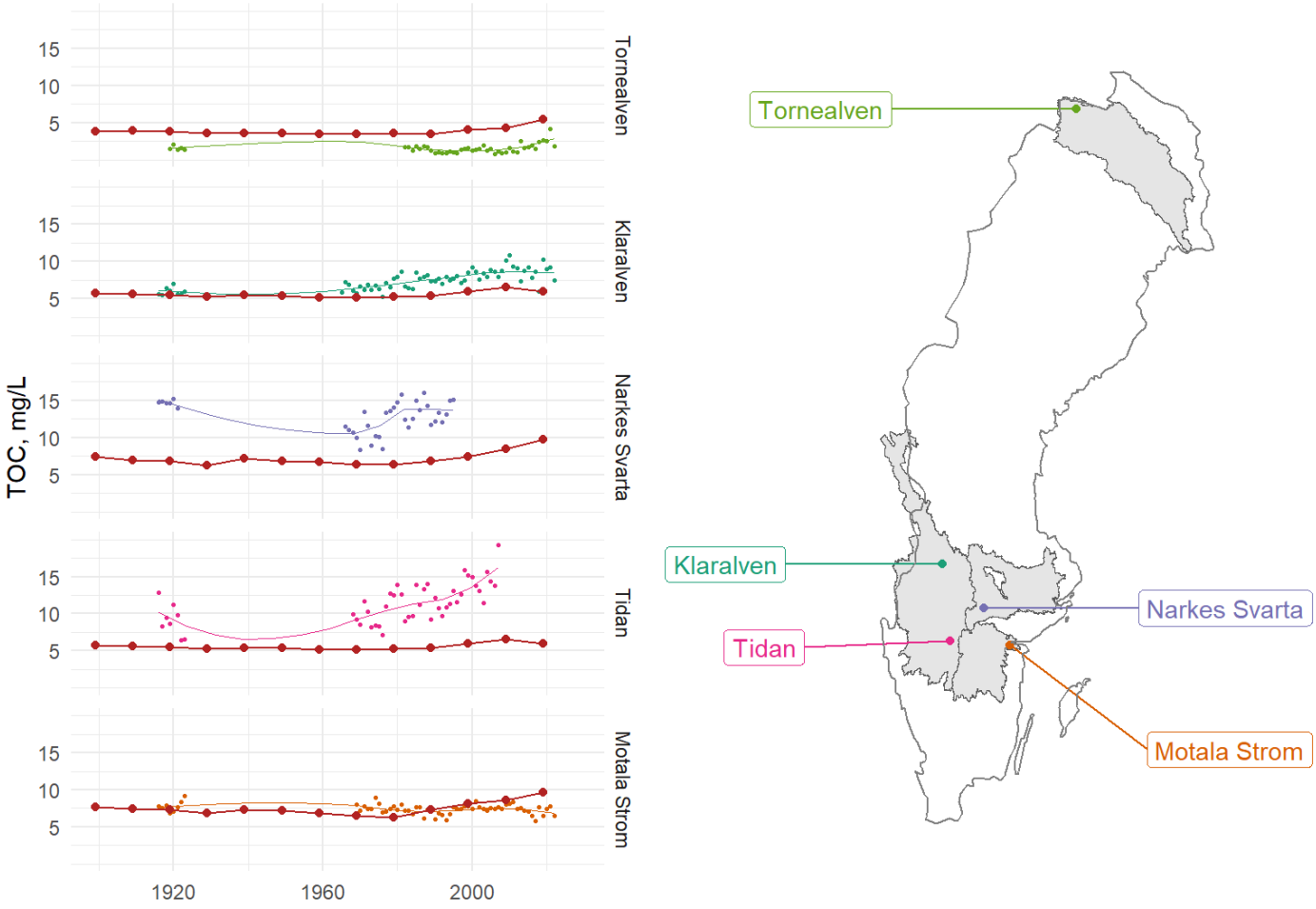

Figure 5 – Evolution of TOC concentration by decade in selected Swedish rivers. In red, the predicted values for the corresponding coastal drainage basin are represented. The observed TOC concentrations are smooth with a loess function, represented by a coloured line.

Table 3 – Characteristics of rivers catchments (from SMHI), compared to the corresponding coastal drainage basin (from NOFA)

River name	Forest, %	Shrubland, %	Cropland %	Catchment area, km2	Average runoff, mm/y	Average TSdep, mg/y
Tornehalven	0.20	0.28	0.0.03	2754	129.5	135.4
Drainage basin	*51.1*	*35.1*	*0.0*	*28261.1*	*166.2*	*106.7*
Klarälven	0.84	0.06	0.02	9493	48.9	467.7
Tidan	0.27	0.02	0.26	940	44.4	424.4
Drainage basin	*0.64.7*	*8.5*	*10.4*	*47556.5*	*84.1*	*371.6*
Narkes Svartå	0.43	0.05	0.0.06	3153	64.4	373.0
Drainage basin	*65.0*	*1.0*	*22.2*	*21527.1*	*75.5*	*349.1*
Motala Ström	0.0	0.2	17.9	3616	48.8	423.1
Drainage basin	*64.7*	*0.5*	*15.9*	*15965.4*	*45.6*	*404.8*

The presence of two of the largest Swedish lakes in the represented coastal drainage basins, namely Vänern in basin 167089 and Vättern in basin 264568, introduces an additional factor to consider. These lakes receive approximately 25% of their water input directly from precipitation, which dilutes the contributions from rivers. In basin 167089, the average predicted TOC concentration does not exceed 8 mg/L at its peak while the observations reach 15 mg/L. Since the model is fitted on lakes and the observations come from rivers, we can conclude that rivers are more directly affected by the surrounding changes compared to these large lakes.

Conclusion

Our findings indicate that a linear model including catchment characteristics as predictors was successful in hindcasting the TOC dynamic in the past. While absolute predicted TOC concentrations must be interpreted with caution, due to the use of averages, our results consistently exhibit the correct order or magnitude and follow the historical trend.

It is acknowledged that a large part of the organic carbon will undergo mineralization or sedimentation processes on their way to the sea. However, we computed the export to the sea as the average TOC concentration in freshwater for a given costal drainage basin, multiplied by surface runoff and area of this basin, without considering these potential sinks. However, we consider the computed export values reasonably close to reality, as the average concentration over the catchment was often under observed averages.

This study shows that the space-for-time approach yields satisfactory results in predicting TOC concentration back in time, given that land cover indicators, together with surface runoff and atmospheric deposition, are included in the model.

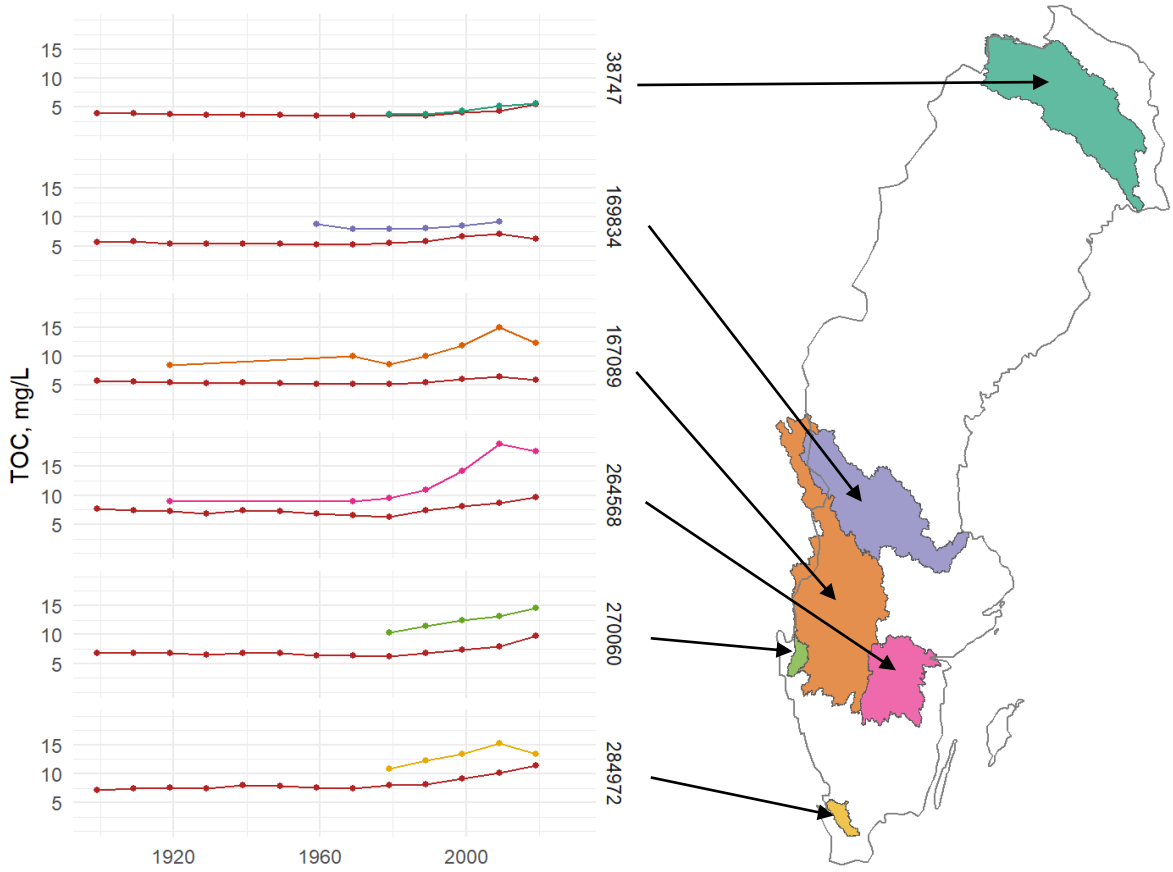

Figure 6 - Evolution of observed average TOC concentration (coloured) and predicted average TOC concentration (red) in selected coastal drainage basins, in mg/L

References

Bentsen, M., I. Bethke, J. B. Debernard, T. Iversen, A. Kirkevåg, Ø. Seland, H. Drange, et al. 2013. "The Norwegian Earth System Model, NorESM1-M – Part 1: Description and Basic Evaluation of the Physical Climate." *Geoscientific Model Development* 6 (3): 687–720. https://doi.org/10.5194/gmd-6-687-2013.

Bivand, Roger. 2019. "Estimation Methods for Models of Spatial Interaction." *CRAN - R Package*. https://doi.org/10.1080/01621459.1975.10480272.

Crapart, Camille, Anders G. Finstad, Dag O. Hessen, Rolf D. Vogt, and Tom Andersen. 2023. "Spatial Predictors and Temporal Forecast of Total Organic Carbon Levels in Boreal Lakes." *Science of the Total Environment* 870 (April): 161676. https://doi.org/10.1016/j.scitotenv.2023.161676.

EMEP. 2022. "EMEP MSC-W HOME." 2022. https://emep.int/mscw/mscw_moddata.html#Comp.

Eriksson, J.V. 1929. "Den Kemiska Denudationen i Sverige (The Chemical Denudation of Sweden)." Stockholm. http://info1.ma.slu.se/max/www_max.acgi$Project?ID=Intro&pID=23.

Finstad, Anders G. 2017. "Environmental Data · NINAnor/NOFA Wiki." 2017. https://github.com/NINAnor/NOFA/wiki/Environmental-data.

Finstad, Anders G., Tom Andersen, Søren Larsen, Koji Tominaga, Stefan Blumentrath, Heleen A. De Wit, Hans Tømmervik, and Dag Olav Hessen. 2016. "From Greening to Browning: Catchment Vegetation Development and Reduced S-Deposition Promote Organic Carbon Load on Decadal Time Scales in Nordic Lakes." *Scientific Reports* 6:31944 (7485): 1–8. https://doi.org/10.1038/srep31944.

Henriksen, Arne, Brit Lisa Skjelvåle, Jaakko Mannio, Anders Wilander, Ron Harriman, Chris Curtis, Jens Peder Jensen, Erik Fjeld, and Tatyana Moiseenko. 1998. "Northern European Lake Survey 1995: Finland, Norway, Sweden, Denmark, Russian Kola, Russian Karelia, Scotland and Wales." *Ambio* 2 (27): 80–91. https://www.jstor.org/stable/4314692.

Larson, Magnus. 2012. "Sweden's Great Lakes." In *Encyclopedia of Lakes and Reservoirs*, 761–64. Springer, DOrdrecht. https://doi.org/10.1007/978-1-4020-4410-6_269.

Monteith, D. T., J. L. Stoddard, C. D. Evans, H. A. De Wit, M. Forsius, T. Høgåsen, A. Wilander, et al. 2007. "Dissolved Organic Carbon Trends Resulting from Changes in Atmospheric Deposition Chemistry." *Nature* 450 (7169): 537–40. https://doi.org/10.1038/nature06316.

R Core Team. 2023. "R: A Language and Environment for Statistical Computing." Vienna, Austria: R Foundation for Statistical Computing. https://www.r-project.org/.

Seland, Øyvind, Mats Bentsen, Dirk Olivié, Thomas Toniazzo, Ada Gjermundsen, Lise Seland Graff, Jens Boldingh Debernard, et al. 2020. *Overview of the Norwegian Earth System Model (NorESM2) and Key Climate Response of CMIP6 DECK, Historical, and Scenario Simulations*. *Geoscientific Model Development*. Vol. 13. https://doi.org/10.5194/gmd-13-6165-2020.

SLU. 2020. “Miljödata MVM.” Swedish University of Agricultural Sciences. 2020. https://miljodata.slu.se/MVM/Search.

Winkler, Karina, Richard Fuchs, Mark Rounsevell, and Martin Herold. 2021. “Global Land Use Changes Are Four Times Greater than Previously Estimated.” *Nature Communications* 12 (1): 1–10. https://doi.org/10.1038/s41467-021-22702-2.

Wit, Heleen A. De, Jan Mulder, Atle Hindar, and Lars Hole. 2007. “Long-Term Increase in Dissolved Organic Carbon in Streamwaters in Norway Is Response to Reduced Acid Deposition.” *Environmental Science and Technology* 41 (22): 7706–13. https://doi.org/10.1021/es070557f.

World Climate Resarch Program. n.d. “CMIP6.” Accessed March 3, 2022. https://www.wcrp-climate.org/wgcm-cmip/wgcm-cmip6

Paper 1: Spatial Predictors and Temporal Forecast of Total Organic Carbon Levels in Boreal Lakes.

Crapart Camille, Anders G. Finstad, Dag Olav Hessen, Rolf David Vogt, and Tom Andersen. 2023.

Science of the Total Environment 870

Photos: Camille Crapart/ Alexander Håland

Science of the Total Environment 870 (2023) 161676

Contents lists available at ScienceDirect

Science of the Total Environment

journal homepage: www.elsevier.com/locate/scitotenv

Spatial predictors and temporal forecast of total organic carbon levels in boreal lakes

Camille Crapart [a,*], Anders G. Finstad [b], Dag O. Hessen [c], Rolf D. Vogt [d], Tom Andersen [c]

[a] Department of Chemistry and Centre for Biogeochemistry in the Anthropocene, University of Oslo, P.O. Box 1033, 0315 Oslo, Norway
[b] Department of Natural History, Centre for Biodiversity Dynamics, Norwegian University of Science and Technology, 7491 Trondheim, Norway
[c] Department of Biosciences and Centre for Biogeochemistry in the Anthropocene, University of Oslo, P.O. Box 1066, 0316 Oslo, Norway
[d] Norwegian Institute for Water Research, Økernveien 94, 0579 Oslo, Norway

HIGHLIGHTS

- TOC concentration in boreal lakes depends on catchment characteristics, in particular on standing biomass.
- A space-for-time approach proves successful to predict future TOC concentration.
- Climate change > 4.5°C will lead to a strong increase in browning of freshwater and export of TOC to coastal waters.

GRAPHICAL ABSTRACT

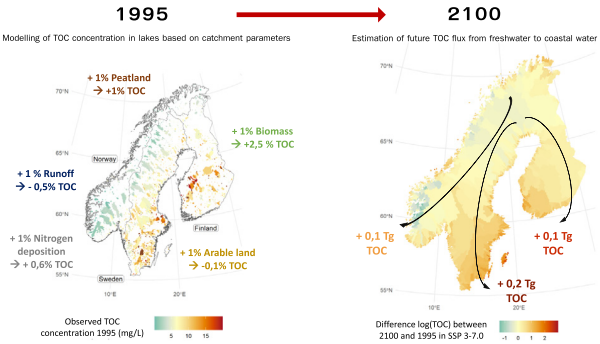

ARTICLE INFO

Editor: Ouyang Wei

Keywords:
TOC
Boreal lakes, catchment characteristics
Forecast
Coastal darkening

ABSTRACT

Browning of Fennoscandian boreal lakes is raising concerns for negative ecosystem impacts as well as reduced drinking water quality. Declined sulfur deposition and warmer climate, along with afforestation, other climate impacts and less outfield grazing, have resulted in increased fluxes of Total Organic Carbon (TOC) from catchments to freshwater, and subsequently to coastal waters. This study assesses the major governing factors for increased TOC levels among several catchment characteristics in almost 5000 Fennoscandian lakes and catchments.

Normalized Difference Vegetation Index (NDVI), a proxy for plant biomass, and the proportions of peatland in the catchment, along with surface runoff intensity and nitrogen deposition loading, were identified as the main spatial predictors for lake TOC concentrations. A multiple linear model, based on these explanatory variables, was used to simulate future TOC concentration in surface runoff from coastal drainage basins in 2050 and 2100, using the forecasts of climatic variables in two of the Shared Socio-economic Pathways (SSP): 1-2.6 (+2 °C) and 3-7.0 (+4,5 °C). These scenarios yield contrasting effects. SSP 1-2.6 predicts an overall decrease of TOC export to coastal waters, while SSP 3-7.0 in contrast leads to an increase in TOC export.

1. Introduction

In many boreal lakes, including Fennoscandian (Finland, Sweden, and Norway), a widespread browning of freshwater has been observed in the last decades. This phenomenon is caused by the increased flux of colored natural organic matter (NOM) from catchments to rivers and lakes (Monteith et al., 2007), and enhanced by a concurrent increase in iron

Abbreviations: TOC, Total Organic Carbon; NDVI, Normalized DIfference Vegetation Index.

* Corresponding author.
E-mail address: c.m.crapart@kjemi.uio.no (C. Crapart).

http://dx.doi.org/10.1016/j.scitotenv.2023.161676
Received 16 September 2022; Received in revised form 21 December 2022; Accepted 13 January 2023
Available online 31 January 2023

(Monteith et al., 2007, Xiao and Riise, 2021, Björnerås et al., 2017, Solberg, 2022). This upward trend in total organic matter (TOC) has been recorded since the 1980s when several monitoring programs were implemented to document the effect of acid deposition abatement policies. The changes in water quality in Norway were also assessed by regional synoptic surveys in 1986 (Henriksen et al., 1989), in 1995 (Northern European Lake Survey, (Henriksen et al., 1998), and in 2019 (Hindar et al., 2020, De Wit et al., 2023). The 1986-study covered 1000 lakes in Norway, while the 1995 survey included also almost 4000 lakes in Sweden, Finland, Denmark, as well as Scotland, Wales and Russian Kola and Karelia, while the 2019 survey again covered the 1000 Norwegian lakes. There was a 50 % decrease in sulfur deposition between the period 1976–85 and the period 1995–2001 (Skjelkvåle, 2003; Aas et al., 2002; Fagerli et al., 2022). This caused an increased solubility of NOM, thereby increasing the concentration of TOC in surface waters (De Wit et al., 2007; Monteith et al., 2007). Sulfur deposition is now back to preindustrial levels, meaning that any further reductions are considered to be marginal (Grennfelt et al., 2020). On the contrary, there are larger uncertainties regarding the reactive nitrogen deposition, which has not decreased as much as the sulfur. This nitrogen contributes both to soil and water acidification (Kanakidou et al., 2016), and promotes the net primary production of forests (Schulte-Uebbing and de Vries, 2018). A potential further increase in surface water NOM will likely not be driven by a further decrease in sulfur deposition, but by other factors, such as changes in nitrogen deposition, hydrology, and temperature, as well as re −/afforestation and other land use changes.

Increased surface runoff is expected to lead to increased flux of NOM from the forest floor to surface waters (De Wit et al., 2016). Higher temperatures provide longer growing seasons. This increases the primary production and thereby the amount of biomass in the catchments, as well as enhanced heterotrophic decomposition of the organic matter. Inherently, this leads to an increased flux of NOM to surface waters causing increased browning (Finstad et al., 2016; Kritzberg et al., 2020; Larsen et al., 2011a). Finstad et al. (2016) modelled the increase of TOC concentrations in 70 Norwegian lakes over 30 years. They found that a temporal increase in Normalized Difference Vegetation Index (NDVI), along with increasing temperature, were the main temporal explanatory parameters for the observed increase in freshwater TOC concentration. NDVI is used as a proxy for the density of vegetation (primarily forest) biomass (Beck et al., 2007). Accumulated reactive nitrogen from long-range atmospheric deposition is also expected to contribute to an increase in biomass (Vries and Schulte-Uebbing, 2019). The intensification of forest management in the 1950ies and 60ies increased the forest volume in Nordic countries. Moreover, abandonment of out-field resources as grazing pastures for husbandry, has resulted in increased standing forest biomass during the last centuries (Myrstener et al., 2021). In the coming decades, afforestation is expected to expand further, as the governments of Norway, Sweden, and Finland (collectively referred to here as Fennoscandia) consider forest as a necessary trade-off leverage for offsetting their carbon emissions and reaching their zero-emission goals (Nordic Council of Ministers, 2021; Vogt et al., 2022). Coniferous forests build up a thick layer of organic soil that increases the amount of NOM available for lateral transport (Škerlep et al., 2020). In addition, practices such as clear-cutting and peatland ditching are likely to promote the release of NOM towards the water system (Nieminen, 2004; Asmala et al., 2019; Finér et al., 2021).

The planned intensification of forest management and re-/afforestation has raised concern for possible effects on water quality (Norsk Vann, 2019). Raw water sources used for producing drinking water in Fennoscandia are predominantly surface waters. Browning has thus a potential impact on the water treatment to ensure potability of water (Eikebrokk et al., 2004). In addition, browning has a suite of ecosystem impacts in lakes, e.g., by increasing light absorbance, and thus reducing primary production (Karlsson, 2007; Thrane et al., 2014). Moreover, the increased influx of allochthonous NOM boosts the heterotrophic degradation, causing increased CO_2 and CH_4 emissions, especially in small lakes (Hessen et al., 1990; Tranvik et al., 2009; Wit et al., 2018; Yang et al., 2015). Increased browning also extends the duration of thermal stratification and affects fish, both via the reduced primary production, but also by the darkening affecting predators by hampering visual hunting (Craig et al., 2017; Finstad et al., 2014; Karlsson et al., 2009). Monitoring of the Secchi depth in the Baltic Sea have shown that the coastal water has steadily become less transparent since the beginning of the 20th century (Fleming-Lehtinen and Laamanen, 2012). Browning of freshwater lakes and rivers cascade along the aquatic continuum from rivers to the coast (Opdal et al., 2019). Increased NOM in surface freshwater thus inherently leads to an increased export of NOM to the coastal water, subsequently causing coastal darkening (Aksnes et al., 2009).

Identifying the governing factors for NOM concentration in space and time and understanding their role under changing anthropogenic and climatic pressures is therefore a prerequisite to forecasting NOMs potential detrimental effects to the water quality and ecosystem services.

Larsen et al. (2011a) developed an empirical model predicting the spatial distribution of TOC concentrations in the 1000 Norwegian lakes of the 1995 Northern European Lake Survey (Henriksen et al., 1998). The model was based on lake catchment characteristics, using catchment NDVI, area fractions of peat (Bog) and area specific surface runoff intensity (Runoff) as predictors. This study concluded that NDVI was a key predictor of surface water TOC concentration, as NDVI explained, together with Bog and Runoff, nearly 80 % of observed spatial variation in TOC.

The 1000 lakes used to fit the model by Larsen et al. cover a very heterogeneous landscape, comprising large gradients in NOM, relative forest and bog coverage, and mean surface runoff, as well as length of growing season, with extensive subalpine and alpine areas. For this reason, the model predictions may not be representative of the more homogeneous boreal biome at large. To test the assumption that the key catchment properties NDVI, Bog and Runoff can serve as explanatory predictors for TOC concentrations at wider spatial scale, this study includes an additional 3735 lakes and their catchments properties from Sweden and Finland. These additional catchments represent more uniform topography and runoff, situated in low-altitude land of Sweden and Finland, with more productive forests, and with extensive areas of bogs. Other conceptually relevant predictors at the catchment level were also included in this study: i.e., mean temperature (Temp) and amount of rain (Precip), proportion of forest (Forest) and farmland (Arable), as well as total nitrogen (TNdep) and sulfur deposition (TSdep).

A Spatial Error Linear Model (SELM) is used as a modelling tool to account for the spatial autocorrelation of the response and predictor variables. The fitted TOC model, built on the optimum set of predictors, is validated on data from the recent re-sampling of the 1000 lakes in Norway (Hindar et al., 2020). Based on the model, the effect size (i.e., relative effect on TOC) of a relative increase of each of the predictor variables are estimated. The model is also used to forecast future average TOC concentration in an ensemble of Fenno-Scandinavian watersheds draining into the sea (here referred to as “coastal drainage basins”). Following the IPCC AR6 report (Masson-Delmotte et al., 2021), two global warming scenarios are considered: i.e., the SSP 1.2-6 scenario, with global warming limited to <2 °C, and the SSP 3-7.0 where global warming can reach up to 4 °C. Finally, these scenarios are compiled to estimate the future export of TOC from Fennoscandian peninsula into its coastal waters.

The aim of the study is to test two distinct hypotheses: 1) that a space-for-time approach, using a spatial “snap-shot” to predict temporal changes, can produce realistic forecast results; and 2) that global warming, including increased surface runoff, together with land-use changes, with increased standing biomass, is likely to exacerbate the ongoing browning of freshwaters and, subsequently, also coastal darkening.

2. Methods

2.1. Data preparation

The main water chemistry dataset assessed in this study (training dataset) comprised the data from 4735 lakes sampled during the Northern

European Lake Survey in 1995 (Henriksen et al., 1998). Except for one outlier, the smallest catchments areas started from 3500 m^2, while the largest watershed was over 5106 km^2. The average being 107 km^2, with a standard deviation of 416 km^2. TOC concentration in each lake, as well as catchment polygons defined with a digital elevation model, were downloaded from the NOFA database (Finstad, 2017). Nine explanatory parameters, describing each of the lake catchments, were compiled as predictor variables: i.e., NDVI; Forest, Arable and Bog; Runoff, Precip and Temp; TNdep and TSdep. These are briefly described below. Lake morphology parameters, such as lake depth, were not available for the Northern Lake Survey dataset and thus not included in the analysis. The complete procedure for preparation, extraction, and compilation, as well as the sources of data are described in Supplementary 1.

The test dataset, provided by the Norwegian Institute for Water Research (NIVA), comprised 1001 lakes sampled in 2019 (Hindar et al., 2020). The sampled lakes were essentially the same ones as for the Norwegian lakes in the training data set. In both surveys, the sampling was completed in the autumn, after the seasonal turnover, so that the surface sample represents the entire water column (De Wit et al., 2023). Each lake of the test dataset was matched with the corresponding lake of the 1995 training dataset, in order to use the same catchment polygons, from the NOFA database (see Supplementary 2).

Some of the variables were not strongly asymmetrical and were log-transformed using the natural logarithm, simply denoted "log" hereafter.

- Total organic carbon (TOC) concentration in mg C/L (Fig. 2) were extracted from the Northern European Lake Survey dataset from 1995 (Henriksen et al., 1998; Finstad, 2017) and from the 1000-lakes-survey in 2019 (Hindar et al., 2020). As the TOC concentration values were skewed, the data were log-transformed (logTOC) to normalize the distribution.
- Normalized difference vegetation index (NDVI) (Fig. 1a) for the summer months (June, July, and August) were downloaded from the GIMMS database (The National Center for Atmospheric Research (2018)) and averaged for 1994, i.e., the year preceding sampling of the Northern European Lake Survey. For the 2019 dataset, data from 2015 are used, as it was the latest available year in the GIMMS database.
- Mean area specific surface runoff (Runoff) values in mm/y (Fig. 1b) were derived from the CORDEX historical model. The period 1970–2000 was used for the 1995 data, and the period 1985–2015 was used for the 2019 data (CORDEX, 2021; Kreienkamp et al., 2012). As the surface runoff intensities were skewed the data were log-transformed (logRunoff).
- Mean annual precipitation (Precip) in mm/y (Fig. 1c) and temperature (Temp) in °C (Fig. 1d) for the years 1970 to 2000 were downloaded from the WorldClim database (WorldClim, n.d.) to be used as representative for the 1995 data. As the precipitation distribution was not normally distributed the data were log transformed (logPrecip). As these climate data were not retained in the final model, they were not downloaded for the 2019 data.
- Proportions of peatland (Bog), arable land (Arable) and forested area (Forest) (Fig. 1e, f, and g, respectively) within each catchment are computed from the Corine Land Cover (CLC) database (Copernicus Land Monitoring Service, n.d.), and correspond to the data of 2000, as land use data prior to this were not available. Several CLC categories were merged to create the three categories used in this study (see Supplementary 1). For the 2019 dataset, Corine Land Cover data for 2018 were used. Although distributions of the different land use are not normally distributed, they were not log-transformed due to many zeros in the data. Other transformations (square, square roots) did not contribute to normalizing the distribution.
- Total reactive nitrogen deposition (TNdep) in $mg.N/m^2$ and total sulfur deposition (TSdep) data in $mg.\ S/m^2$ (Fig. 1h and i, respectively) were extracted from EMEP models as the sum of dry and wet deposition (EMEP, 2022; "The Unified EMEP Model-User Guide", 2012). Data from 2000 were used as these were the earliest available data, resulting in a slight underestimation of TNdep and TSdep since deposition has decreased since the 90s. For the 2019 dataset, EMEP data from 2019 were used.

2.2. Spatial TOC models

Larsen et al. (2011b) used a Multiple Linear regression model (LM) to predict the effect of climate change on the spatial distribution of TOC concentration in 1000 Norwegian lakes. In the present study, including in addition almost 4000 lakes in Sweden and Finland, a similar linear model is reproduced to investigate the explanatory value of the three predictors selected by Larsen et al. (i.e., NDVI, Bog and Runoff), along with other conceptually relevant predictors, for explaining the spatial differences in TOC levels in Fennoscandian lakes. All the statistical analysis were performed in R, version 4.1.2. (R Core Team, 2021).

The spatial autocorrelation of all predictors were determined by computing Moran's I (see details in Supplementary 4). All variables were found to be spatially autocorrelated. To take this into account, a Spatial Error Linear Model (SELM) was fitted with the same predictors as for the LM and the results compared. SELM was fitted using the "errorsarlm" function from the "spatialreg" package, version 1.1-8 (Bivand, 2019). Akaike Information Criterion (AIC) was used to compare the performances of the models.

The SELM and LM models are fitted on the 1995 training dataset and their slope estimates (i.e., slope β as in the simple model $y = \beta x + c$) were evaluated both on scaled and unscaled variables. Scaled estimates β (i.e., computed with centered and standardized variables) expresses the response variable change in standard deviation units per unit standard deviation change in the predictor variable, while unscaled estimates were used to compute effect sizes (expressing the relative change in the response variable for a given change in the predictor). Equations used to calculate effect size for each pair of response/predictor variables are explained in Supplementary 4.

The 2019 dataset of the 1000 Norwegian lakes survey (Hindar et al., 2020) was used to perform a test of the space-for-time model. The model fitted on the Fennoscandic 1995 data was used to predict TOC concentration values in the 1001 lakes in 2019, and the results were compared with actual observations.

2.3. Forecast of TOC prediction in coastal drainage basins

Changes in TOC concentrations in costal drainage basins by year 2100 are predicted using the validated SELM. Polygons representing the coastal drainage basins were used to cover the whole territory of Fennoscandia, not only the studied lakes catchments. These basins are the ensemble of the watercourses that drains into the sea within a coastal section (NVE, n.d.). The coastal drainage basins were defined using an elevation model delineated from a 10 m digital terrain model obtained from The Norwegian, Swedish and Finnish Mapping Authorities (Finstad, 2017). After cleaning, the dataset is composed of 1392 watershed polygons (see Supplementary 3). The smallest coastal drainage basin has an area of 27 km^2, the largest has an area close to 49,000 km^2, while the mean area is 751 km^2 with a standard deviation of 3723 km^2.

Future changes in climate parameters are based on predicted changes in climate drivers derived from the Coupled Model Intercomparison Project (Phase 6) (CMIP6), run by the World Climate Research Program (World Climate Research Program, n.d.) using two different SSPs (Riahi et al., 2017): SSP1-2.6 as the best scenario, assuming the average global warming will be limited to <2 °C, and SSP 3-7.0 as our worst-case scenario (CORDEX, 2021; Hausfather, 2019). Several institutions run the CMIP6 models to forecast future climate. Based on Raju and Kumar (2020), results from the model developed by the Centre National de Recherches Météorologiques (CRNM) were selected to extract future surface runoff intensity.

There is no forecast for NDVI in CMIP6. Summer NDVI values for 2050 and 2100 were instead predicted using a polynomial model based on forecast for temperature and precipitations in the period 2041–2060 and for the period 2081–2100. This model was fitted using summer months

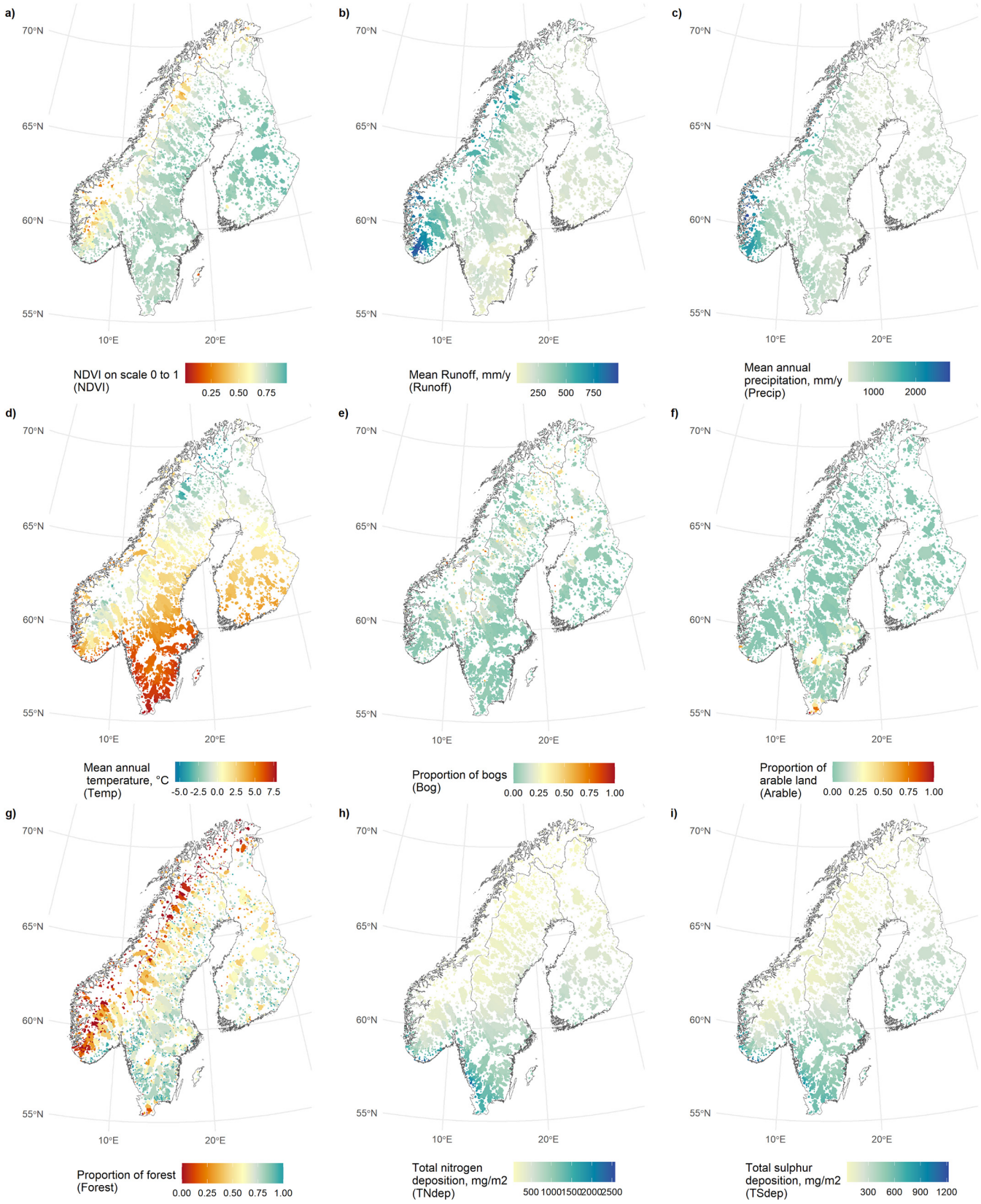

Fig. 1. Maps of the predictor variables: summer NDVI in 1994 (a); mean surface runoff intensity (Runoff, b), temperature (Temp, c), mean annual precipitation (Precip, d) from 1970 to 2000; proportion of peat (Bog, e), proportion of forest (Forest, f), proportion of arable land (Arable, g) for the year 2000; total nitrogen deposition (TNdep, h) and total sulfur deposition (TSdep, i) in the 4735 lake studied catchments in 2000.

NDVI, temperature and precipitations in 1995. The predicted future temperature and precipitation values were extracted from the CRNM model. Modelled summer NDVI and changes in this NDVI in the future are shown in Supplementary 3.

TNdep is also not modelled for the future and is estimated depending on the SSP. Between 2000 and 2020 the TNdep decreased due to reduced emission of both reduced (NH_3) and oxidized nitrogen (NOx), by respectively 8 and 42 % (European Environment Agency, 2021). Future trends in TNdep for the forecasts SSP 1-2.6 and SSP 3-7.0 were assessed based on the estimation for future N emissions described above. According to the Sixth Assessment of the IPCC report (Masson-Delmotte et al., 2021), the NOx emissions will decrease slightly for the SSP 1-2.6 (from 11 to 9 Mt/y globally) and increase for SSP 3-7.0 (from 11 to 21 Mt/y globally), between 1995 and 2100. There are no projections for reduced nitrogen, instead NH_3 is assumed to decrease by around 20 % between 2020 and 2100 in case of the SSP 1-2.6, and to remain constant for SSP 3-7.0.

2.4. Selection of predictor variables

2.4.1. Spatial distribution of predictors

Spatially distributed data of the mean values of summer NDVI, Runoff, Precip, Temp, Bog, Arable, Forest, TNdep and TSdep were assessed as possible predictors to be used in the SELM. Catchment means of these variables, describing each of the 4735 lake catchments in Fennoscandia, are shown in Fig. 1.

2.5. Pearson correlation coefficient, autocorrelation, and variance inflation factor

Predictor variables that are strongly correlated (multi-collinear) reduce the robustness of multiple linear models and the precision of their estimates (Vittinghoff et al., 2012). This intercorrelation is disclosed by investigating the Pearson correlation coefficients (r) for each pair of variables, shown in Table 1. In addition, the Moran's I of each variable was calculated (Fig. 2), estimating the spatial autocorrelation for each variable. Considering the substantial number of observations, the maximum Moran's I value for a non-autocorrelated variable would be $2.1{\cdot}10^{-4}$. All variables in this study had a Moran's I above this limit, indicative of a high degree of autocorrelation. Finally, the Variance Inflation Factor (VIF) (James et al., 2013), indicating the severity of multi-collinearity due to a single predictor, was computed, and presented in Fig. 2.

The Pearson correlation coefficient matrix in Table 1 highlights several groups of predictors that are strongly correlated. TNdep, TSdep and Temp are closely correlated, especially TNdep and TSdep with r = 0.97. The correlation coefficient between TNdep and Temp is 0.85, and the correlation coefficient between TSdep and Temp is 0.88. This is because both N and S deposition are mainly from long-range transported atmospheric pollution from sources in Europe located to the south of Fennoscandia. The deposition of nitrate and sulfate is thus higher in the southern regions of Fennoscandia, where also the temperature is higher. Additionally, the high correlation is partly due to that both S and N deposition are based on emission inventories that are calculated using the same meteorological model. TSdep also has the highest VIF (21.15), followed by TNdep (16.97). Likewise, Temp, TNdep and TSdep have a remarkably high Moran's I (all around 0.9), reflecting their similar spatial pattern. Because of the strong interaction between these three predictors, only one can be used in the model. Although the decrease in TSdep has been documented by several studies as the main driver for the temporal increase in TOC concentration (Monteith et al., 2007), we chose instead to keep TNdep as a predictor for atmospheric deposition in this study. TSdep has decreased substantially since the 80s, though soil acidification is still driven by the deposition of reduced and oxidized nitrogen (Lepori and Keck, 2012). In addition, reactive N is biologically relevant, being generally the limiting factor for terrestrial primary production, and has been shown to enhance C storage in biomass (Schulte-Uebbing and de Vries, 2018) and in soils (Janssens et al., 2010).

Table 1
Correlation plot for predictor variables.

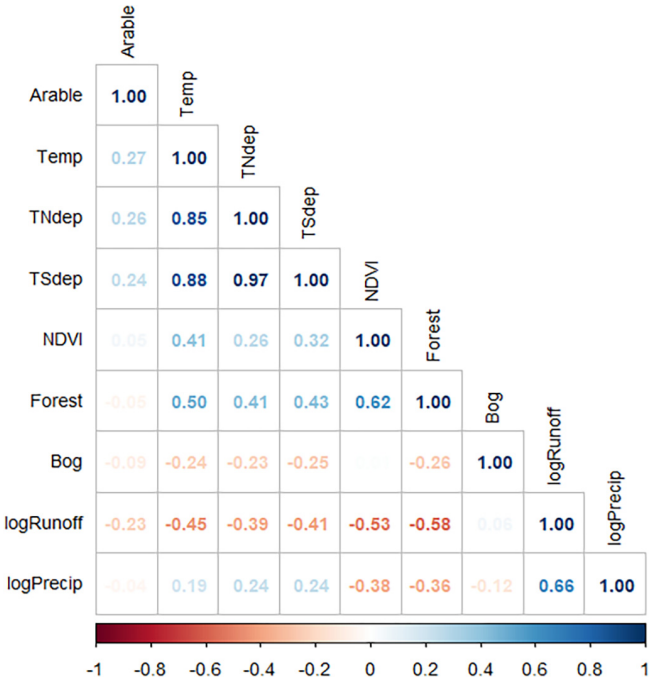

Forest and summer NDVI were also closely correlated (r = 0.58) although they do not match as closely as could perhaps be expected. Despite the finer resolution of the Corine Land Cover dataset for forest land cover, logTOC is slightly stronger correlated to summer NDVI (r = 0.68) than to Forest (r = 0.62). Moreover, NDVI reflects the density of the vegetation, and thus likely represents a better indicator for total standing biomass. Likewise, summer NDVI better reflects the photosynthetic activity of plants by representing greenness. Finally, the VIF of summer NDVI was lower than that of Forest (1.83 compared to 2.59), showing that it is less correlated to the other predictor variables. Therefore, only NDVI was kept as the vegetation biomass proxy in this study.

LogRunoff and logPrecip were also strongly positively correlated (r = 0.58). LogPrecip had a higher VIF than logRunoff (5.17 compared to 5.38), showing more general correlation to the other predictors, and a higher Moran's I (0.89 for logPrecip, compared to 0.79 for logRunoff). Conceptually, surface runoff is a more relevant predictor for TOC export from catchment to surface waters than precipitation, as the part of the precipitation that evapotranspires or infiltrates into ground reservoirs do not reach the surface water bodies. Moreover, logRunoff is stronger correlated to logTOC (r = −0.67) than logPrecip (r = −0.51). LogRunoff was therefore selected as the preferred NOM transport related predictor in the model.

The proportions of Bog and Arable land were not strongly correlated to any other variable (Table 1), and both had low VIF and Moran's I (Fig. 2). Therefore, both were kept in the model as explanatory variables for TOC.

3. Results and discussion

3.1. Modelling of TOC concentration on the Northern Lake Survey dataset

A multiple Linear Model (LM) and a multiple Spatial Error Linear Model (SELM) were fitted for the log of TOC using the 5 predictors selected in the previous section. SELM takes into account the spatial autocorrelation of predictor variables in the error term of the regression. To compare the two models, the Akaike Information Criterion (AIC) was calculated. AIC for each model is presented in Supplementary 1.

Both models were fitted with and without scaled variables. This allows a comparison of scaled estimates with the actual effect size for each predictor

a)

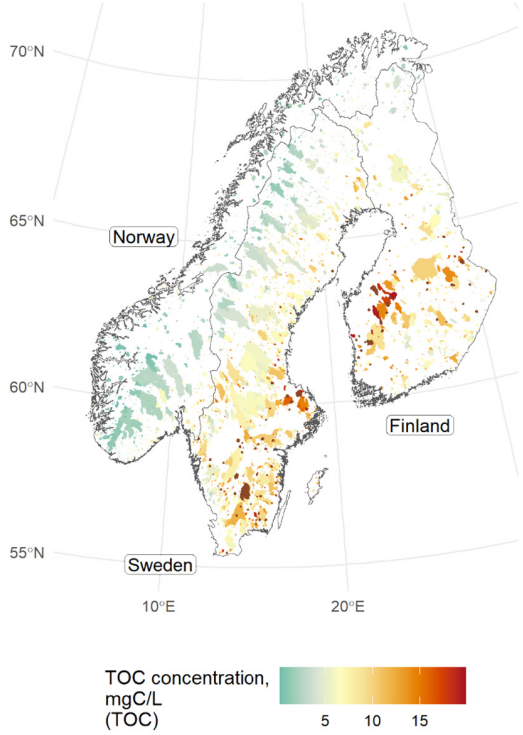

b)

Predictor	Moran's I	VIF	Pearson's r
Temp	**0.9**	**5.56**	0.47
logPrecip	**0.89**	**5.17**	**-0.51**
TNdep	**0.88**	**16.97**	0.32
TSdep	**0.86**	**21.15**	0.36
logRunoff	0.79	**5.38**	**-0.67**
Forest	0.48	2.59	**0.62**
NDVI	0.46	1.83	**0.68**
Bog	0.17	1.23	0.08
Arable	0.12	1.27	0.13

Fig. 2. a) Map of TOC concentration (mg C/L) in Fennoscandian catchments in 1995. b) Moran's I (i.e., spatial autocorrelation), Variance Inflation Factor (VIF) (i.e., multicollinearity) between predictor variables, and Pearson correlation coefficient with logTOC. Moran's I higher than 0.8, VIF higher than 5 and r higher than 0.5 are highlighted in red. (For interpretation of the references to colour in this figure legend, the reader is referred to the web version of this article.)

variable (Fig. 3). Centered and scaled estimates (hereafter referred to as β), fitted on response and predictors variables, show the degree of contribution of each predictor to the response variable value. But this is in units of the local standard deviations of the variables, which complicates the generalization to other regions. The effect sizes are instead expressed as percent change in TOC concentration caused by a 1 % relative change, as explained in Supplementary 4: 1 % increase in summer NDVI (0.01 on the NDVI index); 1 % increase of surface runoff; 1 % increase in either Forest, Bog or Arable land coverage proportion; and a 25 mg/m^2 increase of nitrogen deposition (i.e., 1 % of the max TNdep). These relative changes of 1 % are arbitrarily chosen to represent the relative impact of each predictor variable on a comparable basis. This means that a 1% change of the predictor x, with an effect size δx in catchment A with initial TOC concentration TOC_A would result in a final TOC concentration of $TOC_A + \delta x \times TOC_A$.

Summer NDVI is the strongest predictor for logTOC in both LM and SELM. LM gives a higher impact to NDVI, with an estimate of 0.5 and an effect size of 4.02 %, while SELM gave a scaled estimate of 0.4 and an effect size of 3.27 % (Fig. 3).

LogRunoff had high scaled estimates, especially for the LM with $\beta =$ -0.38, while SELM had $\beta =$ -0.15. The effect size of a 1 % increase in logRunoff has a negative effect on TOC concentration (-0.68 % for LM and $-$ 0.27 % for SELM) (Fig. 3). A plausible conceptual rationale for this negative effect is that the overall dilution effect is on average stronger than the increased episodic flushing of NOM. The spatial distribution of TOC concentration could also impact this result, as the highest surface runoff values are in steep mountain areas in the west coast of Norway, where soils are thin, and TOC concentrations are low.

Bog, despite its low correlation with logTOC (0.08), has relatively high scaled estimates (0.13 for LM and 0.14 for SELM) and effect sizes (0.81 % for LM and 0.9 % for SELM) (Fig. 3). This is bolstering the role of bog coverage as an important spatial predictor for TOC concentration. Still, bogs evolve slowly, and their area-wise proportion is assumed to be constant over timescales relevant for this assessment. They can however experience short-term extreme events, such as droughts that are predicted to occur with increased frequency (Helbig et al., 2020). However, since we base our TOC forecast on 20-year averages of the main predictors (precipitation and temperature to predict NDVI, as well as surface runoff), the impact of extreme events on the TOC average is considered limited.

Arable land has negligible impact on TOC, along with a relatively low negative effect size (0.13 % for LM and 0.1 % for SELM) (Fig. 3). Agricultural soils store indeed less carbon than forest soils and bogs (FAO and ITPS, 2020), though the use of phosphate fertilizers may affect the primary production and thus the levels of autochthonous NOM in lakes through eutrophication. This effect does however not appear to be a preponderant factor governing NOM levels in the studied region.

TNdep has positive impact on TOC concentration ($r = 0.32$), with both relatively high positive scaled estimates (0.08 for LM and 0.1 for SELM) and effect sizes (0.42 % for LM and 0.52 % for SELM) (Fig. 3). The positive effect of TNdep on TOC may on the one hand be surprising as the deposition of acid rain, including the strongly correlated TSdep, is known to have a negative impact on TOC concentration in several studies (Monteith et al., 2007). The positive effect of TNdep may instead be due to a spatial covariation, as the TNdep is higher in the southern and warmer part of Fennoscandia, where high summer NDVI drives the high TOC concentrations. It can also be driven by the fertilizing effect of accumulating TNdep in the biomass. Future impact of reactive nitrogen deposition depends on public policies, as it is linked to combustion of fossil fuel and agricultural practices in central Europe. Here, the effect size is calculated for an increase of 25 mg/m^2 of TNdep, though TNdep might either decrease in the coming decades (SSP 1-2.6) or remain stable (SSP 3-7.0) compared to 1995.

The SELM model had a lower AIC than the LM model (see Supplementary 1). It also resulted in estimates being less extreme than the LM. Especially, summer NDVI and Runoff have lower estimates and effect sizes with SELM than with LM. On the other hand, TNdep had higher estimate and effect size with SELM compared to LM. This shows that the SELM model is more balanced and less likely to over- or underestimate the impact

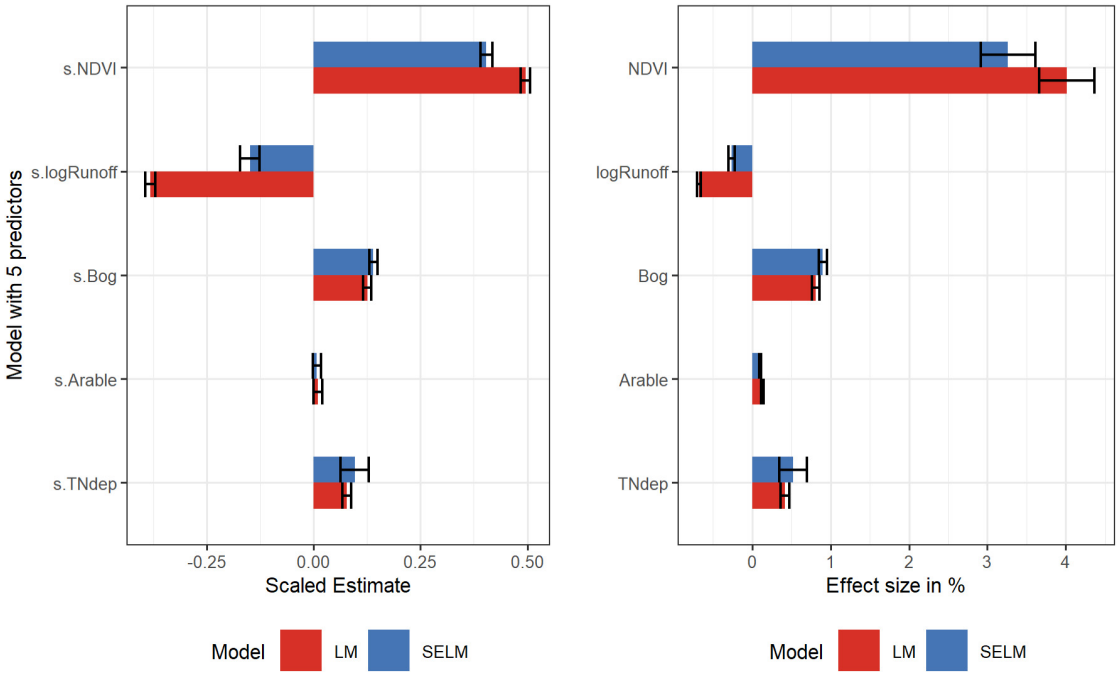

Fig. 3. Comparison of scaled estimates and effect sizes for a 1 % increase in the predictor variables using LM and SELM models, based on the Fennoscandian dataset with the 5 selected predictors. The s. prefix indicates that the variable is centered and scaled.

of each predictor. Moran's I of the residuals is higher for the LM than for the SELM, showing a stronger spatial pattern of the errors in LM. The SELM model performs therefore better in predicting TOC concentration in boreal lakes and is assessed further in the next section.

3.2. Validation against a new 1000-lakes-survey

The results of the validation test of the space-for-time model show that the SELM model fitted with the training data from 1995 of the five selected predictors gives satisfactory results. logTOC predictions were made from the 1995 model using input data from 2019. The Pearson correlation coefficient between these predictions and the actual observations from 2019 was 0.84. However, the model tends to over-estimate TOC concentrations in lakes with very low initial TOC concentrations (< 1 mgC/L), typically alpine oligotrophic lakes, and under-estimate the TOC concentrations in dystrophic lakes that had high initial TOC concentrations (>7,5 mgC/L), particularly in the south-eastern part of Norway (Fig. 4b).

This space-for-time approach employs a set of explanatory values taken at a snap-shot moment in time from a large variety of catchment types to model future changes. The relationships between explanatory parameters and the TOC response parameter at any single site is a result of biogeochemical processes that have evolved in the soils since the last glacial epoch (i.e., about 15,000 years), e.g., the long-term processes of generating the pool of soil organic matter. That catchments in the middle of the Norwegian mountains are predicted to have a higher TOC concentration in 2019 compared to the actual observations (Fig. 4b) is hence likely due to a recent increased NDVI in these regions (i.e., due to climate and land use change), not yet followed by the soil formation that a catchment with a similar NDVI value in 1995 would have had. On the contrary, the TOC concentration of lakes in south-east Norway are mostly under-estimated since in 1995 the TOC was still suppressed by S-deposition. High TNdep, being strongly correlated to TSdep, would have meant low TOC concentration, while in 2019 the role of TNdep as a predictor is more related to the positive fertilizing effect of accumulating reactive N in the watersheds than the negative acid rain effect.

Having in mind these potential discrepancies, this space for time model can be used to obtain an indication of future TOC concentration under various climate scenarios, as the prediction range and the trends predicted in this study nevertheless serves as a good indication in most catchments.

3.3. Forecast with SSP1-2.6 and SSP3-7.0

Future average TOC concentrations were modelled for 1392 coastal drainage basins in Norway, Sweden, and Finland.

As each coastal drainage basins comprise several lakes and catchments, there exists no empirical data for their respective average TOC concentration in their various water bodies. Therefore, the first step was to compute the TOC concentration in 1995 using the SELM model that was fitted and verified in the above section. In a second step, forecasts of the predictor variables Temp, Precip and Runoff were extracted from CMIP6 climate models based on two climate scenarios: i.e., SSP1-2.6 (global warming limited to <2 °C) and SSP 3-7.0 (global warming up to 4 °C). Summer NDVI was then modelled based on the Precip and Temp using a polynomial model, as described in Larsen et al. (2011b), though based on a beta distribution to constrain NDVI predictions between 0 and 1. The linear models were fitted with beta distributed response and logit link using the betareg package (Cribari-Neto and Zeileis, 2010), version 3.1-4, for R (see Supplementary 3).

Future trends in TNdep were assessed based on estimations from IPCC as described above. According to their predictions following the SSP1-2.6 there will be a net decrease in TNdep through 2050 to 2100 and a net increase in the SSP 3-7.0 forecast. Finally, the average TOC concentration was modelled for two time periods: 2041–2060 and 2081–2100 (abbreviated as “2050” and “2100”). The details of predictor extraction and model fitting are presented in Supplementary 3.

Fig. 5 shows the difference between logTOC in 2050 and 2100, fitted for the different climate scenarios, relative to logTOC fitted for the coastal drainage basins based on the 1995 data. Coastal drainage basins are used in order to cover all of Norway, Sweden and Finland, and not only the lakes selected in the Northern Lakes Survey. This provides a better overview of future trends and enables a prediction of TOC export to coastal waters. Over- or under-estimation of TOC concentration, identified by the test on 2019-data, are assumed to be partially compensated by this double-fit. Moreover, the TOC is forecasted as an average over a 20-years

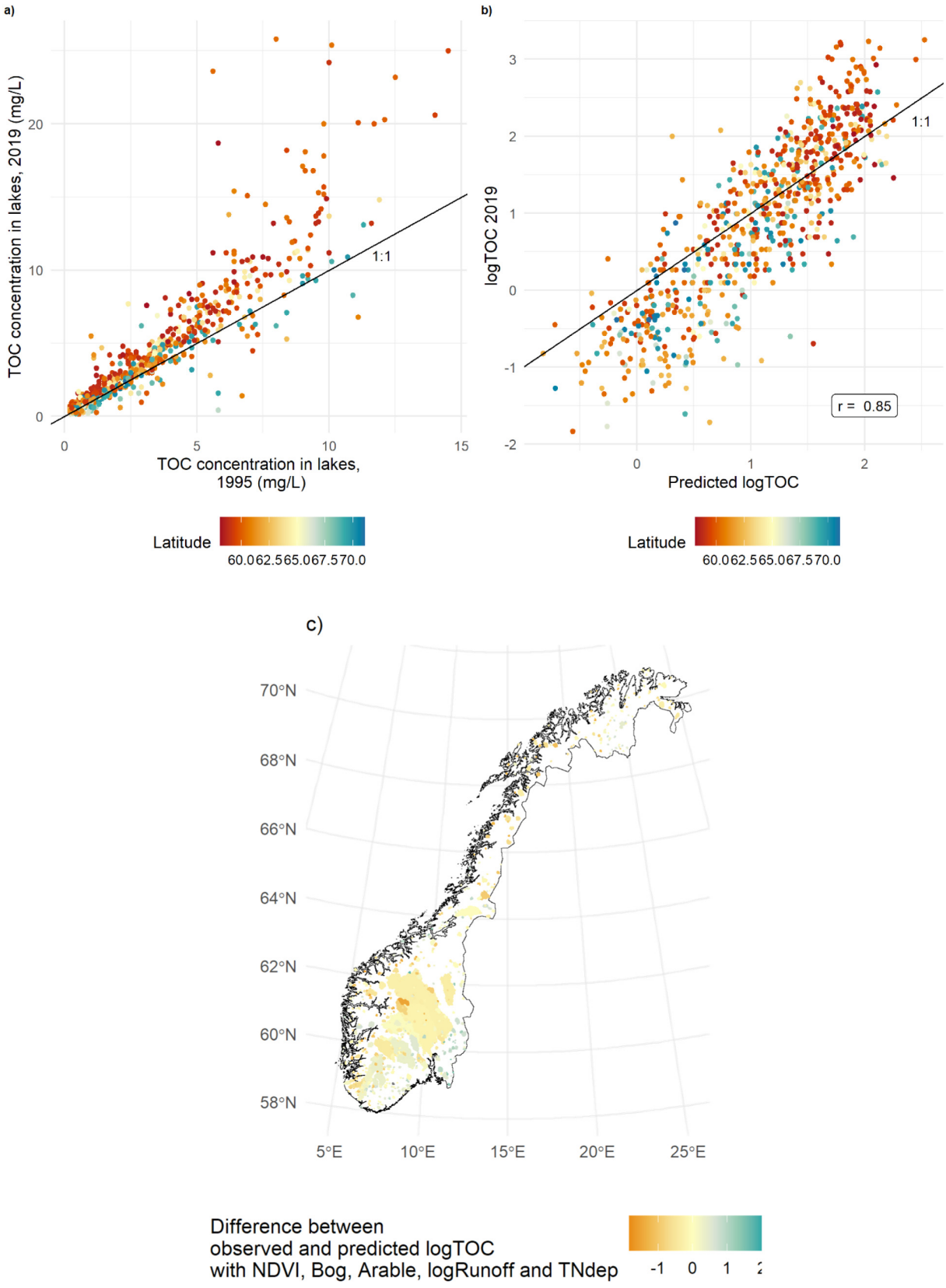

Fig. 4. Test of the SELM model, a) TOC concentration (in mg C/L) in 1995 and in 2019, b) predicted vs. measured logTOC; c) map of the spatial distribution of the difference between measured and fitted logTOC.

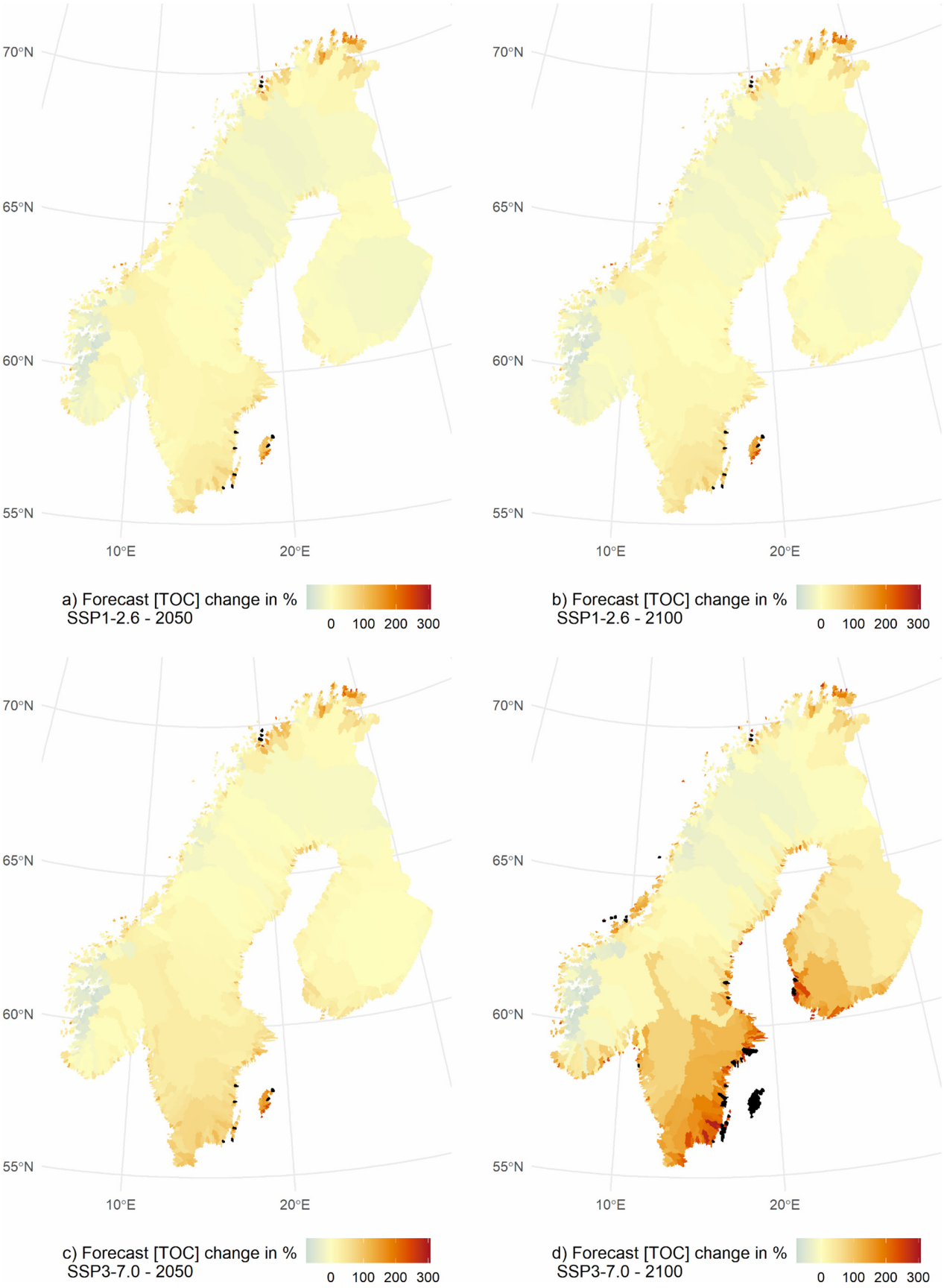

Fig. 5. Forecast of changes in TOC concentration (%) under SSP1-2.6 and SSP3-7.0 climate scenarios. The 5 % basins with the highest increase of TOC (> 307 % increase) are represented in black.

period, which reduce the "snap-shot" effect by considering a certain adaptation time of the system, although it does not account for centennial processes.

The forecasts of average TOC concentration show similar pattern of changes under both the SSP1-2.6 and SSP3-7.0 scenarios, with the latter representing more extreme changes (Fig. 5). The strongest increase in TOC is predicted in the south-east of Sweden and south-west of Finland, while there is predicted a slight decrease in mountain areas in Norway and in some northernmost basins. The modelled changes of TOC are mainly governed by a combination of forecasted changes in NDVI, runoff and TNdep, with different relative effects varying between regions. A loss of TOC from oxidation and sedimentation occurs along the watercourse, inherently dependent on the distance from the headwater origin to the coast (Weyhenmeyer et al., 2012). It should thus be noted that this assessment neglects the potential effect of increased TOC retention due to longer water courses in the coastal drainage basins compared to the catchments used in the training data set.

In the western and northern basins changes in TOC are basically driven by the forecasted changes in NDVI (see Supplementary 3), reflecting the expected changes in biomass, which is mainly governed by the temperature increase. A main effect of this increase is the longer growing seasons and thereby a larger biomass production in forests, along with a faster biodegradation rate of soil organic matter. This increase in growth is supported by sustained amount of precipitation in most of Fennoscandia, if not an increase as for the Norwegian western coast. This limits the potential for soil dryness and water stress, even though water lost by evapotranspiration will increase (D'Orangeville et al., 2018; Gauthier et al., 2015). In mountain regions of the Norwegian west coast, where increase of precipitation is highest, NDVI decreases in both SSP pathways. Indeed, at high altitudes, negative winter temperatures allow for increased snow fall with increased precipitation. This in turn impedes vegetation growth at these high altitudes, which are scarcely vegetated areas that are sensitive to the number of snow cover days (Asam et al., 2018). This can partly explain the predicted decrease in mean TOC concentration in this region.

In this space-for-time approach, the chain of processes between biomass production and carbon storage in forest soils are not integrated. Actually, there will be a delay before the export of TOC from soils to surface starts to increase or decrease in turn. Nevertheless, these results can be used as a good trend indicator. It is worth noting that, in this model, the northernmost, small coastal drainage basins display a significant increase in TOC (up to 300 %), that matches a strong increase in temperature (up to 10 degrees). However, the NDVI model over-estimates the summer NDVI in these regions (see Supplementary 3). On the other hand, the effect of thawing permafrost, as a driver of increased export of TOC (cf. Abbott et al., 2014), is not accounted for in this study since permafrost cover very limited areas in the northernmost areas.

These changes in NDVI do not account for the forest policies implemented by Norway, Sweden, and Finland to capture and sequester carbon dioxide to fulfill their Paris agreement obligations (Vogt et al., 2022). The specific relationship between the proportion of forest in the catchment and TOC concentration are provided in Supplementary 5. Nonetheless, an increase in forest cover would lead to an increase of NDVI, so the results of the model runs may serve as an indication of the impact of this increased planting of climate forest on TOC concentration.

Forecasted trends in surface runoff intensity resemble changes in summer NDVI patterns and often match the TOC concentration evolution in the same manner. A strong decrease of surface runoff was modelled in small coastal drainage basins on the Norwegian western coast. This is likely caused by poor performance of the runoff model in this region due to its steep topography. Still, this has a limited impact on the overall TOC forecast. Besides these small basins, the regions with increased surface runoff (i.e., Norwegian mountains, and some basins in northern Sweden) will, due to stronger dilution, experience less increase or even a decrease in TOC concentration, compared to the regions with decreasing surface runoff, such as southern Sweden and Finland. The largest increases in TOC concentration are predicted to happen in these areas (Fig. 5). In some very small coastal basins, mostly in South-east Sweden, changes are predicted to exceed +400 %. These should be judged with care and are likely caused by the low resolution of the predicting variables in tiny catchments. However, our model also predicts the doubling or tripling of TOC levels in some of the larger basins in south-east Sweden. NDVI is predicted to increase only slightly in these areas, and even to decrease in some coastal basins. The significant decrease in surface runoff could therefore explain this forecast, by reducing the dilution of TOC exported from land to water.

Our model does not consider seasonal patterns of surface runoff, which will be more impacted by climate change than the average yearly surface runoff (Hanssen-Bauer et al., 2017). Summer runoff will decrease in most regions, due to earlier snowmelt and more evapotranspiration, while winter runoff is predicted to increase in most regions. These changes may have antagonistic effects on the yearly average TOC concentration: mobilization of soil organic carbon will increase during the winter and spring (Håland, 2017), while increased residence time of the TOC in lakes will allow for more enhanced photo- and biodegradation of the NOM during the summer. Whether higher fluxes and mineralization rate lead to a net higher or lower yearly average NOM concentration in surface water is subject to discussion (De Wit et al., 2016). The SELM shows that the dilution effect (i.e., more surface runoff means more surface water) prevails over the mobilization effect, though this requires more investigation.

Finally, accumulation of reactive nitrogen also affects regionally the predicted levels of TOC. The TNdep predictions are only based on emissions targets from the AR6 report (see Supplementary 3) and applied evenly on Fennoscandia: the following trend must therefore be interpreted with caution. In the SSP 1-2.6, final levels are reached in 2050. In the SSP 3-7.0, the trend for decrease nitrogen emissions between 1995 and 2015 is reversed during the rest of the century, leading to no overall change. In southern Norway and in the south-western part of Sweden no large changes of TOC levels are predicted, except in SSP 3-7.0 in 2100. A slight increase in NDVI and a decrease in runoff should have led to an increase in TOC concentration, but as TNdep is projected to decrease significantly under SSP1-2.6 scenario, the predicted TOC increase in these regions is limited. On the contrary, under SSP3-7.0, there is no significant change in the rate of TNdep in 2100 compared to 1995. This modelled effect is likely a consequence of the inherent weakness in the space-for-time approach as it likely reflects the spatial location of TOC-rich surface waters in southern catchments with higher mean temperatures, even though there is a potential fertilization effect of TNdep. In addition, chronic TNdep has been reported to have a positive effect on TOC concentration by that TNdep limit microbial respiration and root activities in soils, reducing soil organic matter mineralization rates and thus increasing the pool of TOC readily exportable to surface water (Bowden et al., 2004; Janssens et al., 2010; Ramirez et al., 2012). However, the projected future changes of TNdep were roughly estimated in this study and depend largely on regulations concerning fossil fuels burning and agricultural practices. A finer evaluation of the potential evolution of public policies would be necessary to refine the contribution of future TNdep to TOC concentration in surface waters.

3.4. Coastal darkening

Modelling TOC concentration in coastal drainage basins provides an estimate of future TOC export to the Baltic Sea and the Norwegian coast from Fennoscandia. Most coastal drainage basins in Sweden and Finland drain into to the Baltic Sea (see Supplementary 2), while Norwegian coastal basins drain to Skagerrak, the North Sea, the Norwegian Sea and the Barents Sea (Sætre, 2007). All contribute to the Norwegian coastal current (NCC) freshwater with 50 % coming from the Baltic Sea and 40 % from Norway. The estimated exported TOC from each coastal drainage basin was computed as:

$$TOC_{exp} = [TOC]\left(mg.L^{-1}\right) \times Runoff\left(L.m^2.y^{-1}\right) \times Watershed\ \text{area}\left(m^2\right)$$

Past and future TOC concentrations (*mg C/L*) were obtained by taking the antilog of logTOC. The result of the above equation, giving the amount

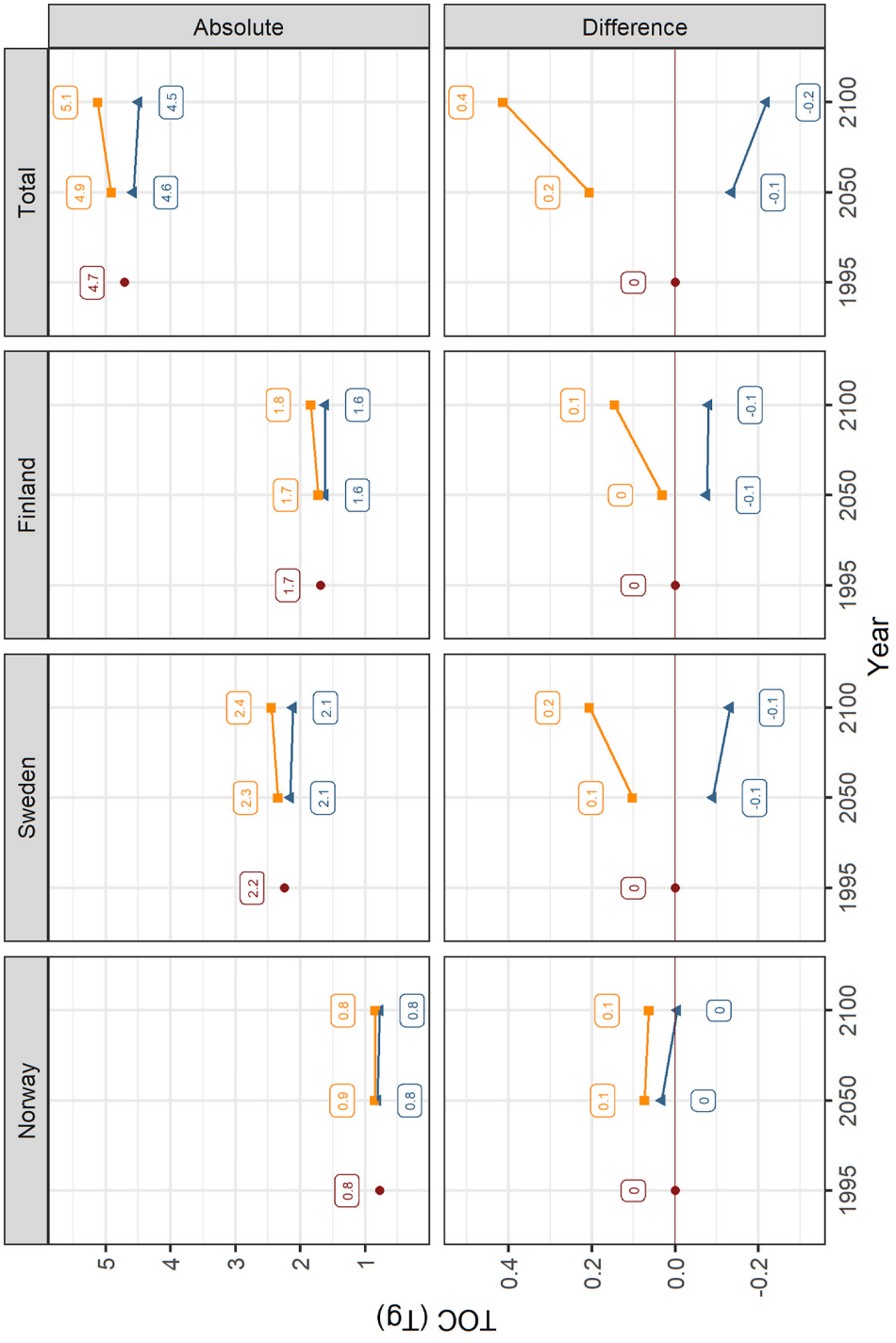

Fig. 6. Forecast of TOC export to coastal waters under SSP 1-2.6 and SSP 3.7-0 (Tg); above: absolute export, below: relative export compared to 1995.

of TOC exported in *mg C/y*, is then converted to *Tg*. Forecasts are presented in Fig. 6.

The amount of TOC exported is in the same order of magnitude as the estimations of De Wit et al. (2015) for Norway, who estimated an export of 0.96 Tg C/y in the period 1990 to 2008, for Norway alone. For Finland, our estimations are higher than those reported in Räike et al. (2016), who reported a yearly export of TOC from Finnish catchments to the Baltic Sea to be 0.92 TgC/y. Under the SSP 1-2.6 scenario, the export of TOC into the NCC will decrease by −0.1 Tg by 2050 compared to 1995, and by −0.2 Tg in 2100. On the contrary, under the SSP 3-7.0 scenario, the total TOC import into the NCC increases by 0.2 Tg in the forecast for 2041–2060, and by 0.4 Tg for the period 2081–2100. Swedish coastal drainage basins would contribute most to these changes. Associated with higher surface temperature, this browning of coastal water could lead to later spring bloom and spawning time.

These estimates do not account for mineralization and sedimentation of TOC along the water continuum, and hence we present a maximum estimate of coastal export where TOC entering the water system is transported all the way to the sea without losses. This "passive pipe" vision has been challenged by Cole et al. (2007), who highlighted the processes that organic matter undergoes along the water system. Photo-mineralization, respiration and sedimentation remove organic carbon from the water (Tranvik et al., 2018). Although the magnitude of this loss remains uncertain, it could be as high as 30 to 70 % (Algesten et al., 2004). In addition, this loss of organic C will, in turn, be impacted by changes in hydrology and temperature. Decreased retention time limits the degree of mineralization. An increase in runoff thus results in the export of less processed, more colored organic carbon to coastal waters (Weyhenmeyer et al., 2012). On the contrary, increased temperature favor higher mineralization rates in soils (Hicks Pries et al., 2017) and in water (Hanson et al., 2011). Moreover, microbial respiration rate also depends on the chemical composition of the freshwater (Crapart et al., 2021), which is impacted by land-use and atmospheric deposition. Sedimentation rates might also increase, without enhancing C-storage because of parallel increased decomposition rates (Velthuis et al., 2018). It should be remarked, however, that since these losses affect both current and future exports, the relative change in export should be less affected by "leaky pipe" processes than the absolute rate estimates.

4. Conclusion

This study demonstrates the relevance of using space-for-time models to forecast future regional environmental changes in TOC concentration in freshwater. The TOC concentration was best predicted by a linear spatial error model, with catchment characteristics as predictors. Long-term processes working on the catchment characteristics are not taken into account in the space-for-time approach. Nevertheless, the simulated changes from 1995 to 2019 were in good agreement with measured values ($r = 0.84$). NDVI, being a good proxy for the amount of biomass in the catchment, is a major predictor for TOC concentration. Surface runoff intensity was also a significant predictor with a negative effect on TOC concentration. The proportion of bogs in the catchment was a good spatial predictor for TOC concentration in lakes, while the proportion of arable land had almost no effect. Finally, a sustained atmospheric deposition of reactive nitrogen will, according to the model, have significant positive effects on the TOC concentration in lakes.

The forecast of TOC changes within this century indicates a slight decrease of total TOC export from Fennoscandia in the SSP1-2.6 scenario (−0.2 Tg in 2100) and an increase in the SSP3-7.0 scenario (+0.4 Tg). Under the SSP1-2.6 scenario, seasonal antagonistic effects of changes in predictors outweigh each other in several of the coastal drainage basins. In particular, the decrease of nitrogen deposition compensates the increase in biomass in southern Norway, limiting the increase of TOC amount in freshwater.

Supplementary data to this article can be found online at https://doi.org/10.1016/j.scitotenv.2023.161676.

CRediT authorship contribution statement

Camille Crapart: Conceptualization; Methodology; Software; Formal Analysis; Investigation; Data Curation; Writing original draft, review and editing; Visualization.

Tom Andersen: Conceptualization; Methodology; Resources; Writing: Review and Editing; Supervision.

Dag O. Hessen: Conceptualization; Resources, Writing: Review and Editing; Project Administration.

Rolf D. Vogt: Writing: Review and Edit.

Anders Finstad: Conceptualization; Resources; Data Curation.

Data availability

The data/code is available on https://camilmc.github.io/TOC_trend_1995/

Declaration of competing interest

The authors declare that they have no known competing financial interests or personal relationships that could have appeared to influence the work reported in this paper.

Acknowledgment

We would like to thank Jose Luis Guerrero (NGI) and Heleen de Wit (NIVA) for the provision of catchment polygons, as well as for the TOC and catchment data of the 1000 lakes survey in 2019. This work was partially supported by the Center for Biogeochemistry of the Anthropocene (CBA) at UiO and by RCN project 287"90 "A green-blue link made browner: how terrestrial climate change affects marine ecology".

References

Aas, W., Tørseth, K., Solberg, S., Berg, T., Manø, S., Yttri, K.E., 2002. Overvåking av langtransportert forurenset luft og nedbør. OR 21/2002. NI https://www.miljodirektoratet.no/publikasjoner/publikasjoner-fra-klif/2004/november/overvaking-av-langtransportert-forurenset-luft-og-nedbor.–atmosfarisk-tilforsel-2002/.

Abbott, B.W., Larouche, J.R., Jones, J.B., Bowden, W.B., Balser, A.W., 2014. Elevated dissolved organic carbon biodegradability from thawing and collapsing permafrost. J. Geophys. Res. Biogeosci. 119, 2049–2063. https://doi.org/10.1002/2014JG002678.

Aksnes, D.L., Dupont, N., Staby, A., Fiksen, Ø., Kaartvedt, S., Aure, J., 2009. Coastal water darkening and implications for mesopelagic regime shifts in Norwegian fjords. Mar. Ecol. Prog. Ser. 387, 39–49. https://doi.org/10.3354/meps08120.

Algesten, G., Sobek, S., Bergström, A.K., Ågren, A., Tranvik, L.J., Jansson, M., 2004. Role of lakes for organic carbon cycling in the boreal zone. Glob. Chang. Biol. 10 (1), 141–147. https://doi.org/10.1111/j.1365-2486.2003.00721.x.

Asam, S., Callegari, M., Matiu, M., Fiore, G., De Gregorio, L., Jacob, A., Menzel, A., Zebisch, M., Notarnicola, C., 2018. Relationship between spatiotemporal variations of climate, snow cover and plant phenology over the Alps-an Earth observation-based analysis. Remote Sens. 10 (11), 1757. https://doi.org/10.3390/rs10111757.

Asmala, E., Carstensen, J., Raike, A., 2019. Multiple anthropogenic drivers behind upward trends in organic carbon concentrations in boreal rivers. Environ. Res. Lett. 14 (12), 124018. https://doi.org/10.1088/1748-9326/ab4fa9.

Beck, P.S.A., Jönsson, P., Høgda, K.A., Karlsen, S.R., Eklundh, L., Skidmore, A.K., 2007. A ground-validated NDVI dataset for monitoring vegetation dynamics and mapping phenology in Fennoscandia and the Kola peninsula. Int. J. Remote Sens. 28, 4311–4330. https://doi.org/10.1080/01431160701241936.

Bivand, R., 2019. Estimation methods for models of spatial interaction. CRAN - R package. https://github.com/r-spatial/spatialreg/issues/.

Björnerås, C., Weyhenmeyer, G.A., Evans, C.D., Gessner, M.O., Grossart, H.-P., Kangur, K., Kritzberg, E.S., 2017. Widespread increases in iron concentration in European and North American freshwaters. Glob. Biogeochem. Cycles 31, 1488–1500. https://doi.org/10.1002/2017GB005749.

Bowden, R.D., Davidson, E., Savage, K., Arabia, C., Steudler, P., 2004. Chronic nitrogen additions reduce total soil respiration and microbial respiration in temperate forest soils at the Harvard Forest. For. Ecol. Manag. 196, 43–56. https://doi.org/10.1016/j.foreco.2004.03.011.

Cole, J.J., Prairie, Y.T., Caraco, N.F., McDowell, W.H., Tranvik, L.J., Striegl, R.G., et al., 2007. Plumbing the global carbon cycle: integrating inland waters into the terrestrial carbon budget. Ecosystems 10 (1), 171–184. https://doi.org/10.1007/s10021-006-9013-8.

Copernicus Land Monitoring Service. CHA 2000-2006 [Internet]. [cited 2022 Jan 26]. Available from: https://land.copernicus.eu/pan-european/corine-land-cover/lcc-2000-2006.

CORDEX, 2021. CORDEX experiment design for dynamical downscaling of CMIP6. 8p. Available at https://cordex.org/wp-content/uploads/2021/05/CORDEX-CMIP6_exp_design_RCM.pdf.
Craig, N., Jones, S.E., Weidel, B.C., Solomon, C.T., 2017. Life history constraints explain negative relationship between fish productivity and dissolved organic carbon in lakes. Ecol. Evol. 7, 6201–6209. https://doi.org/10.1002/ece3.3108.
Crapart, C., Andersen, T., Hessen, D.O., Valiente, N., Vogt, R.D., 2021. Factors governing biodegradability of dissolved natural organic matter in lake water. Water 13 (16), 2210. https://doi.org/10.3390/w13162210.
Cribari-Neto, F., Zeileis, A., 2010. Beta regression in R. J. Stat. Softw. 34 (2), 129–150. https://doi.org/10.18637/jss.v034.i02.
De Wit, H.A., Austnes, K., Hylen, G., Dalsgaard, L., 2015. A carbon balance of Norway: terrestrial and aquatic carbon fluxes. Biogeochemistry 123 (1–2), 147–173. https://doi.org/10.1007/s10533-014-0060-5.
De Wit, H.A., Garmo, ØA., Jackson-Blake, L., Clayer, F., Vogt, R.D., Kaste, Ø, et al., 2023. Changing Water Chemistry in One Thousand Norwegian Lakes During Three Decades of Cleaner Air and Climate Change. Glob. Biogeochem. Cycles 37 (2) Available from https://agupubs.onlinelibrary.wiley.com/doi/full/10.1029/2022GB007509.
De Wit, H.A., Mulder, J., Hindar, A., Hole, L., 2007. Long-term increase in dissolved organic carbon in streamwaters in Norway is response to reduced acid deposition. Environ. Sci. Technol. 41, 7706–7713. https://doi.org/10.1021/es070557f.
De Wit, H.A., Valinia, S., Weyhenmeyer, G.A., Futter, M.N., Kortelainen, P., Austnes, K., Hessen, D.O., Räike, A., Laudon, H., Vuorenmaa, J., 2016. Current browning of surface waters will be further promoted by wetter climate. Environ. Sci. Technol. Lett. 3, 430–435. https://doi.org/10.1021/acs.estlett.6b00396.
D'Orangeville, L., Houle, D., Duchesne, L., Phillips, R.P., Bergeron, Y., Kneeshaw, D., 2018. Beneficial effects of climate warming on boreal tree growth may be transitory. Nat. Commun. 9, 1–10. https://doi.org/10.1038/s41467-018-05705-4.
Eikebrokk, B., Vogt, R.D., Liltved, H., 2004. NOM increase in Northern European source waters: discussion of possible causes and impacts on coagulation/contact filtration processes. Water Supply. IWA Publishing, pp. 47–54 https://doi.org/10.2166/ws.2004.0060.
EMEP, 2022. EMEP MSC-W HOME. Available at https://emep.int/mscw/mscw_moddata.html#Comp.
European Environment Agency, 2021. Emissions of the main air pollutants in Europe. Available at https://www.eea.europa.eu/ims/emissions-of-the-main-air.
Fagerli, H., Benedictow, A., Denby, B.R., Gauss, M., Heinesen, D., Jonson, J.E., Karlsen, K.S., Klein, H., Mortier, A., Segers, A., Simpson, D., Tsyro, S., Wind, P., Aas, W., Hjellbrekke, A., Solberg, S., Platt, S., Yttri, K.E., Matthews, B., Schindlbacher, S., Ullrich, B., Klimont, Z., Scheuschner, T., Fernandez, I.A.G., Kuenen, J.J.P., 2022. Transboundary particulate matter, photo-oxidants, acidifying and eutrophying, components. EMEP Status Report 1/2022. Available at https://emep.int/publ/reports/2022/EMEP_Status_Report_1_2022.pdf.
FAO, ITPS, 2020. Global Soil Organic Carbon Map (GSOCmap) Version 1.5: Technical Report. Rome. https://doi.org/10.4060/ca7597en.
Finér, L., Lepistö, A., Karlsson, K., Räike, A., Härkönen, L., Huttunen, M., et al., 2021. Drainage for forestry increases N, P and TOC export to boreal surface waters. Sci. Total Environ. https://doi.org/10.1016/j.scitotenv.2020.144098.
Finstad, A.G., 2017. Environmental data NINAnor/NOFA Wiki. https://github.com/NINAnor/NOFA/wiki/Environmental-data.
Finstad, A.G., Andersen, T., Larsen, S., Tominaga, K., Blumentrath, S., De Wit, H.A., Tømmervik, H., Hessen, D.O., 2016. From greening to browning: catchment vegetation development and reduced S-deposition promote organic carbon load on decadal time scales in nordic lakes. Sci. Rep. 6 (31944), 1–8. https://doi.org/10.1038/srep31944.
Finstad, A.G., Helland, I.P., Ugedal, O., Hesthagen, T., Hessen, D.O., 2014. Unimodal response of fish yield to dissolved organic carbon. Ecol. Lett. 17, 36–43. https://doi.org/10.1111/ele.12201.
Fleming-Lehtinen, V., Laamanen, M., 2012. Long-term changes in Secchi depth and the role of phytoplankton in explaining light attenuation in the Baltic Sea. Estuar. Coast. Shelf Sci. 102–103, 1–10. https://doi.org/10.1016/j.ecss.2012.02.015.
Gauthier, S., Bernier, P., Kuuluvainen, T., Shvidenko, A.Z., Schepaschenko, D.G., 2015. Boreal forest health and global change. Science 349, 819–822. https://doi.org/10.1126/science.aaa9092.
Grennfelt, P., Engleryd, A., Forsius, M., Hov, Ø., Rodhe, H., Cowling, E., 2020. Acid rain and air pollution: 50 years of progress in environmental science and policy. Ambio 49, 849–864. https://doi.org/10.1007/s13280-019-01244-4.
Håland, A., 2017. Characteristics and Bioavailability of Dissolved Natural Organic Matter in a Boreal Stream During Storm Flow (Master thesis). Available atDUO, University of Oslo, Norway. http://urn.nb.no/URN:NBN:no-61154.
Hanson, P.C., Hamilton, D.P., Stanley, E.H., Preston, N., Langman, O.C., Kara, E.L., 2011. Fate of allochthonous dissolved organic carbon in lakes: a quantitative approach. Plos One https://doi.org/10.1371/journal.pone.0021884.
Hanssen-Bauer, I., Førland, E.J., Haddeland, I., Hisdal, H., Lawrence, D., Mayer, S., Nesje, A., Sandven, S., Sandø, A.B., Sorteberg, A., 2017. Climate in Norway 2100 – a knowledge base for climate adaptation. NCCS report 1/M-714. Available from www.mijodirektoratet.no.
Hausfather, Z., 2019. CMIP6: the next generation of climate models explained. https://www.carbonbrief.org/cmip6-the-next-generation-of-climate-models-explained/ Available at.
Helbig, M., Waddington, J.M., Alekseychik, P., Amiro, B., Aurela, M., Barr, A.G., Black, T.A., Carey, S.K., Chen, J., Chi, J., Desai, A.R., Dunn, A., Euskirchen, E.S., Flanagan, L.B., Friborg, T., Garneau, M., Grelle, A., Harder, S., Heliasz, M., Humphreys, E.R., Ikawa, H., Isabelle, P.E., Iwata, H., Jassal, R., Korkiakoski, M., Kurbatova, J., Kutzbach, L., Lapshina, E., Lindroth, A., Löfvenius, M.O., Lohila, A., Mammarella, I., Marsh, P., Moore, P.A., Maximov, T., Nadeau, D.F., Nicholls, E.M., Nilsson, M.B., Ohta, T., Peichl, M., Petrone, R.M., Prokushkin, A., Quinton, W.L., Roulet, N., Runkle, B.R.K., Sonnentag, O., Strachan, I.B., Taillardat, P., Tuittila, E.S., Tuovinen, J.P., Turner, J., Ueyama, M., Varlagin, A., Vesala, T., Wilmking, M., Zyrianov, V., Schulze, C., 2020. The biophysical climate mitigation potential of boreal peatlands during the growing season. Environ. Res. Lett. 15, 104004. https://doi.org/10.1088/1748-9326/abab34.
Henriksen, A., Lien, L., Rosseland, B.O., Traaen, T.S., Sevaldrud, I.S., 1989. Lake acidification in Norway: present and predicted fish status. Ambio 18, 314–321. https://doi.org/10.2307/4313601.
Henriksen, A., Skjelvåle, B.L., Mannio, J., Wilander, A., Harriman, R., Curtis, C., Jensen, J.P., Fjeld, E., Moiseenko, T., 1998. Northern European Lake Survey 1995: Finland, Norway, Sweden, Denmark, Russian Kola, Russian Karelia, Scotland and Wales. Ambio 2, 80–91. https://www.jstor.org/stable/4314692.
Hessen, D.O., Andersen, T., Lyche, A., 1990. Carbon metabolism in a humic lake: pool sizes and cycling through zooplankton. Limnol. Oceanogr. 35, 84–99. https://doi.org/10.4319/lo.1990.35.1.0084.
Hicks Pries, C.E., Castanha, C., Porras, R., Torn, M.S., 2017. The whole-soil carbon flux in response to warming. Science 355 (6332), 1420–1423. https://doi.org/10.1126/science.aal1319.
Hindar, A., Garmo, Ø., Austnes, K., Sample, J.E., 2020. Nasjonal innsjøundersøkelse 2019. NIVA Report No. 7530-2020/M-1870-2020 86p. Available from www.mijodirektoratet.no.
James, G., Witten, D., Hastie, T., Tibshirani, R., 2013. An Introduction to Statistical Learning. Available from:Springer Texts in Statistics , p. 618 p.. https://www.statlearning.com/.
Janssens, I.A., Dieleman, W., Luyssaert, S., Subke, J.A., Reichstein, M., Ceulemans, R., Ciais, P., Dolman, A.J., Grace, J., Matteucci, G., Papale, D., Piao, S.L., Schulze, E.D., Tang, J., Law, B.E., 2010. Reduction of Forest Soil Respiration in Response to Nitrogen Deposition. https://doi.org/10.1038/ngeo844.
Kanakidou, M, Myriokefalitakis, S, Daskalakis, N, Fanourgakis, G, Nenes, A, Baker, AR, et al., 2016. Past, present, and future atmospheric nitrogen deposition. J Atmos Sci 73 (5), 2039–2047. https://journals.ametsoc.org/view/journals/atsc/73/5/jas-d-15-0278.1.xml.
Karlsson, J., 2007. Different carbon support for respiration and secondary production in unproductive lakes. Oikos 116, 1691–1696. https://doi.org/10.1111/j.0030-1299.2007.15825.x.
Karlsson, J., Byström, P., Ask, J., Ask, P., Persson, L., Jansson, M., 2009. Light limitation of nutrient-poor lake ecosystems. Nature 460, 506–509. https://doi.org/10.1038/nature08179.
Kreienkamp, F., Huebener, H., Linke, C., Spekat, A., 2012. Good practice for the usage of climate model simulation results - a discussion paper. Environ. Syst. Res. 1, 9. https://doi.org/10.1186/2193-2697-1-9.
Kritzberg, E.S., Hasselquist, E.M., Škerlep, M., Löfgren, S., Olsson, O., Stadmark, J., Valinia, S., Hansson, L.A., Laudon, H., 2020. Browning of freshwaters: consequences to ecosystem services, underlying drivers, and potential mitigation measures. Ambio 49, 375–390. https://doi.org/10.1007/s13280-019-01227-5.
Larsen, S., Andersen, T., Hessen, D.O., 2011a. Predicting organic carbon in lakes from climate drivers and catchment properties. Glob. Biogeochem. Cycles 25. https://doi.org/10.1029/2010GB003908.
Larsen, S., Andersen, T., Hessen, D.O., 2011b. Climate change predicted to cause severe increase of organic carbon in lakes. Glob. Chang. Biol. 17, 1186–1192. https://doi.org/10.1111/j.1365-2486.2010.02257.x.
Lepori, F., Keck, F., 2012. Effects of atmospheric nitrogen deposition on remote freshwater ecosystems [Internet]. cited 2022 Oct 2641. Ambio, Springer, pp. 235–246 Available from: https://link.springer.com/article/10.1007/s13280-012-0250-0.
Masson-Delmotte, V., Zhai, P., Pirani, A., Connors, S.L., Péan, C., Berger, S., Caud, N., Chen, Y., Goldfarb, L., Gomis, M.I., Huang, M., Leitzell, K., Lonnoy, E., Matthews, J.B.R., Maycock, T.K., Waterfield, T., Yelekçi, O., Yu, R., Zhou, B., 2021. IPCC. 2021: summary for policymakers. Available atClimate Change 2021: The Physical Science Basis. Contribution of Working Group i to the Sixth Assessment Report of the Intergovernmental Panel on Climate Change. IPCC, Cambridge, United Kingdom; New Yoak, USA , pp. 3–32. https://www.ipcc.ch/report/ar6/wg1/.
Monteith, D.T., Stoddard, J.L., Evans, C.D., De Wit, H.A., Forsius, M., Høgåsen, T., Wilander, A., Skjelkvåle, B.L., Jeffries, D.S., Vuorenmaa, J., Keller, B., Kopécek, J., Vesely, J., 2007. Dissolved organic carbon trends resulting from changes in atmospheric deposition chemistry. Nature 450, 537–540. https://doi.org/10.1038/nature06316.
Myrstener, E., Ninnes, S., Meyer-Jacob, C., Mighall, T., Bindler, R., 2021. Long-term development and trajectories of inferred lake-water organic carbon and pH in naturally acidic boreal lakes. Limnol. Oceanogr. 66, 2408–2422. https://doi.org/10.1002/lno.11761.
Nieminen, M., 2004. Export of dissolved organic carbon, nitrogen and phosphorus following clear-cutting of three Norway spruce forests growing on drained peatlands in southern Finland. Silva Fenn. 38 (2), 123–132. https://doi.org/10.14214/sf.422.. http://dx.doi.org/10.14214/sf.422.
Nordic Council of Ministers, 2021. Policies for the Promotion of BECCS in the Nordic Countries. TemaNord 2021:538. Available at https://pub.norden.org/temanord2021-538/.
Norsk Vann, 2019. Drinking water sources need to be protected against pollution (In Norwegian). Available atNorsk Vann mener – Vannkilder . https://norskvann.no/vannforsyning-og-drikkevann/vannkilder/.
NVE, https://www.nve.no/kart/kartdata/vassdragsdata/nedborfelt-regine/ (In Norwegian). Available at.
Opdal, A.F., Lindemann, C., Aksnes, D.L., 2019. Centennial decline in North Sea water clarity causes strong delay in phytoplankton bloom timing. Glob. Chang. Biol. 25, 3946–3953. https://doi.org/10.1111/gcb.14810.
World Climate Research Program, n.d.World Climate Research Program, n.d. CMIP Phase 6. Available at https://www.wcrp-climate.org/wgcm-cmip/wgcm-cmip6.
R Core Team, 2021. R: A Language and Environment for Statistical Computing. 2021. Available at R Foundation for Statistical Computing, Vienna, Austria. https://www.r-project.org/.
Räike, A., Kortelainen, P., Mattsson, T., Thomas, D.N., 2016. Long-term trends (1975–2014) in the concentrations and export of carbon from finnish rivers to the Baltic Sea: organic and inorganic components compared. Aquat. Sci. 78 (3), 505–523. https://doi.org/10.1007/s00027-015-0451-2.

Raju, K.S., Kumar, D.N., 2020. Review of approaches for selection and ensembling of GCMS. J. Water Clim. Chang. 11, 577–599. https://doi.org/10.2166/wcc.2020.128.

Ramirez, K.S., Craine, J.M., Fierer, N., 2012. Consistent effects of nitrogen amendments on soil microbial communities and processes across biomes. Glob. Chang. Biol. 18, 1918–1927. https://doi.org/10.1111/j.1365-2486.2012.02639.x.

Riahi, K., Vuuren, D.P.van, Kriegler, E., Edmonds, J., O'Neill, B.C., Fujimori, S., Bauer, N., Calvin, K., Dellink, R., Fricko, O., Lutz, W., Popp, A., Cuaresma, J.C., KC, S., Leimbach, M., Jiang, L., Kram, T., Rao, S., Emmerling, J., Ebi, K., Hasegawa, T., Havlik, P., Humpenöder, F., Da Silva, L.A., Smith, S., Stehfest, E., Bosetti, V., Eom, J., Gernaat, D., Masui, T., Rogelj, J., Strefler, J., Drouet, L., Krey, V., Luderer, G., Harmsen, M., Takahashi, K., Baumstark, L., Doelman, J.C., Kainuma, M., Klimont, Z., Marangoni, G., Lotze-Campen, H., Obersteiner, M., Tabeau, A., Tavoni, M., 2017. The Shared Socioeconomic Pathways and their energy, land use, and greenhouse gas emissions implications: an overview. Glob. Environ. Chang. 42, 153–168. https://doi.org/10.1016/j.gloenvcha.2016.05.009.

Sætre, R., 2007. The Norwegian Coastal Current - Oceanography and Climate. Tapir Academic Publisher, Trondheim, Norway.

Schulte-Uebbing, L., de Vries, W., 2018. Global-scale impacts of nitrogen deposition on tree carbon sequestration in tropical, temperate, and boreal forests: A meta-analysis. Glob. Chang Biol. 24 (2), 416–431 Available from: https://onlinelibrary.wiley.com/doi/full/10.1111/gcb.13862.

Škerlep, M., Steiner, E., Axelsson, A.L., Kritzberg, E.S., 2020. Afforestation driving long-term surface water browning. Glob. Chang. Biol. 26 (3), 1390–1399. https://doi.org/10.1111/gcb.14891.

Skjelkvåle, B.L., 2003. The 15-year report: assessment and monitoring of surface waters in Europe and North America; acidification and recovery, dynamic modelling and heavy metals. ICP-Waters report 73-2003Norwegian Institute of Water Research, Oslo, Norway. https://niva.brage.unit.no/niva-xmlui/handle/11250/212201.

Solberg, Carina O., 2022. Clarifying the Role of Ferric Iron for Dissolved Natural Organic Matter Ultraviolet and Visible Light Absorbance. MSc. ThesisUniversity of Oslo. DUO MSc. Thesis.

The National Center for Atmospheric Research, 2018. Global GIMMS NDVI3g v1 dataset (1981-2015), A Big Earth Data Platform for Three Poles. http://poles.tpdc.ac.cn/en/data/9775f2b4-7370-4e5e-a537-3482c9a83d88/.

The Unified EMEP Model - User Guide. https://wiki.met.no/_media/emep/page1/userguide092012.pdf.

Thrane, J.E., Hessen, D.O., Andersen, T., 2014. The absorption of light in lakes: negative impact of dissolved organic carbon on primary productivity. Ecosystems 17, 1040–1052. https://doi.org/10.1007/s10021-014-9776-2.

Tranvik, L.J., Cole, J.J., Prairie, Y.T., 2018. The study of carbon in inland waters—from isolated ecosystems to players in the global carbon cycle. Limnol. Oceanogr. Lett. 3, 41–48. https://doi.org/10.1002/lol2.10068.

Tranvik, L.J., Downing, J.A., Cotner, J.B., Loiselle, S.A., Striegl, R.G., Ballatore, T.J., Dillon, P., Finlay, K., Fortino, K., Knoll, L.B., Kortelainen, P.L., Kutser, T., Larsen, S., Laurion, I., Leech, D.M., Leigh McCallister, S., McKnight, D.M., Melack, J.M., Overholt, E., Porter, J.A., Prairie, Y., Renwick, W.H., Roland, F., Sherman, B.S., Schindler, D.W., Sobek, S., Tremblay, A., Vanni, M.J., Verschoor, A.M., Von Wachenfeldt, E., Weyhenmeyer, G.A., 2009. Lakes and reservoirs as regulators of carbon cycling and climate. Limnol. Oceanogr. 54, 2298–2314. https://doi.org/10.4319/lo.2009.54.6_part_2.2298.

Velthuis, M., Kosten, S., Aben, R., Kazanjian, G., Hilt, S., Peeters, E.T.H.M., 2018. Warming enhances sedimentation and decomposition of organic carbon in shallow macrophyte-dominated systems with zero net effect on carbon burial. Glob. Chang. Biol. 24, 5231–5242. https://doi.org/10.1111/gcb.14387.

Vittinghoff, E., Glidden, D.V., Shiboski, S.C., Mcculloch, C.E., 2012. Regression Methods in Biostatistics - Introduction. https://doi.org/10.1142/S0129065712030037.

Vogt, R.D., De Wit, H.A., Koponen, K., 2022. Case study on impacts of large-scale re-/afforestation on ecosystem services in Nordic regions. Available fromQuantifying and Deploying Responsible Negative Emissions in Climate Resilient Pathway. Negemproject.eu 3.1.4 . https://www.negemproject.eu.

Vries, W.de, Schulte-Uebbing, L., 2019. Impacts of nitrogen deposition on forest ecosystem services and biodiversity. Atlas of Ecosystem Services. Springer, Cham, pp. 183–189 https://doi.org/10.1007/978-3-319-96229-0_29.

Weyhenmeyer, G.A., Fröberg, M., Karltun, E., Khalili, M., Kothawala, D., Temnerud, J., Tranvik, L.J., 2012. Selective decay of terrestrial organic carbon during transport from land to sea. Glob. Chang. Biol. 18 (1), 349–355. https://doi.org/10.1111/j.1365-2486.2011.02544.x.

Wit, H.A., Couture, R.M., Jackson-Blake, L., Futter, M.N., Valinia, S., Austnes, K., Guerrero, J.L., Lin, Y., 2018. Pipes or chimneys? For carbon cycling in small boreal lakes, precipitation matters most. Limnol. Oceanogr. Lett. 3, 275–284. https://doi.org/10.1002/lol2.10077.

WorldClim, n.d.WorldClim, n.d. Data format — WorldClim 1 documentation. Available at https://worldclim.org/data/v1.4/formats.html.

Xiao, Y., Riise, G., 2021. Coupling between increased lake color and iron in boreal lakes. Sci. Total Environ. 767, 145104. https://doi.org/10.1016/j.scitotenv.2021.145104.

Yang, H., Andersen, T., Dörsch, P., Tominaga, K., Thrane, J.E., Hessen, D.O., 2015. Greenhouse gas metabolism in nordic boreal lakes. Biogeochemistry 126, 211–225. https://doi.org/10.1007/s10533-015-0154-8.

Paper 2: Factors Governing Biodegradability of Dissolved Natural Organic Matter in Lake Water.

Crapart Camille, Tom Andersen, Dag Olav Hessen, Nicolas Valiente, and Rolf David Vogt. 2021.

Water (Switzerland) 13 (16)

Photo: Camille Crapart/Alexander Håland

water

MDPI

Article

Factors Governing Biodegradability of Dissolved Natural Organic Matter in Lake Water

Camille Crapart [1,*], Tom Andersen [2], Dag Olav Hessen [2], Nicolas Valiente [2] and Rolf David Vogt [1]

[1] Center of Biogeochemistry in the Anthropocene, Department of Chemistry, University of Oslo, P.O. Box 1033, 0371 Oslo, Norway; r.d.vogt@kjemi.uio.no
[2] Center of Biogeochemistry in the Anthropocene, Department of Biosciences, University of Oslo, P.O. Box 1066, 0371 Oslo, Norway; tom.andersen@ibv.uio.no (T.A.); d.o.hessen@mn.uio.no (D.O.H.); n.v.parra@ibv.uio.no (N.V.)
* Correspondence: c.m.crapart@kjemi.uio.no

Abstract: Dissolved Natural Organic Matter (DNOM) is a heterogeneous mixture of partly degraded, oxidised and resynthesised organic compounds of terrestrial or aquatic origin. In the boreal biome, it plays a central role in element cycling and practically all biogeochemical processes governing the physico-chemistry of surface waters. Because it plays a central role in multiple aquatic processes, especially microbial respiration, an improved understanding of the biodegradability of the DNOM in surface water is needed. Here the current study, we used a relatively cheap and non-laborious analytical method to determine the biodegradability of DNOM, based on the rate and the time lapse at which it is decomposed. This was achieved by monitoring the rate of oxygen consumption during incubation with addition of nutrients. A synoptic method study, using a set of lake water samples from southeast Norway, showed that the maximum respiration rate (RR) and the normalised RR (respiration rate per unit of carbon) of the DNOM in the lakes varied significantly. This RR is conceived as a proxy for the biodegradability of the DNOM. The sUVa of the DNOM and the C:N ratio were the main predictors of the RR. This implies that the biodegradability of DNOM in these predominantly oligotrophic and dystrophic lake waters was mainly governed by their molecular size and aromaticity, in addition to its C:N ratio in the same manner as found for soil organic matter. The normalised RR (independently of the overall concentration of DOC) was predicted by the molecular weight and by the origin of the organic matter. The duration of the first phase of rapid biodegradation of the DNOM (BdgT) was found to be higher in lakes with a mixture of autochthonous and allochthonous DNOM, in addition to the amount of biodegradable DNOM.

Keywords: biodegradability; DNOM; sUVa; nutrient status; boreal lakes; browning

Citation: Crapart, C.; Andersen, T.; Hessen, D.O.; Valiente, N.; Vogt, R.D. Factors Governing Biodegradability of Dissolved Natural Organic Matter in Lake Water. *Water* **2021**, *13*, 2210. https://doi.org/10.3390/w13162210

Academic Editors: Tea Zuliani and Tina Kosjek

Received: 31 May 2021
Accepted: 9 August 2021
Published: 13 August 2021

1. Introduction

The amount of Dissolved Natural Organic Matter (DNOM) in boreal surface waters typically exceeds in mass the content of inorganic constituents, and carbon associated with DNOM by far exceeds the biotic pools of C [1]. This DNOM, being a very heterogeneous mix of partly degraded organic compounds, has a profound effect on the cycling of carbon (C) and associated elements such as nitrogen (N) and phosphorus (P), in addition to the physicochemical characteristics of surface waters. During recent decades, the concentrations of DNOM in surface water have increased, especially in boreal lakes [2]. In these aqueous systems most of the DNOM is allochthonous, i.e., derived from the catchment [3]. The main driver for the ongoing rise in DNOM is the increase in terrestrial biomass (greening), rendering more organic matter in the soils available to be partly decomposed and leached out, causing surface water browning [4,5]. This is due to the rise in mean temperatures and to the increase in forest biomass [6], which, e.g., reached 29% in southeast Norway between 1971 and 2000 [7]. A concomitant factor is the increasing runoff and runoff intensity. This causes shifts in soil–water flow paths, with more water flowing

through the organic-rich forest floor horizons before entering the stream, bypassing the absorptive capacity of the deeper mineral soil. A third major factor applies to regions heavily exposed to acid deposition in the 1970–1980s. Since then, sulphur (S) deposition has decreased by up to 90% in the previously most affected areas in southern Norway. The subsequent decrease in ionic strength, in addition to Al^{3+} and H^{+} concentrations, has increased DNOM solubility and reduced its flocculation, increasing its flux to surface waters [8,9]. However, the decrease in S deposition has subsided, and the effect of this driver no longer contributes significantly to the present increase in DNOM.

The increased concentrations of DNOM in lakes have, in turn, significant impacts on the lake ecosystem. The increasing content of chromophoric DNOM (CDOM) reduces light penetration and thereby the depth of photosynthetic active radiation [10]. Concurrently, the increased contribution of allochthonous carbon boosts microbial metabolism and therefore enhances heterotrophic respiration. This is potentially boosting the net emission of the greenhouse gases (GHGs) CO_2 and CH_4 [11], promoting the role of boreal lakes as hot-spots for GHG emissions [3].

The bioavailability of DNOM to bacterial respiration is known to mainly depend on its molecular weight and aromaticity, with the low molecular weight (LMW) and more saturated moieties of the DNOM being most biodegradable [12]. Allochthonous DNOM has a generally higher molecular weight (HMW) and is more aromatic than DNOM produced in situ (autochthonous) [13]. Nevertheless, due to the large flux of DNOM from boreal catchments, the allochthonous DNOM constitutes a significant fraction of the bioavailable organic C in their surface waters. In addition, the DNOM contents of key nutrients, such as N and P, are important for both autotroph and heterotroph production of boreal lakes [11]. In addition, photodegradation, or photobleaching, transforms the aromatic HMW DNOM moieties into more saturated and more LMW DNOM compounds that are thus more bioavailable [14]. Insights into the factors governing the microbial respiration of DNOM (i.e., its biodegradability) are important for assessing the transformation of organic C to CO_2.

The objective of this study was to assess the temporal dynamics of DNOM biodegradability in a wide range of boreal lakes with different quantities and qualities of DNOM. This measure of biodegradability differs from end-point measurements of the biodegradable amount of organic carbon (BDOM), estimated either by the decline in oxygen concentration or the increase in CO_2 emissions, or by analysing the content of DOC [15]. During incubation, the decline in oxygen (O_2) concentration is monitored over time with gas sensors, providing a measure of the maximum speed at which bacteria consume O_2 (i.e., respiration rate (RR), DOC normalised RR (RRn), and duration of rapid biodegradation (BdgT)) that relates to the physicochemical properties of the DNOM and other water quality properties. Optical sensors for dissolved oxygen have previously been used to measure the biodegradability of organic pollutants under incubation [16]. The estimation of the respiration rate of organic matter with optical sensors has been previously undertaken in our group [17–20]. The large scale of the current study allows a standardisation of the method, including the development of a script for the extraction of biodegradability parameters and the comparison of the respiration rates in a large variety of samples.

2. Materials and Methods

2.1. Water Sampling

Surface water samples from 73 lakes in southeast Norway (Figure 1) were collected in autumn 2019 for detailed biogeochemical studies by the Centre for Biogeochemistry (CBA) at the University of Oslo, Norway. They were selected as a subset of the lakes sampled during the national lake survey, itself repeating the sampling of previous campaigns conducted in 1986 and 1995 [21,22]. These lakes span a wide range of water quality properties, notably DNOM, covering different catchment sizes and elevations. Most Norwegian lakes are oligotrophic or dystrophic, although a few of the lakes in the selection have mesotrophic or eutrophic characteristics (Figure S1).

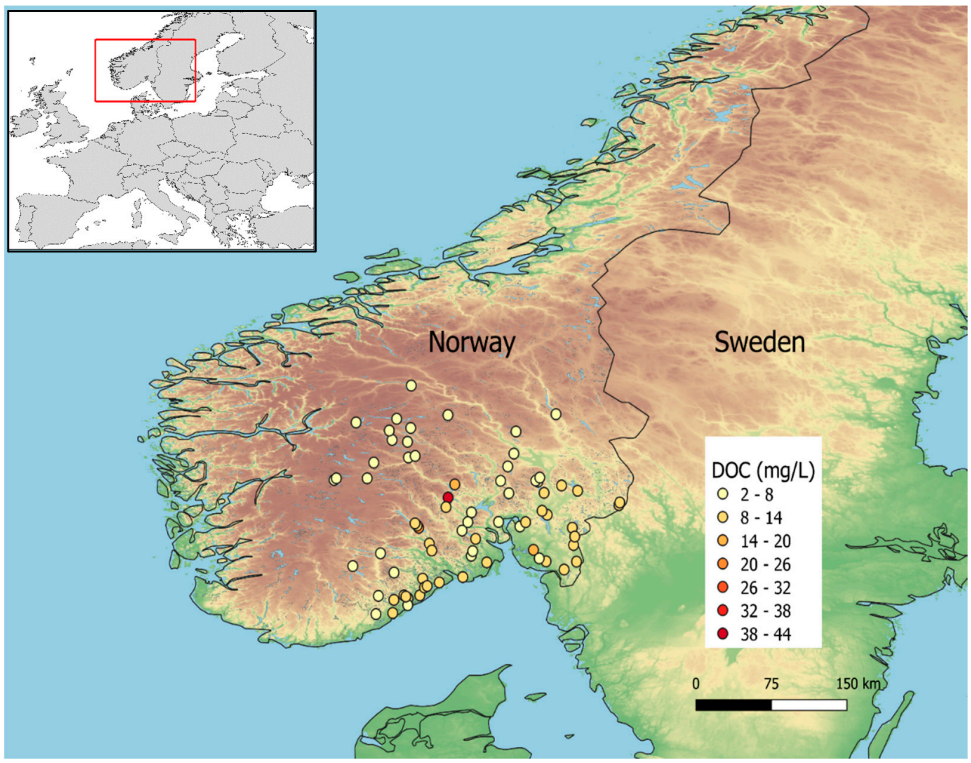

Figure 1. Map of South Norway with the 73 sampled lakes and their DOC concentration (in mg/L) as a proxy for DNOM.

2.2. Explanatory Water Quality Factors

The biodegradability of DNOM (RR, RRn and BdgT) from the 73 sampled lakes was related to more than 80 variables, describing the DNOM quality, in addition to the physical, chemical, and biological characteristics of the lake samples. The complete dataset and details about the experimental settings for the measurement of these variables are available on an online repository dedicated to the survey [23] and a summary is available in the Supplementary Material (Table S1). From these 80 parameters, 27 were selected as explanatory parameters based on their conceptual relevance. Empirical and conceptual links between the derived biodegradability descriptors and the following explanatory parameters were thus assessed: DOC normalised UV and VIS absorbance (sUVa = Aλ254 nm/DOC, sVISa = Aλ400 nm/DOC), UV/VIS absorbance ratio (SARuv), and spectral slope ratio (SR = Aλ275–295/Aλ350–400), along with DOC concentration, pH, alkalinity, lake temperature (T), conductivity (EC), O_2, CO_2, N_2O and CH_4 concentration, consumption and production, major cations (Calcium (Ca), Magnesium (Mg), Sodium (Na), Potassium (K)) and anions (Sulphate (SO_4), Chloride (Cl)), Iron (Fe), Aluminium (Al), dissolved reactive Nitrogen and -Phosphorus (DN, DP), carbon to nutrient ratios (C:N, C:P), and bacterial abundance. The gas concentration, consumption, and production were obtained from a concomitant experiment, independent of the biodegradability measurements [11,24]. It should be noted that the nutrient concentrations applied for the statistical analysis is the original concentration in the sample water, not the concentration after the addition of nutrients for the incubation experiment.

As commonly found for environmental concentration variables, most of the ion and nutrient concentration data were not normally distributed, but rather skewed towards higher concentrations. Therefore, the concentration data were log transformed prior to analysis, except for pH, which is already in logarithmic form. Optical proxies of DNOM characteristics and cell counts where normally distributed and thus not log transformed. The dataset was standardised prior to regression analysis in order to ease the comparison of the effect size [25].

2.3. Determination of Biodegradability

A detailed description of the experiment protocol is available online [26] and provided in the Supplementary Material (Chapter B). The main principles and concepts are summarised in the following.

2.3.1. Sample Preparation for Biodegradability Analysis

At the sampling sites, a bucket of raw water was collected with a sampling rod close to the outlet of the lake, approximately 4 m from the shore. A quantity of 50 mL of raw water was filtered through a sterile 0.22 µm cartridge (Sterivex-GP Pressure unit filter, rinsed by pipetting 120 mL raw water through cartridge before sampling) to remove bacteria and eucaryotes. The samples were transported and stored at 10 °C in polyethylene bottles. Biodegradability measurements were conducted within 7 days after sampling. All batches of inoculum were prepared from a 50 L sample of water containing natural microbial communities (mainly bacteria) collected on September 8th, 2019, from one of the 73 sites, the dystrophic lake Langtjern ecological monitoring station (NIVA, 2021). After sampling, the water was filtered through 2.0 µm Isopore Membrane Filters to remove zooplankton. The water was then stored until use at in a closed tank at 10 °C with water circulation.

Three to five days prior to each incubation, the inoculum was prepared with 100 mL of the filtered water withdrawn from the tank and 1 mL of a solution of nutrients (5 mM ammonium nitrate and 5 mM dipotassium phosphate) to ensure unlimited growth of the bacterial community.

2.3.2. Incubation

The inoculum was added to each sample prior to the incubation, along with ample amounts of nutrients (same solution of 2:1 N:P as for the inoculum). N and P were added to ensure that the only limitation for the respiration rate at maximum O_2 consumption was the biodegradability of the DNOM substrate, and thus that the biodegradability was primarily governed by the DNOM quantity and quality. A quantity of 0.25 mL of the inoculum solution and 0.25 mL of nutrient solution were added to 25.0 mL of the water sample, which means that 1% of the sample volume was added of both solutions. Therefore, the final concentration of nutrients in the biodegradation samples was 4- to 20-fold higher than that of the lake water with respect to N, and around 1000-fold for P. Aliquots of 5 mL samples were transferred into gas-tight PreSens SensorVials and placed on a PreSens plate (PreSens Precision Sensing, Regensburg, Germany) that holds 24 vials. Five samples with 4 replicates each were run in parallel, along with 3 blanks (5 mL of Type-1 water) and a house standard (solution of 20 mg C/L, prepared from Reverse Osmosis and freeze-dried isolate from Hellerudmyra, the source of The Nordic Humus Standard [27]). We did not include samples without added nutrients, because pilot studies showed very little biodegradation during the incubation period in that case. The 5 mM concentration for the stock solution of phosphate and ammonium nitrate was based on pilot studies, showing an increasing effect on biodegradation up to 5 mM, which levelled off above this concentration.

Three phases are commonly observed during incubation experiments [28]. During the initial phase, or "lag phase", the inoculated bacterial community adapts to its new environment and substrate. During this phase oxygen consumption is low. Some activity is nevertheless taking place because the bacteria are synthesising new enzymes adapted to the new substrate, though no significant biodegradation occurs [28]. Following this phase, the bacterial respiration of the DNOM increases. The maximum rate of oxygen consumption obtained during a linear phase is used as a measure of RR of the DNOM and thus a proxy for its biodegradability. Eventually, a decrease in respiration occurs due to limitation in BDOM, lack of O_2, or an accumulation of toxic wastes from the bacterial community. This phase subsides on a stationary plateau where the decrease in O_2 is low.

2.3.3. Inoculum Composition

A standardised inoculum from one site was used in this study. This could represent a bias relative to site-specific properties and CDOM qualities. It was nevertheless assumed that the large biodiversity of bacteria in freshwater enables the population to adapt during the lag phase to the range of water qualities and DNOM substrates assessed in this study [29]. To test the assumption of microbial similarity, the bacterial community composition in Langtjern (the origin of the inoculum) was compared with that of the other 72 lakes. For this purpose, the Sterivex filter cartridges, used to remove bacteria and eucaryotes from the samples (Section 2.3.1), were liquid nitrogen frozen immediately after use on-site. Total DNA was extracted from each filter using a DNesay PowerWater Sterivex Kit (Qiagen, Hilden, Germany). Bacterial SSU rRNA gene amplicons were sequenced using an Illumina MiSeq with a 2 × 300 bp chemistry MiSeq (Illumina, San Diego, USA) at IMR sequencing facility (Dalhousie University, Halifax, Canada) following procedures from Comeau et al. [30]. As forward and reverse primers, 515FB (5′-GTGYCAGCMGCCGCGGTAA-3′) and 806RB (5′-GGACTACNVGGGTWTCTAAT-3′) were used, respectively. Raw sequences were trimmed of primers with CUTADAPT [31] and analysed with the R package dada2, version 1.18.0 [32] for de-replicating, de-noising, and sequence-pair assembly. Finally, taxonomy was assigned using the SILVA138 database.

A total of 1181 genera were found, confirming the large diversity of bacteria. To simplify the analysis, the genera, families, and orders were grouped by class taxonomic rank so that the sample sites could be clustered depending on the number of occurrence of bacteria from a given class. The ideal number of clusters was determined using the silhouette method [33]. This resulted in 3 site clusters, represented in Figure 2. An analysis of variance of the dependent variables based on these three clusters is presented in Section 3.1. All the computations were performed using the "factoextra" [34] and "dendextend" [35] packages in R.

Figure 2. Dendrogram of the 73 sampling sites sorted by similar bacteria classes. Different colours show the three main clusters. The inoculum was sampled in "Langtjern". Computations were performed with the "factoextra" and "dendextend" packages in R.

2.3.4. Instrumentation

PreSens Oxygen sensors measure the oxygen concentration in samples by its quenching of fluorescence decay (PreSens Precision Sensing, Regensburg, Germany). The sensors contain a dye that is excited once every minute. The dye subsequently emits a fluorescence signal detected by the instrument. Oxygen molecules present in the solution collide with the excited dye, quenching the fluorescence, and thereby decreasing its intensity. Hence, the higher the oxygen concentration, the more collisions and the shorter the fluorescence lifetime. The lifetime of the fluorescence is recorded and converted to oxygen concentration using the Stern–Volmer equation. The oxygen sensors are situated in the bottom of the Sensor Vials, which are set on a plate with 24 wells. The plates are mounted on the Sensor Reader in an incubator (Digital incubator Incu-line 23 L, VWR International, Oslo, Norway), maintaining a constant temperature at 25 °C during the 30 h incubation period. The incubation time was chosen empirically as the time at which most samples have reached the last phase plateau.

2.3.5. Data Processing

The oxygen concentration in each vial was monitored every minute by the PreSens software (SDR_v4.0.0). Typically, the curve of oxygen concentration with time had a negatively sigmoid shape (Figure 3). A R script was developed to extract descriptive parameters for the biodegradability of DNOM from each curve by the following steps.

Data were removed from the initial hours of incubation, due to an unstable temperature and the lag phase (Section 2.3.2), and measurement after 30 h.

1. The oxygen concentration values ($[O_2]_{t,initial}$) were normalised ($[O_2]_{t,corrected}$) by the ratio of oxygen concentration in the corresponding blanks ($[O_2]_{t,blank}$) divided by the mean of all the blanks, according to the following equation:

$$[O_2]_{t,\ corrected} = \frac{[O_2]_{t,initial}}{\frac{[O_2]_{t,blank}}{mean([O_2]_{blank})}}$$

2. The decline in oxygen concentration in each vial was fitted as a constrained spline (median R^2 = 0.97) and the derivative of the equation was calculated ("scam" and "base" package on R). Typically, the derivative curve displays a peak, corresponding to the maximum rate of oxygen consumption. Two parameters were extracted from this peak, as shown in Figure 4: the maximum respiration rate (RR) and the biodegradation period (BdgT). The first half of the peak was used to determine the BdgT to avoid effects of limited O_2 or accumulation of toxic wastes from the bacterial community (Section 2.3.2).
3. RR and BdgT (Table 1) were determined for each of the 73 lakes as the median of 4 replicate samples. The area under the curve of the derivative was strongly correlated with RR (r = 0.93). It thus provided no new information and was therefore not included in the assessment.

Table 1. Parameters describing the biodegradability of DNOM.

Parameter	Definition	Interpretation
Maximum Respiration rate (RR)	Maximum biodegradation speed ($\mu molO_2\ L^{-1}\ h^{-1}$)	The maximum speed at which the microorganisms consume the DNOM, thus a proxy of the biodegradability of DNOM
Normalised respiration rate (RRn)	Respiration rate divided by the DOC ($\mu molO_2\ h^{-1}\ mgC^{-1}$)	The normalised respiration rate is a quality factor describing the relative speed of biodegradability, independent of the amount of DNOM.
Biodegradation period (BdgT)	Width of the half-peak (h)	The biodegradation period reflects the heterogeneity of DNOM quality, and balance of RR on the one hand and the amount of biodegradable matter on the other.

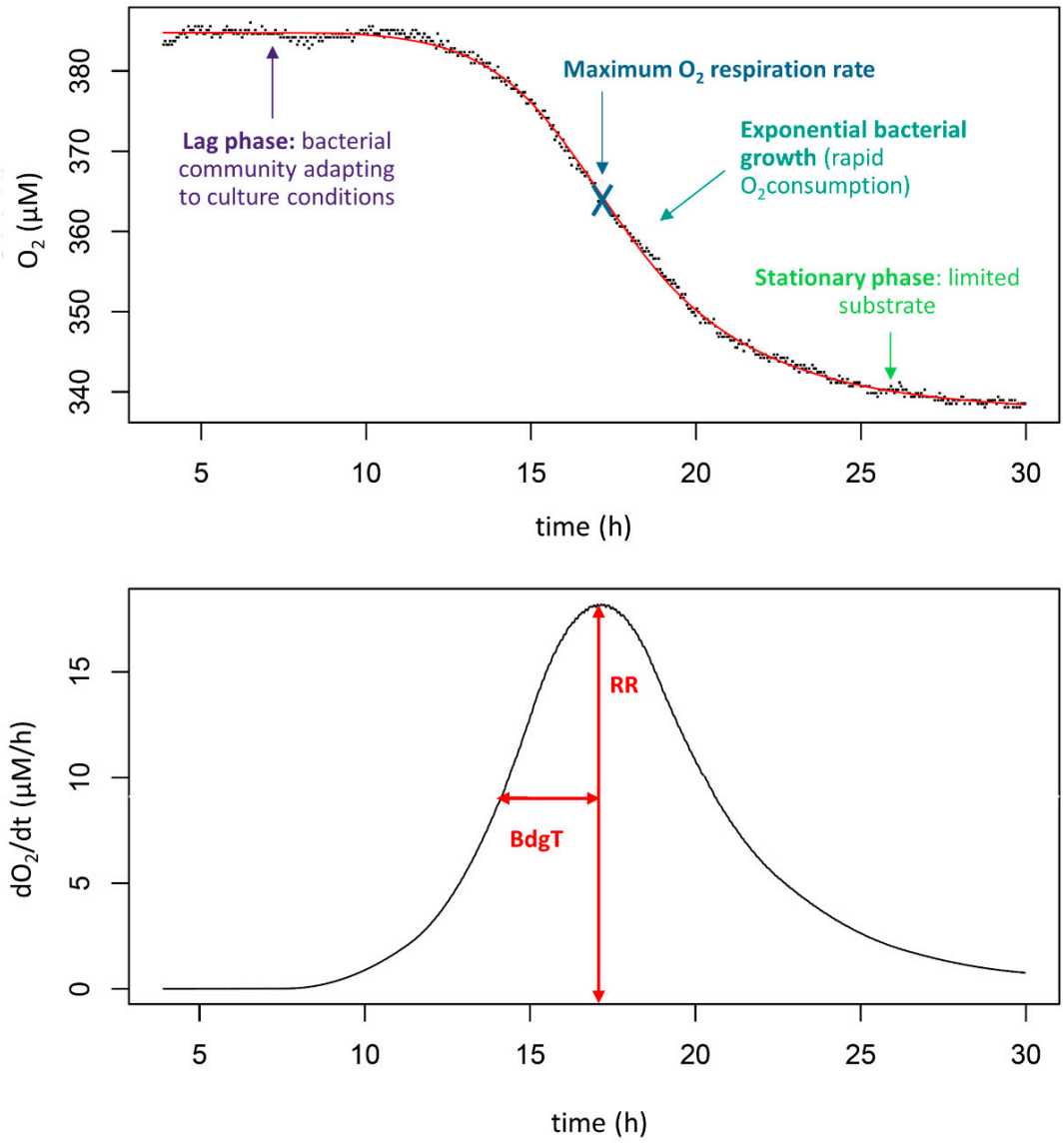

Figure 3. Typical O_2 concentration curve (top panel) and corresponding derivative (bottom panel). RR is the respiration rate and BdgT is the biodegradation Period (see Table 1).

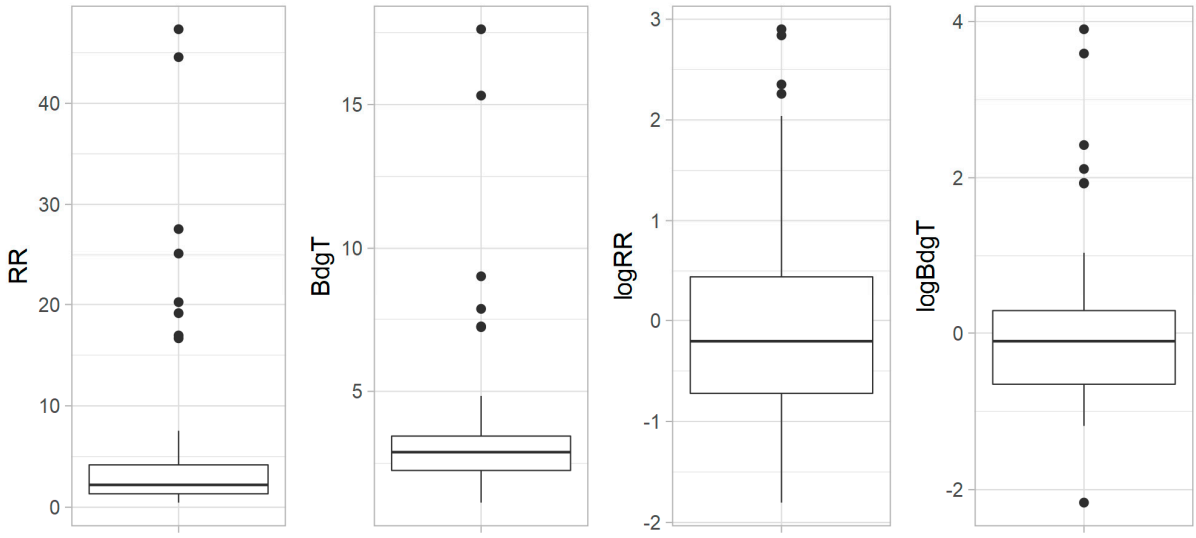

Figure 4. Boxplots of respiration rate (RR) and biodegradability period (BdgT) and their log transformed data, showing the distribution of these parameters in the 73 sampled lakes. The line inside the box represents the median value, and the upper and lower sections of the box show the upper and lower quartiles. The whiskers represent 1.5 times the interquartile range. Outliers are marked as points outside the whiskers.

2.4. Assessment of Factors Governing Biodegradability

Statistical analysis was conducted in R 4.0.3 [30], using the 27 conceptually relevant parameters selected from the CBA-100 lakes survey as predictors (Section 2.2) for the respiration rate (RR), normalised RR (RRn), and the biodegradability period (BdgrT) as response variables. The response variables and the relevant parameters, and the summary statistics of the 73 lakes, are presented in the Supplementary Material (Part A Table S1). Eight missing values in the dataset (summarised in the last column of the Table S1) were imputed by multiple imputation (50 imputations) using the "mice" package in R [36]. The multiple imputations process is described in the Supplementary Material, Part B Figure S5.

Correlation analysis on parameters that were not normally distributed was also conducted on log-transformed data (Section 2.2). A screening of the covariates was then performed to remove covariates with high correlations [37], using the correlation matrix ("micombine.cor") function in the mice package.

Multivariate analysis was performed using a lasso (least absolute shrinkage and selection operator) regression model [38] on the 50 imputed datasets. The lasso model selects relevant parameters by shrinking the estimates of unimportant variables to 0. The estimates are selected by minimising the expression $RSS + \lambda\Sigma|\beta_j|$, where RSS is the residual sum of squares in the model, and λ is the penalty term used to shrink the estimate β [39]. Several **λ** might be obtained depending on how the dataset is separated between a training and a test subset. Cross-validation was applied to each model to select the best lambda (penalty) parameter each time, and the estimates of the covariates were computed and pooled. Pooling of lasso estimates consists of averaging the estimates for each dataset if the estimates were retained for more than half of the 50 lasso regression results. These analyses were undertaken using the cv.glmnet function in the "glmnetUtils" package in the R software environment [40]. The selected parameters were used to compute a multiple linear regression model ("Gauss-lasso regression"). The merits of the resulting models were compared by their mean absolute error (MAE).

3. Results

3.1. Respiration Rate and Time-Lapse of Biodegradability

Most RR values ranged between 0.46 and 7.55 μmol O_2 h^{-1}, though eight samples had higher values up to 47.3 μmol O_2 h^{-1} (Figure 4). Similarly, most BdgT values ranged

from 1.14 h to 4.84 h, with outliers as high as 17.6 h. As is evident from Figure 5, the RR and BdgT data were not normally distributed, but skewed towards higher values. The data were thus log transformed for the following analysis.

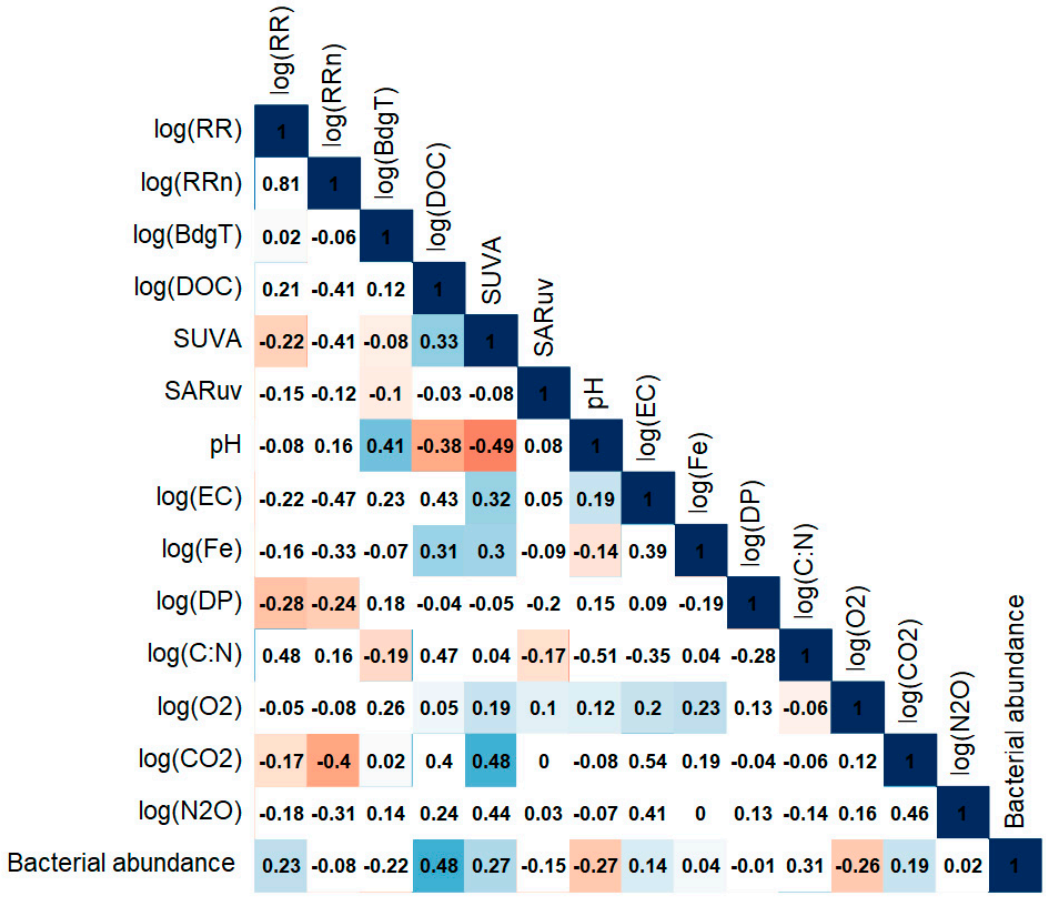

Figure 5. Correlation plot of log transformed response variables log(RR), log(RRn), and log(BdgT), and the 12 selected explanatory variables. Blue and red coloured squares indicate positive and negative significant correlation coefficients ($p < 0.05$), respectively.

The respiration rate (RR) and biodegradation period (BdgT) were calculated from the derivate of the O_2 slope data. RR is not correlated to BdgT (confidence interval for R being $(-0.25; 0.21)$), indicating that RR and BdgT reflect different aspects of the microbial degradation process. An ANOVA showed that there was no significant difference between the three site clusters of bacterial composition (Section 2.3.3) and mean RR ($p = 0.7$) and BdgT ($p = 0.9$). The use of a non-indigenous inoculum does thus not appear to have affected the biodegradation parameters.

3.2. Covariation of Variables

A total of 27 potential explanatory parameters were selected from the CBA lake survey (see Section 2.2). However, regression models are sensitive to collinearity between covariates. Therefore, a correlation matrix with Pearson correlation coefficients was calculated for the 27 potential explanatory variables. The full matrix is presented in the Supplementary Material (Part D Figure S2). Only covariates with a correlation coefficient lower than 0.5 were kept, in order to avoid interaction effects in the models. The resulting 12 selected explanatory parameters are presented in Table 2 and a correlation matrix with the log transformed response variables is presented in Figure 5.

Table 2. Selected 12 explanatory parameter and their aliased covariates.

Selected Explanatory Parameter	Aliased (Covariates with r > 0.5, p < 0.05 Are Indicated by an Asterisk (*))	
	Positive Correlations	**Negative Correlations**
log(DOC)	log(C:P) *, SR, log(DN), log(B)	
sUVa	log(CH_4) *, sVISa	
SARuv	None	
pH	log(Alkalinity) *, log(Ca) *	Log(Al) *, log(C:N)
log(EC)	log(Alkalinity) *, log(Ca) *, log(Mg) *, log(Na) *, log(SO_4) *, log(Cl) *, log(B) *, log(DN) *, log(K), log(CO_2)	
log(Fe)	None	
log(DP)		log(C:P) *
log(C:N)	Log(C:P)	Log(SO_4) *, log(DN) *
Log(O_2)		log(T) *
Log(CO_2)	Log(EC), Log(B), log(CH_4)	
Log(N_2O)	sVISa	
Cells	None	

Log(RR) is significantly correlated (p-value < 0.05) with sUVa (r = −0.22), log(DP) (−0.28), log(CO_2) (−0.17), and cells counts (0.23) (Figure 5). It is also strongly, though not significantly, correlated with log(C:N). The correlation coefficient between log(RRn) and log(RR) is high (r = 0.81), although the p-value is higher than 0.05. Therefore, this correlation is not significant. Log(RR) has negative significant correlations with log(DP) (r = −0.24) and log(CO_2) (r = −0.4). Log(BdgT) is not correlated with log(RR) or log(RRn), but is significantly correlated with pH (r = 0.41) and log(C:N) (r = −0.19). It has also weak significant correlations with sUVa and SARuv (r = −0.08 and r = −0.1).

3.3. Selection of Drivers of Biodegradability

Lasso multiple linear regressions were applied to the dataset of 12 selected explanatory parameters (Table 2) for each of the three log transformed response variables. The lasso regression is a statistical tool allowing covariates with little explanatory power to be discarded, thus only keeping significant covariates. The fitted vs. observed values of the multiple linear regression models are plotted in Figure 6. Their performances are presented by residual plots in the Supplementary Material (Part E Figures S7–S9). The mean absolute error of each of the models was low, but the normal Q-Q plots display residuals skewed to the right, and not following the normal distribution. The estimates for each lasso regression model are plotted in Figure 7.

The lasso regression model with log(RR) as response variable selected six covariates of the 12 (Table 2). Because the dataset was standardised, the estimates reflect the effect size of each variable, not the absolute effect. Log(C:N) was the parameter with the highest explanatory value on log(RR) with β = 0.34. On the contrary, the estimate for log(DP) was β = −0.13. Nutrient concentrations were based on the concentration in the original sample, before addition of nutrients for the incubation experiment. Log(RR) was thus found to increase with an increasing original C:N ratio, and decrease with increasing original DP concentration. sUVa also had a high explanatory value with β = −0.16. (RRn). Cells count, log(Fe), and SARuv were also selected by the model, with estimates of β = 0.07, β = −0.06, and β = −0.04, respectively.

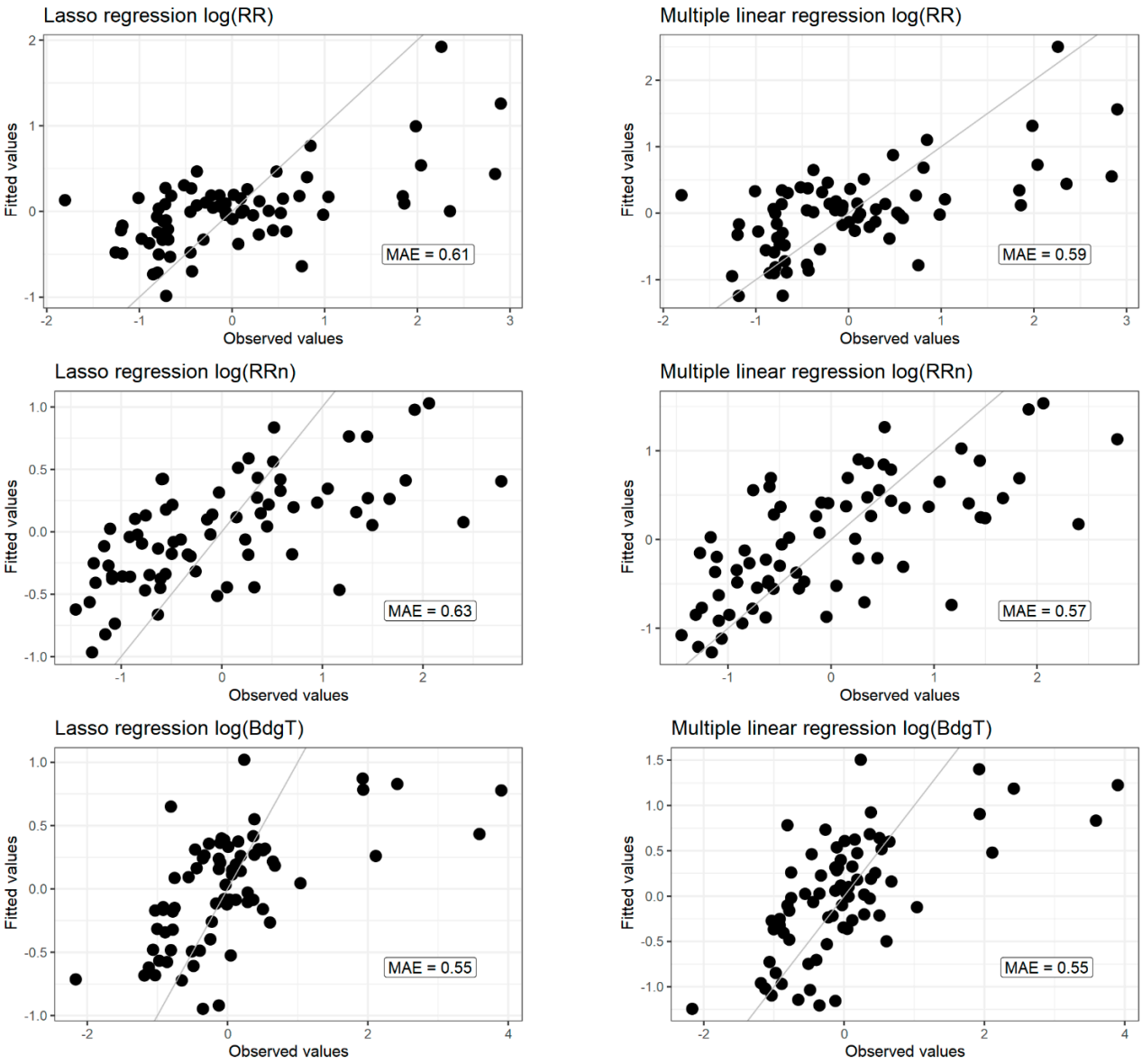

Figure 6. Predicted vs. observed values for lasso regression and multiple linear regression.

For the modelling of log(RRn), seven covariates were selected by the lasso regression, all with a negative effect. Log(EC) had the largest effect with β = −017, followed by sUVa with −0.15. Moreover, log(DP), log(DOC), and log(Fe) had negative estimates, in addition to log(CO_2) and log(SARuv) (β = −0.13, −0.12, −0.06, and −0.05 and −0.04 respectively). This suggests that the normalised respiration rate (the respiration rate divided by the organic carbon concentration) decreases with increasing DOC and phosphate concentrations, and with increasing conductivity (a proxy for ionic strength).

Of the 12 selected covariates, nine were selected for log(BdgT). The estimates with the highest coefficients were the pH with β = 0.38, followed by log(DOC) with β = 0.29, and log(O_2) with β = 0.10. Cells count and SARuv had a negative effect on log(BdgT), with β = 0.17 and β = 0.09, respectively. Log(DP), log(N_2O), log(C:N), and log(Fe) were also selected but had minor effects (β being 0.02, 0.01, −0.01, and −0.05, respectively). The effect of the nutrient concentration on log(BdgT) was opposite to the one observed for log(RR).

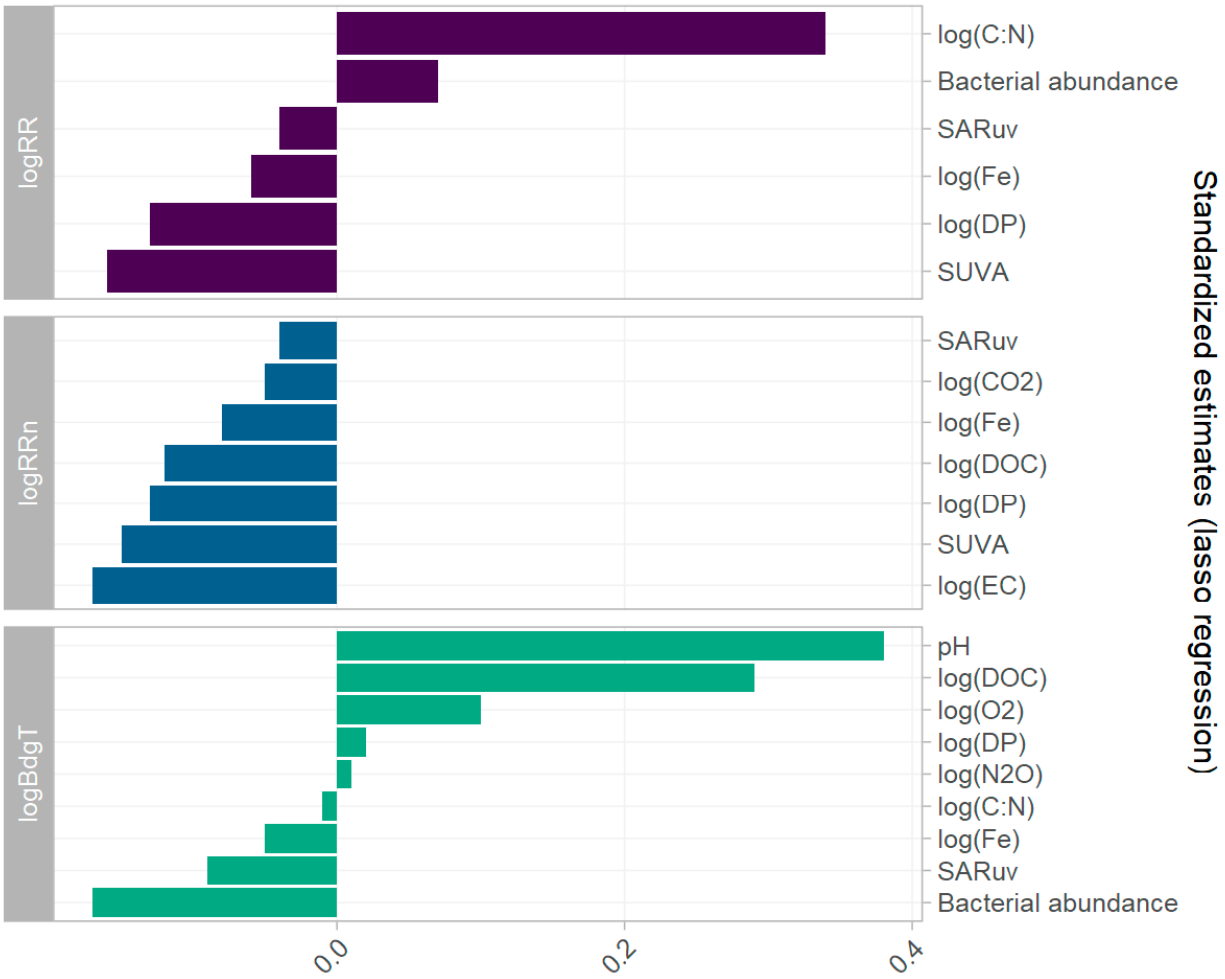

Figure 7. Estimates (pooled for n > 25) of parameter coefficients in lasso regression models of log(RR), log(RRn), and log(BdgT).

3.4. Significance of the Selected Drivers of Biodegradabilityz

Multiple linear regression models for each of the three variables describing the biodegradability of DNOM were constructed based on only the explanatory variables selected by lasso regression (Section 3.3). Each model was performed on the 50 imputed datasets and the resulting estimates, residuals, and predicted values were pooled. The fitted vs. observed values are represented in Figure 7. The residual plots of the model are presented in the Supplementary Material (Part F Figures S10–S12).

The mean absolute errors of the models are similar to those obtained with the lasso regression. Despite the log transformation, residuals are skewed to the right and there is still heteroscedasticity of the data. Moreover, certain data points had high leverage in the model, but no lake had both high leverage and high studentised residual (>3), so all the points were retained in the model. Estimates for the covariates are represented for each model in Figure 8. Only the significant estimates with a *p*-value less than 0.05 are represented (Supplementary Material Part F Table S3). Compared to the lasso regression, few covariates remained significant.

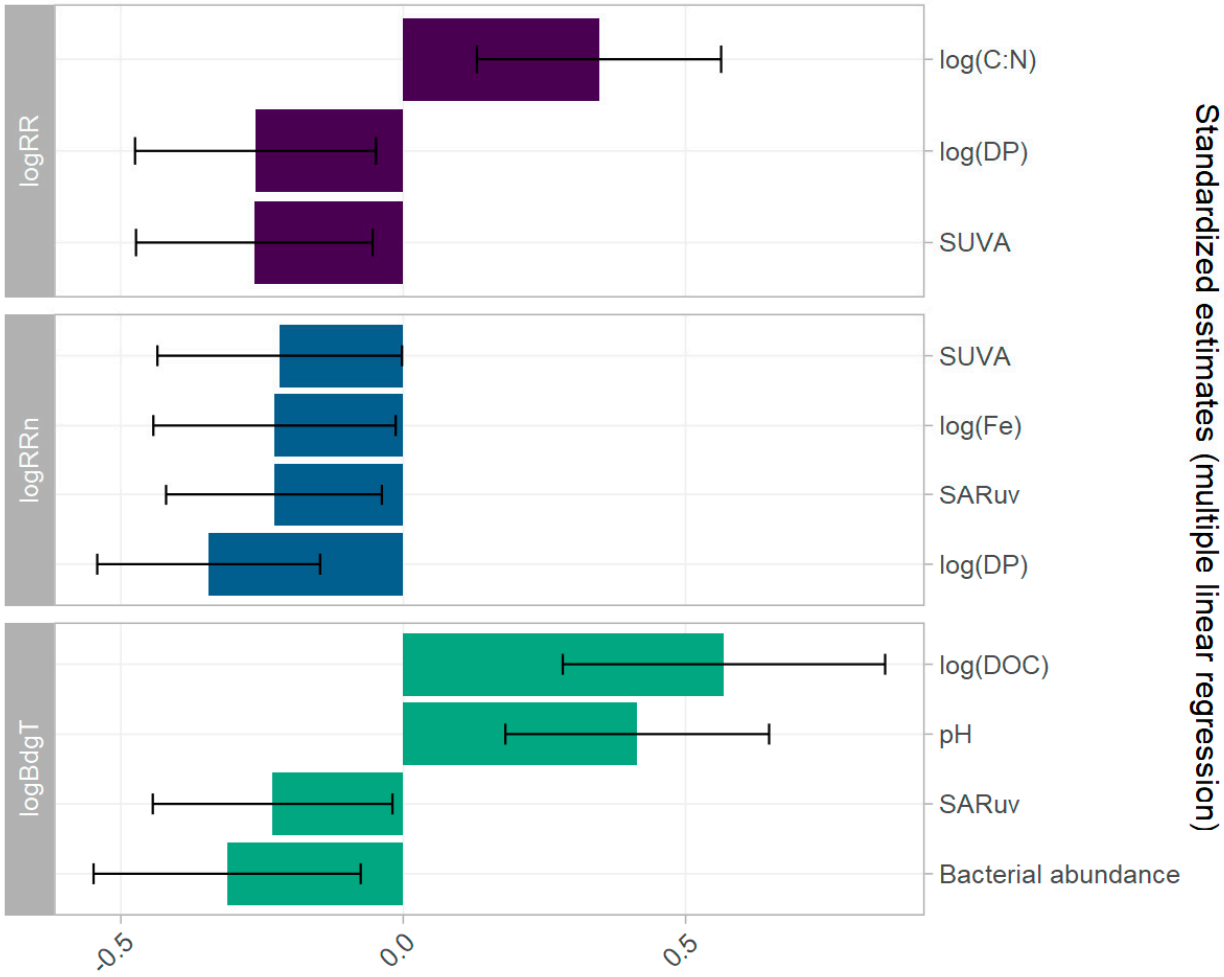

Figure 8. Estimates of the covariates in multiple linear regressions of log(RR), log(RRn), and log(BdgT). Error bars show the confidence interval for each estimate.

Log(RR) is exclusively dependent on sUVa, log(C:N), and log(DP), with log(C:N) remaining as the predictor with the highest impact ($\beta = 0.35$), followed by sUVa and log(DP), both with $\beta = -0.26$.

Log(RRn) is negatively impacted by sUVa and log(DP) in a similar manner as log(RR), with $\beta = -0.22$ and -0.34, respectively. In addition, log(Fe) and SARuv had equally important effects ($\beta = -0.23$). Four explanatory variables were kept for log(BdgT): log(DOC), pH, SARuv, and Cells count (i.e., bacterial abundance) with respective estimates of 0.57, 0.41 and -0.23, and -0.31.

4. Discussion

4.1. Priming Effect Boosting the Respiration Rate

The specific UV absorbance (sUVa) had an explanatory value for the observed variation of log(RR) and log(RRn), both in the correlation analysis and in the lasso and multiple linear regressions. A high sUVa value is an indicator of HMW and of a high degree of aromaticity of the DNOM [36]. Several authors have shown that DNOM with a low sUVa is preferably degraded compared to DNOM with a high sUVa. For example, Zhou et al. [41] highlighted a negative correlation between the BDOM and the sUVa value, and Abbott et al. [42] showed that the sUVa increases during the first 10 days of an incubation experiment, meaning that the HMW aromatic compounds were less degraded than the LMW saturated moieties. Our incubation experiment, focusing on the first hours of bacterial decomposition of the DNOM, confirms that bacterial communities consume preferentially

the LMW and more saturated moieties of the DNOM pool. Even if the residence time of the water in the studied lakes can extend up to 8 years [43] (as represented by Mjøsa, Norway's largest lake), the bacterial community will prioritise fresh, light moieties of DNOM over the remaining HMW compounds. The log normalised respiration rate (log(RRn)) was also negatively associated with sUVa in the lasso and multiple linear regression models, although this relationship may be inherent because both variables are derived by dividing by DOC. Log(Fe) was also found to have a slight negative explanatory value on log(RR) and log(RRn). Practically all Fe in these generally oxic surface waters is complexed to the DNOM. Typically, the HMW moieties of the DNOM have higher Fe content [44,45]. The role of log(Fe) as an explanatory factor for log(RR) and log(RRn) may thus reflect a covariation to the larger size of the DNOM, and thereby lower biodegradability, as reflected by sUVa ($r = 0.3$, Figure 6).

Although the log(C:N) ratio was not significantly correlated with log(RR) (Figure 6), it excelled as an explanatory predictor, both in the lasso and in the multiple linear regression models of log(RR) (Figures 7 and 8). The C:N ratio was calculated as the molar ratio of DOC/DN, both DOC and DN being measured in filtered water (0.45 um). In the assessed lake water samples, it displayed a pronounced variation, ranging from 9.33 to 450, with a mean of 49.0. This greatly exceeds the Redfield ratio observed in marine phytoplankton cells (the molar Redfield ratio for C:N being 6.6), which would be assumed to represent the C:N ratio of algae-derived, autochthonous DOM. Large deviations from this stoichiometry are commonly observed in inland waters [46,47] and oceans [48]. The relatively high C:N ratio indicates recalcitrant, terrestrially derived organic matter, potentially already partially degraded by a microbial community, contrary to autochthonous and algae-derived DNOM [49,50]. N-poor DNOM implies that proteins and amino acids are depleted, yielding low-quality DNOM for bacterial consumption. This is due to the large import of allochthonous DNOM [51] to surface waters in the boreal biome, and the long residence time in the lake [52]. In addition, the degradation of the most recalcitrant moieties of DNOM may primarily be restricted by the N limitation [37]. Therefore, the addition of nutrients in our incubation experiment might have led to a "priming effect", making the relatively LMW and more saturated DNOM moieties with a high C:N ratio available for microbial degradation. Such a priming effect occurs naturally in boreal lakes, for instance, during seasonal turnovers, when the water from the hypolimnion is mixed with the nutrient-depleted water of the epilimnion [53].

The respiration rate was also partly explained by log(DP), which was negatively correlated with log(RR) ($r = -0.28$, Figure 6) and had a negative impact in the lasso and multiple linear regression models (Figures 7 and 8). Abbott et al. [54] found that DP in their permafrost leachate samples was a good positive indicator of the percentage of BDOC. Similarly, Allesson et al. [18] reported a higher turnover of BDOM in lakes in which P was in surplus. In our incubation experiment, all treatments received N and P to avoid the effects of nutrient limitation, in order to specifically test the role of DNOM quality on respiration. Nonetheless, the negative effect of log(DP) appears counterintuitive but may be because, in more nutrient-rich systems, the available DNOM was previously degraded. This supports the hypothesis of the priming effect in nutrient-poor samples.

4.2. Slower Biodegradation in Autotrophic Lakes

Log(BdgT) was positively associated with log(DOC) in the lasso and linear regressions (Figures 7 and 8). This is an inherent baseline condition for the biodegradation: the more DNOM and thereby BDOM to degrade, the longer the biodegradation period. However, log(BdgT) was negatively correlated with log(C:N) (Figure 6), which suggests a longer biodegradation time for labile DNOM. A possible explanation for this apparent contradiction is that the bacterial community faces a more heterogeneous pool of BDOM in lakes with a higher share of labile DNOM.

This is supported by the association between the biodegradation period (BdgT) and autotrophic conditions. First, log(O_2) appeared as the main explanatory positively corre-

lated variable in the lasso regression for log(BdgT) (Figure 8). High oxygen concentrations are common in the epilimnion of autotrophic lakes where the primary production releases dissolved oxygen in the layer of photosynthesis active radiation (PAR) [55]. As the samples in this study were collected from the surface, elevated O_2 concentration likely indicates high primary production in the raw water. The positive effect of log(DP) and the negative effect of log(C:N) in the lasso regression (Figure 8) also support this hypothesis. In addition, pH was a positive explanatory factor for BdgT in the lasso and multiple linear regression (Figures 7 and 8). It was itself positively related to log(Alkalinity) and log(Ca) (Table 2). Typically, these lakes are eutrophic with an inherent significant production of autochthonous BDOM [56,57].

As shown above, lighter BDOM is degraded preferentially even though the nutrient limitation is removed. Therefore, in lakes comprising both autochthonous and allochthonous DNOM, the biodegradation phase lasts longer because both the light BDOM and the less recalcitrant share of allochthonous DNOM are degraded by the bacterial community.

4.3. Enhanced Bacterial Respiration in Dystrophic Lakes

The speed and duration of respiration by the bacterial community was measured, assuming that for one molar unit of oxygen gas consumed, the bacterial community consumed one molar unit of carbon. However, this is based on the theorical value for glucose degradation. In reality, the degradation of compounds of lower molecular weight, containing more oxygen, could yield an RQ well above 1 [17,58]. In this case, the respiration of DNOM with a large share of autochthonous, light DNOM would be underestimated by controlling only the oxygen consumption. The higher respiration rate in samples from dystrophic lakes may reflect a RQ closer to 1, contrarily to the respiration rate in samples from mesotrophic lakes, where more autochthonous DNOM is available.

In addition, the microbial fixation of DNOM was not measured. The actual concurrence of these two processes can also explain the behaviour of the bacterial community in meso/eutrophic lakes and in dystrophic lakes, with a longer biodegradability lapse in the former and a higher respiration rate in the latter. Indeed, community respiration reflects both the cell-specific and the overall heterotrophic community activity. Situations with "excess C" may yield high cell-specific respiration (typically high RR), whereas higher levels of nutrients may lead to reduced cell-specific respiration, although with increased bacterial biomass and thus increased overall respiration (high BdgT) [59].

Abbott et al. [42] observed that, in samples with higher inorganic nitrogen concentration, a larger proportion of the DNOM was mineralised after the nutrient addition. They suggested that nutrient addition enhances preferentially the complete degradation of labile organic matter to CO_2, rather than causing a priming effect by making recalcitrant organic matter available. In that case, high RR is a means for the microorganisms to spend excess C [59–62], thereby lowering the C:N ratio. This is supported by the fact that log(RR) and log(RRn) were negatively associated with proxies indicating higher nutrient lake status. First, log(RR) and log(RRn) were both negatively correlated with log(CO_2) (Figure 6). Low CO_2 concentrations are usually associated with autotrophic lakes, due to the autotrophic fixation of the CO_2 [63]. Secondly, log(RRn) was negatively associated with log(EC) in the lasso regression (Figure 8). Log(EC) is a proxy of the trophic state because it is correlated with the ionic strength. Indeed, most eutrophic lakes are found in agricultural regions that are located below the marine limit with elevated levels of HCO_3, Ca, Na and Cl, in addition to DP. Moreover, few dystrophic lakes have high levels of inorganic ions [64].

This is consistent with the findings of Allesson et al. [18], who also suggested that at a community level, bacterial production increases relative to the bacterial respiration in nutrient-rich lakes. We thus suggest that in meso- and eutrophic lakes, the bacterial community uses a large proportion of the DNOM to grow and respire, although only a small part is used to provide energy for this growth. Meso- and eutrophic lakes contain a high share of autochthonous, labile DNOM, which can be directly used for anabolism.

This causes the bacterial community to use the available oxygen at a slower pace, and for a longer time. On the contrary, in dystrophic lakes, the bacterial community uses a larger proportion of the DNOM pool for respiration and a smaller part for assimilation, leading to high respiration rates and faster oxygen depletion.

5. Conclusions

We tested the applicability of an analytical method to determine the biodegradability of DNOM, based on the rate of oxygen consumption by bacteria during incubation under optimal conditions. The respiration rate (RR) and the DOC normalized RR (RRn), in addition to the duration of rapid biodegradation (BdgT) of the DNOM, showed significant spatial variation among boreal lakes in southeast Norway.

The variation in the RR was mainly driven by the characteristics of the DNOM. HMW and aromatic DNOM was respired more slowly than LMW and hydrogen saturated DNOM. Indeed, the sUVa was a main predictor of both the RR and RRn. The RR was also governed by the trophic state of the lake. However, dystrophic lakes, with a high proportion of recalcitrant DNOM and a low nutrient concentration, had the highest RR. It is likely that the amount of BDOM left in these dystrophic lake water samples is low due to the long residence time of lake water. It is thus hypothesised that the high RR is due to a priming effect, caused by the addition of nutrients for the incubation experiment. Because the studied lakes are generally lower-mesotrophic and dystrophic, the addition of nitrogen and phosphate allowed an increased respiration rate. This implies that the rate of heterotrophic respiration in these nutrient-poor lakes is mainly governed by the availability of reactive nutrients and, in particular, nitrogen, with the C:N ratio being a main predictor of the respiration rate.

Nutrient-rich lakes with high pH and oxygen concentration displayed a longer BdgT. These lakes are also prone to contain more autochthonous DNOM, which is generally more readily biodegradable. This suggests that the longer biodegradation period reflects a greater variety in the DNOM quality, due to a mix of autochthonous and allochthonous organic matter, which forces the bacteria community to adjust and thus extend its growth phase. Although the RR is faster for lakes with a higher proportion of labile organic matter, the biodegradation period may last longer due to the larger heterogeneity of the biodegradable matter, in addition to a greater quantity of BDOM to degrade.

Our findings suggest that the balance between rapid RR and long BdgT may be partly governed by the balance between bacterial respiration and assimilation. A DNOM pool with a lower proportion of labile nutrient compounds (i.e., high C:N), such as in dystrophic lakes, would enhance the bacterial respiration, hence resulting in a faster RR. On the contrary, a DNOM pool with a high proportion of bioavailable autochthonous compounds, such as those found in eutrophic lakes, would be better suited for bacterial assimilation, hence leading to a longer biodegradation duration.

Supplementary Materials: The following are available online at https://www.mdpi.com/article/10.3390/w13162210/s1: Figure S1: Repartition of the 73 lakes depending on their trophic state, based on Carlson's Trophic State Index; Figure S2: Organization of a sensor plate. Figure; S3: Snapshot of the SDS interface; Figure S4: Example of the oxygen concentration in a natural lake water sample; Figure S5: Multiple imputation process; Figure S6: Correlation plot the 27 covariates; Figure S7: Residual plots for lasso regression with log(RR) as response variable; Figure S8: Residual plots for lasso regression with log(RRn) as response variable; Figure S9: Residual plots for lasso regression with log(BdgT) as response variable; Figure S10: Residual plots for linear model with log(RR) as response variable; Figure S11: Residual plots for linear model with log(RRn) as response variable; Figure S12: Residual plots for linear model with log(BdgT) as response variable; Table S1: Summary of the dataset from the CBA 100 lakes survey; Table S2: Lasso regression estimates (pooled for n > 25); Table S3: Linear model estimates and *p*-values (pooled for n > 25).

Author Contributions: Conceptualization, R.D.V., D.O.H. and C.C.; methodology, R.D.V. and C.C.; formal analysis, C.C. and T.A.; investigation, C.C. and N.V.; data curation, C.C. and N.V.; writing—original draft preparation, C.C.; writing—review and editing, R.D.V., D.O.H., T.A. and N.V.; visual-

ization, C.C.; supervision, R.D.V., D.O.H. and T.A.; project administration, R.D.V. All authors have read and agreed to the published version of the manuscript.

Funding: This research was funded by the Center of Biogeochemistry in the Anthropocene (University of Oslo).

Institutional Review Board Statement: Not applicable.

Informed Consent Statement: Not applicable.

Data Availability Statement: The data used in this study is available on the open access repository Open Science Forum, to any person with a user account. https://osf.io/r39ng/?view_only=e9a3b3de84794bfc9883db481cb9a483 (accessed on 17 July 2021). The R code written for this study is published on Github and freely available: https://github.com/CamilMC/100_lakes_2019 (accessed on 17 July 2021).

Acknowledgments: We thank all of the participants of the CBA-100 lakes survey, who took part in the sampling of the lakes presented in this article. Eline Mosleth Fægerstad and Ragna Othilie Lie contributed significantly to the incubation experiment. Per-Johan Færøvig provided additional Presens sensors. Alexander Eiler and Laurent Fontaine developed the pipeline for amplicon analysis and Jing Wei undertook the microbial DNA extraction.

Conflicts of Interest: The authors declare no conflict of interest.

References

1. Hessen, D.; Andersen, T.; Lyehe, A. Carbon metabolism in a humic lake: Pool sires and cycling through zooplankton. *Limnol. Oceanogr.* **1990**, *35*, 84–99. [CrossRef]
2. Garmo, Ø.A. *Trends and Patterns in Surface Water Chemistry in Europe and North America between 1990 and 2016, with Particular Focus on Changes in Land Use as a Confounding Factor for Recovery*; NIVA REPORT SNO 7556-2020; The Norwegian Institute for Water Research: Oslo, Norway, 2020.
3. Tranvik, L.J.; Downing, J.A.; Cotner, J.; Loiselle, S.; Striegl, R.G.; Ballatore, T.J.; Dillon, P.; Finlay, K.; Fortino, K.; Knoll, L.B.; et al. Lakes and reservoirs as regulators of carbon cycling and climate. *Limnol. Oceanogr.* **2009**, *54*, 2298–2314. [CrossRef]
4. Larsen, S.; Andersen, T.; Hessen, D.O. Predicting organic carbon in lakes from climate drivers and catchment properties. *Glob. Biogeochem. Cycles* **2011**, *25*. [CrossRef]
5. Finstad, A.G.; Andersen, T.; Larsen, S.; Tominaga, K.; Blumentrath, S.; A de Wit, H.; Tømmervik, H.; Hessen, D.O. From greening to browning: Catchment vegetation development and reduced S-deposition promote organic carbon load on decadal time scales in Nordic lakes. *Sci. Rep.* **2016**, *6*, 31944. [CrossRef]
6. Mattsson, T.; Kortelainen, P.; Räike, A. Export of DOM from Boreal Catchments: Impacts of Land Use Cover and Climate. *Biogeochemistry* **2005**, *76*, 373–394. [CrossRef]
7. De Wit, H.A.; Palosuo, T.; Hylen, G.; Liski, J. A carbon budget of forest biomass and soils in southeast Norway calculated using a widely applicable method. *For. Ecol. Manag.* **2006**, *225*, 15–26. [CrossRef]
8. Sawicka, K.; Rowe, E.C.; Evans, C.D.; Monteith, D.T.; Vanguelova, E.I.; Wade, A.J.; Clark, J.M. Modelling impacts of atmospheric deposition and temperature on long-term DOC trends. *Sci. Total Environ.* **2017**, *578*, 323–336. [CrossRef]
9. De Wit, H.A.; Mulder, J.; Hindar, A.; Hole, L. Long-Term Increase in Dissolved Organic Carbon in Streamwaters in Norway Is Response to Reduced Acid Deposition. *Environ. Sci. Technol.* **2007**, *41*, 7706–7713. [CrossRef] [PubMed]
10. Thrane, J.-E.; Hessen, D.O.; Andersen, T. The Absorption of Light in Lakes: Negative Impact of Dissolved Organic Carbon on Primary Productivity. *Ecosystems* **2014**, *17*, 1040–1052. [CrossRef]
11. Yang, H.; Andersen, T.; Dörsch, P.; Tominaga, K.; Thrane, J.-E.; Hessen, D.O. Greenhouse gas metabolism in Nordic boreal lakes. *Biogeochemistry* **2015**, *126*, 211–225. [CrossRef]
12. Rajakumar, J. Effect of Photo-Oxidation on Size, Structure and Biodegradability of Dissolved Natural Organic Matter. Master's Thesis, University of Oslo, Oslo, Norway, 2018.
13. Liu, S.; He, Z.; Tang, Z.; Liu, L.; Hou, J.; Li, T.; Zhang, Y.; Shi, Q.; Giesy, J.P.; Wu, F. Linking the molecular composition of autochthonous dissolved organic matter to source identification for freshwater lake ecosystems by combination of optical spectroscopy and FT-ICR-MS analysis. *Sci. Total Environ.* **2020**, *703*, 134764. [CrossRef] [PubMed]
14. Hansen, A.M.; Kraus, T.; Pellerin, B.; Fleck, J.A.; Downing, B.; Bergamaschi, B. Optical properties of dissolved organic matter (DOM): Effects of biological and photolytic degradation. *Limnol. Oceanogr.* **2016**, *61*, 1015–1032. [CrossRef]
15. Marschner, B.; Kalbitz, K. Controls of bioavailability and biodegradability of dissolved organic matter in soils. *Geoderma* **2003**, *113*, 211–235. [CrossRef]
16. Brown, D.M.; Hughes, C.B.; Spence, M.; Bonte, M.; Whale, G. Assessing the suitability of a manometric test system for determining the biodegradability of volatile hydrocarbons. *Chemosphere* **2018**, *195*, 381–389. [CrossRef]
17. Allesson, L.; Ström, L.; Berggren, M. Impact of photochemical processing of DOC on the bacterioplankton respiratory quotient in aquatic ecosystems. *Geophys. Res. Lett.* **2016**, *43*, 7538–7545. [CrossRef]

18. Allesson, L.; Andersen, T.; Dörsch, P.; Eiler, A.; Wei, J.; Hessen, D.O. Phosphorus Availability Promotes Bacterial DOC-Mineralization, but Not Cumulative CO_2-Production. *Front. Microbiol.* **2020**, *11*. [CrossRef]
19. Håland, A. Characteristics and Bioavailability of Dissolved Natural Organic Matter in a Boreal Stream during Storm Flow. Master's Thesis, University of Oslo, Oslo, Norway, 2017.
20. Færgestad, E.M. Biodegradability and Spectroscopic Properties of DNOM Affected by Mercury Transport and Uptake. Master's Thesis, University of Oslo, Oslo, Norway, 2019.
21. Henriksen, A.; Brit, L.S.; Jaakko, M. *Results of National Lake Surveys 1995 in Finland, Norway, Sweden, Denmark, Russian Kola, Russian Karelia, Scotland and Wales*; Technical Report; U.S. Department of Energy: Washington, DC, USA, 1997.
22. Henriksen, A.; Brit, L.S.; Jaakko, M.; Anders, W.; Ron, H.; Chris, C.; Jens, P.J.; Erik, F.; Tatyana, M. Northern European Lake Survey 1995: Finland, Norway, Sweden, Denmark, Russian Kola, Russian Karelia, Scotland and Wales. *Ambio* **1998**, *27*, 80–91.
23. Crapart, C.; Parra, N. CBA 100 Lakes. Available online: https://osf.io/r39ng/?view_only=e9a3b3de84794bfc9883db481cb9a483 (accessed on 17 July).
24. Åberg, J.; Wallin, M. Evaluating a fast headspace method for measuring DIC and subsequent calculation of pCO_2 in freshwater systems. *Inland Waters* **2014**, *4*, 157–166. [CrossRef]
25. Schielzeth, H. Simple means to improve the interpretability of regression coefficients. *Methods Ecol. Evol.* **2010**, *1*, 103–113. [CrossRef]
26. Biodegradability of DNOM. Available online: https://www.protocols.io/view/biodegradability-of-dnom-biyykfxw (accessed on 2 August 2020).
27. Gjessing, E.; Egeberg, P.; Håkedal, J. Natural organic matter in drinking water ? The ?NOM-typing project?, background and basic characteristics of original water samples and NOM isolates. *Environ. Int.* **1999**, *25*, 145–159. [CrossRef]
28. Najafpour, G.D. Growth Kinetics. In *Biogeochemical Engineering and Biotechnology*; Elsevier B.V.: Amsterdam, The Netherlands, 2017; pp. 81–141.
29. Langenheder, S.; Lindström, E.; Tranvik, L.J. Weak coupling between community composition and functioning of aquatic bacteria. *Limnol. Oceanogr.* **2005**, *50*, 957–967. [CrossRef]
30. Comeau, A.M.; Douglas, G.M.; Langille, M.G.I. Microbiome Helper: A Custom and Streamlined Workflow for Microbiome Research. *mSystems* **2017**, *2*, e00127-16. [CrossRef] [PubMed]
31. Martin, M. Cutadapt removes adapter sequences from high-throughput sequencing reads. *EMBnet. J.* **2011**, *17*, 10–12. [CrossRef]
32. Callahan, B.J.; McMurdie, P.J.; Rosen, M.J.; Han, A.W.; Johnson, A.J.A.; Holmes, S.P. DADA2: High-resolution sample inference from Illumina amplicon data. *Nat. Methods* **2016**, *13*, 581–583. [CrossRef] [PubMed]
33. Charrad, M.; Ghazzali, N.; Boiteau, V.; Niknafs, A. Nbclust: An R package for determining the relevant number of clusters in a data set. *J. Stat. Softw.* **2014**, *61*, 1–36. [CrossRef]
34. Kassambara, A.; Mundt, F. *Factoextra: Extract and Visualize the Results of Multivariate Data Analyses*. Available online: https://cran.r-project.org/package=factoextra (accessed on 17 July 2021).
35. Galili, T. dendextend: An R package for visualizing, adjusting and comparing trees of hierarchical clustering. *Bioinformatics* **2015**, *31*, 3718–3720. [CrossRef] [PubMed]
36. Van Buren, S. *Flexible Imputation of Missing Data*; CRC Press: Boca Raton, FL, USA, 2018; Available online: https://stefvanbuuren.name/fimd/foreword.html (accessed on 8 February 2021).
37. Zuur, A.F.; Ieno, E.N.; Elphick, C.S. A protocol for data exploration to avoid common statistical problems: Data exploration. *Methods Ecol. Evol.* **2010**, *1*, 3–14. [CrossRef]
38. Casella, G.; Fienberg, S.; Olkin, I. *An Introduction to Statistical Learning*; Springer: New York, NY, USA, 2013.
39. Boehmke, B.; Greenwell, B. Chapter 6 Regularized Regression. In *Hands-On Machine Learning with R*; CRC Press: Boca Raton, FL, USA, 2020; Available online: https://bradleyboehmke.github.io/HOML/regularized-regression.html (accessed on 7 April 2021).
40. Ooi, H. *Glmnetutils: Utilities for 'Glmnet*. 2021. Available online: https://cran.r-project.org/web/packages/glmnetUtils/index.html (accessed on 17 July 2021).
41. Zhou, L.; Zhou, Y.; Tang, X.; Zhang, Y.; Jeppesen, E. Biodegradable dissolved organic carbon shapes bacterial community structures and co-occurrence patterns in large eutrophic Lake Taihu. *J. Environ. Sci.* **2021**, *107*, 205–217. [CrossRef]
42. Toosi, E.R.; Clinton, P.W.; Beare, M.H.; Norton, D.A. Biodegradation of Soluble Organic Matter as Affected by Land-Use and Soil Depth. *Soil Sci. Soc. Am. J.* **2012**, *76*, 1667–1677. [CrossRef]
43. NVE Temakart. Available online: https://temakart.nve.no/tema/innsjodatabase (accessed on 17 July 2021).
44. Du, Y.; Ramirez, C.E.; Jaffé, R. Fractionation of Dissolved Organic Matter by Co-Precipitation with Iron: Effects of Composition. *Environ. Process.* **2018**, *5*, 5–21. [CrossRef]
45. Xiao, Y.; Riise, G. Coupling between increased lake color and iron in boreal lakes. *Sci. Total Environ.* **2021**, *767*, 145104. [CrossRef]
46. They, N.H.; Amado, A.M.; Cotner, J. Redfield Ratios in Inland Waters: Higher Biological Control of C:N:P Ratios in Tropical Semi-arid High Water Residence Time Lakes. *Front. Microbiol.* **2017**, *8*, 1505. [CrossRef] [PubMed]
47. Andersen, T.; Hessen, D.O. Carbon, nitrogen, and phosphorus content of freshwater zooplankton. *Limnol. Oceanogr.* **1991**, *36*, 807–814. [CrossRef]
48. Hopkinson, C.S.; Vallino, J. Efficient export of carbon to the deep ocean through dissolved organic matter. *Nat. Cell Biol.* **2005**, *433*, 142–145. [CrossRef] [PubMed]

49. Kähler, P.; Koeve, W. Marine dissolved organic matter: Can its C:N ratio explain carbon overconsumption? *Deep. Sea Res. Part I Oceanogr. Res. Pap.* **2001**, *48*, 49–62. [CrossRef]
50. Rantala, M.V.; Nevalainen, L.; Rautio, M.; Galkin, A.; Luoto, T.P. Sources and controls of organic carbon in lakes across the subarctic treeline. *Biogeochemistry* **2016**, *129*, 235–253. [CrossRef]
51. Sepp, M.; Kõiv, T.; Nõges, P.; Nõges, T. The role of catchment soils and land cover on dissolved organic matter (DOM) properties in temperate lakes. *J. Hydrol.* **2019**, *570*, 281–291. [CrossRef]
52. Jonsson, A.; Algesten, G.; Bergström, A.-K.; Bishop, K.; Sobek, S.; Tranvik, L.J.; Jansson, M. Integrating aquatic carbon fluxes in a boreal catchment carbon budget. *J. Hydrol.* **2007**, *334*, 141–150. [CrossRef]
53. Bellido, J.L.; Peltomaa, E.; Ojala, A. An urban boreal lake basin as a source of CO_2 and CH_4. *Environ. Pollut.* **2011**, *159*, 1649–1659. [CrossRef] [PubMed]
54. Abbott, B.W.; Larouche, J.R.; Jones, J.B.; Bowden, W.B.; Balser, A. Elevated dissolved organic carbon biodegradability from thawing and collapsing permafrost. *J. Geophys. Res. Biogeosciences* **2014**, *119*, 2049–2063. [CrossRef]
55. Laas, A.; Cremona, F.; Meinson, P.; Rõõm, E.-I.; Nõges, T.; Nõges, P. Summer depth distribution profiles of dissolved CO_2 and O_2 in shallow temperate lakes reveal trophic state and lake type specific differences. *Sci. Total Environ.* **2016**, *566–567*, 63–75. [CrossRef]
56. Ryder, R.A. The Morphoedaphic Index—Use, Abuse, and Fundamental Concepts. *Trans. Am. Fish. Soc.* **1982**, *111*, 154–164. [CrossRef]
57. Cole, J.J.; Findlay, S.; Pace, M.L. Bacterial production in fresh and saltwater ecosystems: A cross-system overview. *Mar. Ecol. Prog. Ser.* **1988**, *43*, 1–10. [CrossRef]
58. Berggren, M.; Lapierre, J.-F.; del Giorgio, P. Magnitude and regulation of bacterioplankton respiratory quotient across freshwater environmental gradients. *ISME J.* **2011**, *6*, 984–993. [CrossRef] [PubMed]
59. Hessen, D.O.; Anderson, T.R. Excess carbon in aquatic organisms and ecosystems: Physiological, ecological, and evolutionary implications. *Limnol. Oceanogr.* **2008**, *53*, 1685–1696. [CrossRef]
60. Jansson, M.; Bergström, A.-K.; Lymer, D.; Vrede, K.; Karlsson, J. Bacterioplankton Growth and Nutrient Use Efficiencies Under Variable Organic Carbon and Inorganic Phosphorus Ratios. *Microb. Ecol.* **2006**, *52*, 358–364. [CrossRef] [PubMed]
61. Berggren, M.; Laudon, H.; Jansson, M. Landscape regulation of bacterial growth efficiency in boreal freshwaters. *Glob. Biogeochem. Cycles* **2007**, *21*. [CrossRef]
62. Spohn, M. Microbial respiration per unit microbial biomass depends on litter layer carbon-to-nitrogen ratio. *Biogeosciences* **2015**, *12*, 817–823. [CrossRef]
63. Balmer, M.B.; Downing, J.A. Carbon dioxide concentrations in eutrophic lakes: Undersaturation implies atmospheric uptake. *Inland Waters* **2011**, *1*, 125–132. [CrossRef]
64. Tranvik, L.J. Dystrophy. In *Encyclopedia of Inland Waters*; Elsevier: Amsterdam, The Netherlands, 2009; pp. 405–410.

Paper 3: Effect of Organic Carbon Concentration on CO_2 Evasion from Boreal Lakes

Crapart, Camille, Dag Olav Hessen, Tom Andersen

Submitted to Biogeochemistry

Photo: Camille Crapart